

A Thesis entitled

A STUDY OF THE PROBLEMS OF A
CHANNELLED IMAGE ELECTRON MULTIPLIER

by

EDWARD ALLEN FLINN, B.Sc., A.R.C.S.

submitted for the degree of
Doctor of Philosophy in
the University of London.

Instrument Technology Section,
Physics Department,
Imperial College,
London, S.W.7.

January 1963.

Abstract

After a brief discussion of the advantages of the photo-emissive cathode in comparison with other light detectors, various forms of imaging device using photocathodes are examined and compared. It is shown that a channelled electron-multiplying system has considerable potential advantages over other types of image tube. The theoretical properties of such a tube are considered; its resolution and its performance at low light levels are discussed, together with the possible gain.

The problem of choosing a suitable electrode form is next considered, and several possible dynode systems are discussed. The methods used to determine the optimum structure are described, and the results obtained with the various systems are detailed.

Some possible secondary emitting materials are discussed in Chapter IV. Experiments with several secondary emitters are described and the techniques of activation used, together with the yields obtained, are given.

Chapter V describes the methods and techniques used in the construction of channelled image intensifiers. As a result of work with the earlier tubes, an improved method of construction was devised which largely eliminated several problems initially encountered.

In Chapter VI, the results of measurements on various channelled intensifiers are given. The theoretical resolution is in fact obtained, and this can be further improved by the use of "dynamic viewing". The gains of tubes with varying numbers of multiplying stages are given. A ten-stage tube, working at 530 volts per stage, gave an electron gain of 2.10^4 and a usable blue light gain of 5.10^4 . These figures could readily be increased by the addition of further multiplying stages, a simple process with the channelled tube, and the use of a thicker aluminium backing layer on the phosphor. It is concluded that image intensifiers of this type are indeed practicable, their limited resolution being outweighed for many applications by their small size, high gain and simplicity of operation, since very modest power supplies are required

in comparison with other intensifiers.

Finally, suggestions are made for an improved method of construction, and a possible application as a colour image intensifier, for which the channelled tube is uniquely suited, is suggested.

Contents

1.

Chapter		<u>Page No.</u>
I	<u>Comparison of various image detectors</u>	
	<u>1.1</u> Introduction	
	<u>1.2.</u> Brief comparison of a few light detectors.	4
	1.2.1. Requirements of the ideal detector.	4
	1.2.2. The photo-emissive surface.	5
	1.2.3. The photographic emulsion.	6
	1.2.4. The eye.	6
	<u>1.3.</u> Photo-electronic image devices.	7
	1.3.1. The simple intensifier.	7
	1.3.2. The cascaded intensifier.	8
	1.3.3. The transmission secondary emission intensifier.	10
	1.3.4. The channelled secondary emission intensifier.	11
	1.3.5. Television pickup tubes.	13
	1.3.6. Electronographic tubes.	14
II	<u>Theoretical parameters of a channelled tube</u>	
	<u>2.1.</u> Statistics of the multiplication process.	17
	<u>2.2.</u> Minimum detectable flux.	18
	<u>2.3.</u> Light gain.	24
	<u>2.4.</u> Resolution.	25
	<u>2.5.</u> Dynamic viewing.	28
	<u>2.6.</u> Cell size, dynode area and picture quality.	31

Chapter		2.
III	<u>The choice of electrode structure</u>	<u>Page no.</u>
	<u>3.1.</u> Introduction.	34
	<u>3.2.</u> The Modified Venetian Blind Structure.	36
	<u>3.3.</u> The symmetrical cylindrical structure.	38
	<u>3.4.</u> The asymmetrical cylindrical structure.	44
IV	<u>Choice of secondary emitting surface</u>	
	<u>4.1.</u> Review of three possible materials.	49
	<u>4.2.</u> Antimony-caesium	50
	<u>4.3.</u> Potassium chloride.	50
	<u>4.4.</u> Magnesium oxide.	53
	<u>4.5.</u> Summary.	58
V	<u>Construction of image tubes</u>	
	<u>5.1.</u> Dynode fabrication.	60
	<u>5.2.</u> Preparation of secondary emitting surfaces.	66
	5.2.1. MgO surfaces.	67
	5.2.2. KCl surfaces.	69
	<u>5.3.</u> Assembly of tubes.	72
	5.3.1. Early tubes.	72
	5.3.2. An improved design.	76
	<u>5.4.</u> Processing.	81
	<u>5.5.</u> Modifications in design.	82

VI	<u>Results obtained with imaging tubes</u>	<u>Page no.</u>
	<u>6.1.</u> Measurement techniques.	85
	6.1.1. Measurement of electron gain.	85
	6.1.2. Measurement of light gain.	87
	6.1.3. Measurement of resolution.	89
	<u>6.2.</u> Gains obtained.	89
	<u>6.3.</u> Resolution - Static and Dynamic.	97
	<u>6.4.</u> Contrast.	103
	<u>6.5.</u> Background.	104
	<u>6.6.</u> Conclusion.	104
VII	<u>The future</u>	
	<u>7.1.</u> Suggested scheme for a new design of channelled tube.	105
	<u>7.2.</u> A colour image intensifier.	107
	Acknowledgments.	108
Appendices:	I Statistics of Multiplication	109
	(a) The exponential distribution.	
	(b) Probability distribution of photo-electrons.	
	II Constructional Techniques	112
	(a) Activation of an Sb-Cs photocathode.	
	(b) Settling and aluminising of fluorescent screens.	
	References.	115

1.1. Introduction

There exists today in many fields a pressing need for a simple device which will render visible or recordable optical images of very low intensity. Such a device would be useful not only to extend the range of nocturnal human vision, but also in the scientific field for the study of many phenomena involving faint images. These are found for instance in the study of weak spectral lines, the investigation of particle tracks in scintillation chambers, and the astronomy of very faint objects. In some cases, the need is for a reduction in the period of observation required, in others for the extension of measurements to light levels below those attainable by present techniques. In yet others, however, the total amount of information available may be limited, so that every possible quantum of light must be utilised. This is so in the case of a particle passing through a scintillation chamber, where the whole of the available light may comprise only a few thousand or even a few hundred photons. Under such circumstances, a detecting device is required which is more efficient than those commonly in use, and the photo-emissive surface is becoming increasingly prominent in such applications.

In the next section, the advantages of the photo-emissive surface as the sensitive element in an image detecting device are briefly discussed, in comparison with the two other detectors most commonly used; the eye and the photographic emulsion.

1.2. Brief comparison of a few light detectors.

1.2.1. Requirements of the ideal detector

The most important requirement of a light detector is that it should unmistakably record the maximum possible proportion of the incident photons, giving equal weight to each individual quantum.

It is useful here to define the concept of "quantum efficiency". This is the fraction of the incoming photons which produce an observable effect on the detector, and is normally expressed as a percentage. Thus, if on average the arrival of one hundred photons results in one detectable event, such as the emission of a photo-electron, or the blackening of one grain in an emulsion, the quantum efficiency is said to be 1%.

The ideal detector would have a quantum efficiency of 100% for all wavelengths and under all conditions of stimulation, giving an equal response to each photon, and would consequently be perfectly linear. It would respond instantaneously, so as to allow the study of rapid variations in the input intensity. In practice the quantum sensitivity of most detectors varies with the wavelength of the incident light, and often with its intensity and duration also.

1.2.2. The photo-emissive surface

Oxidised antimony - caesium layers have been produced with a peak quantum sensitivity, in the blue, of some 25%.^{1,2} The mean efficiency over the visible spectrum is normally taken as 10%. The tri-alkali (Sb-Na-K-Cs) surface has a rather higher peak quantum sensitivity of about 35-40%.² and an extended red and infra-red response, so that its mean quantum efficiency over the visible region may be taken as about 15-20%.^{2,3,4} The response time is very brief,⁵ and for all practical purposes the emission process may be considered instantaneous. In addition, the response is perfectly linear over many orders of magnitude, from the emission of a single photo-electron up to the point where the electrical resistivity of the emitting surface begins to cause significant variations in potential across its area.

Photo-emissive surfaces can be prepared which will respond to any one region of the spectrum, from the infra-red to the vacuum ultra-violet (14,000 - 1,000 Å), with a higher efficiency than any other detector.

1.2.3. The photographic emulsion

This has a relatively low quantum efficiency which varies with intensity of illumination, and shows extreme non-linearity at high exposure densities. The peak quantum efficiency for a fast blue-sensitive film under normal conditions of use is generally taken as 0.1%,^{6, 7.} although Fellgett⁸ states that a blue-sensitive emulsion of 1 μ grain size may have a peak monochromatic quantum sensitivity of 1.1% when exposed to the very low density of 0.25 above fog. At this exposure density, however, the information storage capacity of the plate is too low for most applications. As the density is increased, more and more photons strike grains already exposed, reducing the quantum efficiency and giving rise to the non-linearity mentioned above. At very low light levels, reciprocity failure is observed. This causes the quantum efficiency to fall as the level of illumination is reduced, until below a certain threshold level the emulsion is completely insensitive.

1.2.4. The eye

This is the most commonly-used detector and in many respects the most efficient, sensitive and versatile. It has a high quantum efficiency, though various workers differ as to the exact value. The scotopic eye appears to have an efficiency in the region of 2-5% for white light^{9, 10, 11.} and the photopic eye about 0.2-0.5%. The peak sensitivities are about five times these mean values.

The eye is usable over the range of scene illumination from 10^{-7} to 10^4 ft. lamberts,⁹ although many hours are required for full dark adaptation to be attained. Reasonable efficiency is maintained over the region 10^{-6} to 10^2 ft. lamberts, and the full usable range of 10^{11} is many orders of magnitude greater than that of any other device.

The eye has however a fixed integrating time, variously given

as 0.1-0.2^{9,11} seconds according to the experimental conditions. This means that very brief images at a level sufficiently high to make them detectable if of longer duration cannot be seen, and rapid fluctuations in intensity go undetected. In addition, images at low light levels which would be detectable with a longer period of integration remain invisible. It is thus clear that the photo-emissive surface approaches more closely to the ideal detector than other devices, in particular at very low light levels, and the next section discusses possible methods of applying its advantages in an imaging device.

1.3. Image Devices

It is possible to devise a very large variety of image-forming detectors using photocathodes in conjunction with various other elements, but only the most important of these will be discussed here. They are:-

- a) The simple image intensifier.
- b) The cascaded image intensifier.
- c) The transmission secondary emission intensifier.
- d) The channelled secondary emission intensifier.
- e) Television pickup tubes.
- f) Electronographic devices.

1.3.1. The Simple Intensifier

This consists essentially of a photocathode and a fluorescent screen only. Electrons from the cathode are accelerated and focused on to the phosphor, and if given sufficient energy will produce an intensified image. The maximum possible gain of such a tube for a given accelerating voltage may be calculated from a knowledge of the cathode and phosphor efficiencies. Mandel¹³ discusses the case of an Sb-Cs photocathode used with a 5,400^oK. light source (i.e. one

having the same spectral distribution as sunlight) and an aluminium-backed ZnS:Ag phosphor. The maximum light gain with an accelerating voltage of 20 k V is 32. For a blue light input with the same spectral distribution as the light from a ZnS:Ag phosphor, the gain rises to about 200, since the emission curve for ZnS:Ag and the response curve for the Sb-Cs surface are very similar in form, both having maxima at about 4,500 Å. In fact a blue light gain of 100 has been achieved in such a tube, using an accelerating voltage of 25kV.¹⁶

Although at first sight this gain appears quite useful, in practice the losses in any associated optical system reduce the overall gain to a very low value. For example, two ideal F/1 lenses used face to face at unity magnification would transmit only 20% of the emitted light, while losses in any practical system would reduce this to about 13%, if a transmission factor of 80% is assumed for each lens. The useful gain is then reduced to 13. Fibre optics allow image transfer with slightly lower losses, but the improvement obtained by their use would still be insufficient to render the system practical, even if vacuum tight fibre windows were readily obtainable.

For certain specialised applications, primarily astronomical, where a photographic record is required, these losses can be almost eliminated by depositing the phosphor on a thin transparent vacuum-tight membrane, against which the photographic emulsion is pressed.^{14,15.} Photographic gains of 100¹⁶ have been realised in such tubes, using mica windows 12-15 μ thick, with solenoidal focusing, to give a resolution of 30 lp/mm. over an area approximately 1 in. in diameter. Such tubes are limited in their application, however, and for most purposes considerably higher gains are required.

1.3.2. The cascaded image intensifier

The obvious development of the simple intensifier is to cascade several such tubes in series. It is theoretically possible to do

this by means of coupling lenses, but the large losses, and the expense and complication of such a system, make the method impracticable. In 1928, workers in the laboratories of Philips Gloeilampenfabrieken¹⁷ suggested the use of several such tubes in a single envelope, the phosphor of one stage and the cathode of the next being deposited on opposite sides of a thin transparent membrane. (Early efforts to construct such tubes were unsuccessful, but more recently several successful tubes have been made. The device constructed by Zavoitski et al.¹⁸ is particularly noteworthy, as the first intensifier to permit photographic recording of single photo-electrons.

Tubes with from two to five intensifying sandwiches have been reported, and light gains of 10^5 appear to be readily obtainable.^{19, 20.} For instance, Stoudenheimer¹⁹ quotes a three-stage electrostatically-focused tube as having a light gain of 10^5 and a resolution of 15 lp/mm. at the centre of the screen, falling to 8 lp/mm at a radius of $\frac{1}{2}$ in. In magnetically focused tubes, a resolution of 15 lp/mm across the whole screen is typically obtained.

Thus the cascade tube is capable of giving high gain with fairly good resolution. High voltage supplies are necessary, however, values of 50 kV or more being typical. This tube has one great advantage over most other multi-stage intensifiers in that the gain per stage is high - up to 100. This means that the variation in brightness of output scintillations produced by individual photo-electrons will be small, if non-uniformity in the phosphor layer is neglected. If the gain per stage is G , ther.m.s.deviation in the number of electrons resulting from the multiplication of a single photo-electron will be \sqrt{G} , and the fractional deviation $\frac{1}{\sqrt{G}}$, if Poissonian statistics are assumed. Thus a tube with a gain of 100 per stage would show a mean deviation of around 10% in the brightness of the output scintillations, since this value is determined primarily by the gain of the first stage.

In contrast with this we may consider the transmission secondary emission intensifier, with a stage gain of 5, giving a theoretical deviation of the order of 45%. Thus in the latter tube there will be many occasions when it is impossible to decide whether a given scintillation represents one, two, or even three photo-electrons, whereas such a situation would be very rare in a cascade tube, with its high stage gain.

1.3.3. The transmission secondary emission intensifier

In the transmission multiplying tube the multiplying material, usually KCl or BaF₂, is deposited in a layer a few hundred Å thick on an electron-permeable supporting membrane of aluminium oxide. A thin conducting layer of aluminium is interposed between the two to avoid charging of the surface, since both aluminium oxide and the alkali halides are good insulators.

These dynodes are supported in the tube parallel with each other and with the cathode and screen. In operation, electrons from the photocathode are accelerated and focused on the first dynode, where they penetrate the aluminium oxide and aluminium layers to liberate secondary electrons from the multiplying layer. These secondaries in turn are focused on the next dynode, and so on. Finally the multiplied electrons are projected on to the phosphor screen to give an intensified image.

The first really satisfactory tube of this type²² used four dynodes with KCl secondary emitting layers to give a gain per stage of slightly over five, with a primary energy of 4.5 keV. The photon gain was about $8 \cdot 10^4$, and the background at room temperature corresponded to less than $100 \text{ el. cm}^{-2} \text{ sec}^{-1}$. A resolution of 15 lp/mm. was obtained. Later tubes²³ with five dynodes and a more uniform magnetic focusing field gave a resolution of 23 lp/mm.

Owing to the relatively low gain per stage, the statistics of

the tube are fairly poor. Results obtained by Emberson, Todkill and Wilcock²³ appear to show that the brightness distribution of output scintillations for single photo-electrons is exponential, so that an even wider variation is observed than if the multiplication process were Poissonian, as is usually assumed. There is a finite possibility that any given photo-electron will produce no output scintillation at all, and Emberson et al. estimate that about 20% of the photo-electrons are lost at the first dynode in this way when the gain per stage has its maximum value of 5. Recent experimental work at Imperial College suggests that this figure may in fact be very much higher - possibly as high as 60%.

The use of the alkali halides for secondary emitting surfaces has certain disadvantages. The yield is found to fall off under electron bombardment, as chlorine atoms are liberated from the crystal lattice. The free chlorine then attacks the photocathode, causing a fall in sensitivity. The rate of decay of secondary emission yield with bombardment is somewhat uncertain: for KCl, Anderson²¹ quotes a fall of 50% in the yield after bombardment with a total charge of $72 \mu\text{coul}/\text{cm}^2$. Ba F₂ was rather better, the initial yield of 8 per dynode falling by only 3% on bombardment with this quantity of charge. In contrast to Anderson's results, Todkill of this department found that a charge of 25 millicoul/cm² was required to reduce the yield of a KCl dynode by 50% : a large discrepancy.

1.3.4. The channelled secondary emission intensifier

The channelled image intensifier was independently proposed by McGee²⁴ and by Roberts and Kruper²⁵ in 1953. It is essentially a development of the well-known photomultiplier. Photomultipliers are commercially available which will give an electron gain of 10^9 at an overall voltage of only a few kV, and it is clear that an imaging device with similar characteristics would be extremely valuable.

To achieve the desired image-forming properties, it is necessary that during the multiplication process electrons originating from a given area of the photocathode should be kept separate from those originating in other parts of the surface. This is most conveniently done by using a channelled electrode system, so that in effect an array of minute photomultipliers is used, one for each elementary area of the photocathode. After multiplication the electrons are projected on to a suitable detector - normally a fluorescent screen. The resolution is intrinsically limited by the dynode structure, since brightness variations smaller in size than a single channel diameter will not be distinguishable. On the other hand, the resolution is independent of the number of stages, so that many stages of multiplication can be used, to give a very high gain without further loss in resolution.

The voltage requirements of such a tube are very modest in comparison with those of other high-gain intensifiers: satisfactory secondary emission yields can be obtained with primary electron energies of only a few hundred electron volts, so that a potential of a few kV suffices for the multiplier section of the tube, while an accelerating voltage of the same order is required for the phosphor stage. Since the focusing is purely electrostatic, no focusing solenoids, with their stabilised current supplies, are required, and the E.H.T. supply need not be highly stabilised. The dynode structure of a channelled tube is extremely short (one or two cm.) compared with those of other tubes, and the construction of tubes of large sensitive area should be possible, since the very solid dynode structure may be made to support the end plate of the tube. This renders the channelled intensifier potentially ideally suited to such applications as X-ray fluoroscopy and fibre scintillation chamber observations, where the small sensitive area of other intensifiers is a serious handicap. In the latter case, the limited resolution is comparatively unimportant, since the scintillation fibres used are not normally less than $\frac{1}{2}$ mm. in diameter²⁶. Another

potential field of application may be in various satellite experiments, where power supplies are strictly limited, and the use of magnetic fields must be avoided as far as possible, since their presence causes difficulty in maintaining the attitude of the satellite. Here the electrostatic focusing of the channelled tube and its minimal power requirements, together with the small physical size, should prove valuable advantages.

1.3.5. Television pickup tubes

In a television camera tube the incoming light image is transformed into an electrical image, normally in the form of electric charge stored on an insulating target. The electrical image is then discharged, generally by means of a sharply focused electron beam, which is scanned across the surface of the target so that the whole surface is discharged in a short period of time, of the order of .04 second. As the electron beam discharges each image point in turn, the instantaneous discharge current is proportional to the quantity of charge stored, and consequently to the intensity at the corresponding point of the original light image. Thus the spatial intensity distribution of the light image is transformed into a time-varying electrical signal, which can then be handled by the usual techniques of electronic engineering. Normally the signal is amplified, and after the addition of synchronising pulses, is transferred to the display device, which may be at a considerable distance from the camera. It may however be magnetically recorded, so that the original image is conveniently preserved for later use.

Fundamentally, the sensitivity of a television camera tube is limited by the efficiency of the photocathode, as in other photo-electronic devices. In practical devices, however, the noise of the scanning beam, or that introduced by the head amplifier, is much greater than that due to the process of photo-emission, and it is these factors which normally limit the sensitivity of camera tubes.

Attempts have been made to alter this situation by adding one or more stages of intensification prior to the scanning process, so that the level of the incoming signal is raised to a point where beam and amplifier noise are of minor importance. According to Morton²⁷, an image orthicon with a single stage of intensification can resolve a 200-line picture at a cathode illumination of 10^{-6} ft. candles, whereas a selected wide-spaced image orthicon of the normal type requires a cathode illumination of 5.10^{-5} ft. candles to give the same resolution. A tube with three stages of intensification is said to allow the observation of single photo-electrons. Such tubes are very complicated and expensive, however, requiring a large quantity of auxiliary equipment in addition to the normal television channel.

It can thus be seen that although television systems have many advantages, in particular the facilities for remote display and read-recording of the image, they are unlikely to find wide application for work at very low light levels, owing to the cost and relative complexity of the associated electronic equipment.

1.3.6. Electronographic Tubes

In electronographic systems the output element is an electron-sensitive emulsion on to which the electrons are accelerated and focused. Since each electron may produce a large number of developable grains, a valuable gain in sensitivity over unaided photography can be attained. An additional advantage lies in the fact that electronographic emulsions are extremely fine-grained, so that a large quantity of information may be stored, while the response is considerably more linear than that of a photo-sensitive emulsion, which is normally exposed to a much higher density in order to give reasonable information storage.

Successful continuously-pumped tubes in which the cathode and emulsion are in the same vacuum compartment have been constructed by Lallemand and his co-workers.^{28, 29, 30, 31.} In these devices the

emulsion is refrigerated to reduce poisoning of the photocathode by organic vapours. Gains of up to 100 in exposure time over unaided photography are reported, with a resolution of 70 lp/mm. Lallemand et al. also found that for Ilford G5 nuclear emulsion the developed density is proportional to photocathode illumination over a brightness range of more than 10:1.

Sealed-off tubes based on the same principle have been constructed by McGee and Wheeler^{32, 33}. These tubes are terminated by a thin vacuum-tight mica membrane 6-8 μ thick, and 0.5 cm. x 3.0 cm. in area. Photoelectrons are accelerated to 50 keV and focused on this window, against which the emulsion is tightly pressed. About 75% of them pass through the mica, striking the emulsion with energies ranging from 10 keV upwards. The mica window takes on a pronounced curvature under atmospheric pressure, so that glass-backed plates are unsuitable, and nuclear stripping emulsions have normally been used. A resolution of 48 lp/mm. has been obtained with a window 6 μ thick, and McGee and Wheeler quote for Ilford G5 emulsion a photographic speed gain of ten over Tri-X exposed to the same density. It should be noted, however, that when both emulsions are exposed to the same density, a much larger quantity of information is stored on the fine-grained electronographic emulsion, and it seems probable that the performance of this tube is comparable with that of Lallemand's device. It is however much more compact, long-lived and simple to use.

A tube of intermediate type has been studied by several workers^{34, 35, 36, 37}. In this, an electron permeable membrane is used to isolate the photocathode from the emulsion, both compartments being separately pumped. The membrane can be made extremely thin, as it is not called upon to withstand atmospheric pressure, so that the electrons pass through it with little loss in energy. The emulsion must be placed as close as possible to the membrane, however, so that resolution is not lost owing to scattering during transmission. Such

tubes have not in general proved satisfactory, although work on them is still in progress.

It is clear that electronographic tubes are valuable where a photographic record is required and a moderate gain will suffice, but their applications are strictly limited owing to the high working voltages required and the consequent high dark current.

From this brief examination of the range of practical photo-electronic image tubes, it may be seen that no really simple high-gain intensifier is yet available. The channelled tube offers promise of being such a system, and it seems certain that in many applications its advantages would outweigh the handicap of limited resolution. The remainder of this thesis describes work done on the problems of constructing such a device.

2.1. Statistics of the multiplication process

The question of the statistical distribution appropriate to the emission of secondary electrons is one of considerable interest. If all the secondary electrons emitted are completely independent of one another, the number of secondaries produced by a single primary will follow a Poisson distribution, and this is the form considered by Zworykin and Morton,³⁸ and by Morton.³⁹ Then, if one primary electron produces ν secondaries, p primary electrons will produce n secondaries,

$$\begin{aligned} \text{where } \bar{n} &= \bar{p} \bar{\nu} \\ \text{and } \overline{\Delta^2 n} &= \bar{\nu}^2 \overline{\Delta^2 p} + \bar{p} \overline{\Delta^2 \nu} \\ &= \bar{\nu}^2 \bar{p} + \bar{p} \bar{\nu} \end{aligned}$$

Then, if N_0 primaries enter an r -stage multiplying system with mean stage gain $\bar{\nu}$, the number of electrons leaving the system is given by

$$\begin{aligned} \bar{N}_r &= \bar{\nu}^r \bar{N}_0 \\ \text{and } \overline{\Delta^2 N_r} &= \bar{N}_0 (\bar{\nu}^{2r} + \bar{\nu}^{2r-1} + \dots + \bar{\nu}^r) \\ \therefore \frac{\overline{\Delta^2 N_r}}{\bar{N}_r^2} &= \bar{N}_0 \frac{\bar{\nu} - 1}{\bar{\nu} - \frac{1}{\bar{\nu}^r}} \end{aligned}$$

Thus, if $\bar{\nu}^r$ is large, the signal to noise ratio is decreased by a factor $\sqrt{1 - 1/\bar{\nu}^r}$

In fact, however, measurements on the signal-to-noise ratio of electron multipliers yield results not in agreement with the above expression. For example, using Morton's values for the parameters of the RCA 5819, one may calculate a change in signal to noise ratio of $13\frac{1}{2}\%$ during multiplication, whereas the measured change is actually 19%.³⁹ This indicates that the r.m.s. deviation of the distribution is greater than that assumed, so that the assumption of a Poissonian distribution must be incorrect. Ziegler⁴¹ arrives at the same conclusion by studying the deviation for interactions resulting in small numbers of secondaries. He suggests that secondaries resulting from the same primary are not independent of each other, since the escape probability

of an electron depends on the depth at which it is liberated. The figures quoted by Ziegler indicate a change in signal-to-noise ratio of some 20%-30%, depending on the primary voltage, for a multi-stage device. This is in passable agreement with Morton's experimental results.

According to Ziegler, the large r.m.s. deviation precludes the presence of a maximum in the distribution curve, as would be found with a Poisson distribution. Lombard and Martin⁴² come to the same conclusion.

Several workers^{23, 43.} have reported an exponential pulse height distribution at the output of a photomultiplier, for single input electrons. It can be shown that a sufficient (but possibly not necessary) condition for this output distribution is an exponential distribution at each multiplication. An exponential output distribution gives a fall in signal-to-noise ratio on multiplication of 30%, (See Appendix Ia) and is consequently not in good agreement with Morton's results.

2.2. Minimum light flux detectable by a channelled tube

The minimum flux detectable by any photosensitive device is determined by two factors:

- a) The random nature of the photon stream and the consequent statistical fluctuations.
- b) Noise generated inside the detecting device.

In the case of a multiplying tube, b) may be sub-divided.

- i) Statistical noise generated in the photo-emissive process.
- ii) Statistical noise generated in the multiplication process.
- iii) Spurious emission.

i) Owing to the comparatively low efficiency of the photo-emissive process, the signal-to-noise ratio of the incoming signal is severely

reduced at this stage. The arrival of photons is known to obey a Poisson distribution,⁴⁴ so that if only first-order interactions occur at the cathode the photo-electron distribution must also be Poissonian (See Appendix Ib). Then, for a photocathode with a quantum efficiency of 10%, the signal to noise ratio of the input will be reduced by a factor $\sqrt{10}$ during the process of photo-emission.

ii) The change in signal to noise ratio due to the multiplication process is remarkably small, and more or less independent of the actual gain, if this is large. The exact figure depends on the probability distribution of the secondary electrons, but for the purposes of this examination, a loss of 30% in signal-to-noise ratio is assumed. This is the fall produced if the properties of the system are such that single photo-electrons give an exponential pulse height distribution at the output. Such a distribution appears to be the one most commonly observed by experimenters, although there is a considerable amount of controversy on the subject.

iii) In theory there are many possible sources of dark emission, but in practice only two are of importance. These are field emission and thermionic emission. Field emission becomes important at field strengths greater than 10^6 volts/cm.⁴⁵, which is considerably higher than the designed field strength in most intensifiers. Unfortunately it is almost impossible to eliminate microscopic irregularities on the surfaces of the tube walls and electrodes, and the local field strength at these points may attain extremely high values, so that they form sources of spurious emission. Sharp edges on electrodes also may be troublesome, but these can be largely eliminated by the use of suitable techniques. Since field emission from these sources is a very variable phenomenon, and is not a fundamental limitation, but a matter of technique, only thermionic emission will be considered in the following

theoretical discussion.

In a normal tube, the only important sources of thermionic emission are the photosurface itself and any other surface in the tube which has been caesiated during the activation of the photocathode. The latter source can be effectively eliminated by careful design, and thermionic emission from the photocathode can be reduced to a very low level, by suitable processing. For example, Sharpe quotes an experimental Sb-Cs cathode of 4% peak quantum efficiency as having a dark current of $2 \text{ el. cm.}^{-2} \text{ sec.}^{-1}$ although for a normal Sb-Cs surface of 16% peak quantum efficiency he quotes a dark current of $4,000 \text{ el. cm.}^{-2} \text{ sec.}^{-1}$ at room temperature. Other workers have claimed substantially lower figures; e.g. McGee, in a private communication, has described an Sb-Cs cathode with a sensitivity of $40 \mu \text{ A/lm}$, or about 10% peak quantum efficiency, which had a dark current of only $1 \text{ el. cm.}^{-2} \text{ sec.}^{-1}$ at 0° C . All these figures can be greatly reduced by cooling the photocathode, although the high resistivity of the Sb-Cs cathode precludes its use below CO_2 snow temperature.

The tri-alkali surface, in spite of its greater red and infra-red sensitivity, gives in general less thermionic emission than the Sb-Cs cathode; Engstrom et al.⁴ quote a figure of $1,000 \text{ el. cm.}^{-2} \text{ sec.}^{-1}$ at room temperature for a cathode of unspecified sensitivity. Also, the tri-alkali cathode has a comparatively low resistivity, and can be cooled to liquid air temperature, with a large drop in the thermionic emission.

Thermionic emission, like photo-emission, is a random process, and the statistical fluctuations in the rate of emission present themselves in the form of noise, which is additive with that inherent in the photo-electron stream.

Now let us consider a single picture-element, corresponding to a single channel of the system. Assume N photo-electrons/sec. and N_t thermal electrons/sec. are emitted from this area, and consider an observation time t .

Poissonian statistics are applicable, and the standard deviation of the total number of electrons is given by $\sqrt{Nt + N_t t}$. The smallest detectable change in signal is then given by $K\sqrt{Nt + N_t t}$, where K is the "coefficient of certainty", and defines the minimum signal to noise ratio which can be detected with reasonable certainty. A further factor d, which will always be less than 1, must be introduced, to allow for the loss in signal-to-noise ratio during multiplication. If then a half-tone image is being viewed, and it is desired to distinguish B separate brightness steps, the number of photo-electrons required at the brightest picture points is given by

$$N_{\max} t = B \frac{K}{d} \sqrt{N_{\max} t + N_t t}$$

This expression is not exact, since the minimum distinguishable brightness change will be smaller than this in regions of lower brightness, but it will serve to form an estimate of the number of photo-electrons required.

In early work on this subject,^{12, 47.} K was commonly taken as 5, a value which would ensure almost complete certainty of detection. This is a rather pessimistic figure, however, since in images which exhibit a definite structure, as opposed to a random distribution of half-tones, a value for K of 2 or 3 gives quite acceptable images. Here, the conservative value of 5 will be assumed. B may be taken as 10, which is sufficient for quite a good picture. 1 mm. picture points have been satisfactorily used in channelled intensifiers, and for a tri-alkali cathode, N_t may then be taken as 10 el/sec/picture point. For visual observation, $t = 0.1$ sec., the integration time of the eye. $d = 0.7$, for an exponential output distribution.

$$\text{Then } 0.1 N_{\max} = 5 \times 10 \times \frac{1}{0.7} \sqrt{0.1 N_{\max} + 1}$$

$$\therefore N_{\max} = 51,000 \text{ photo electrons/picture point/ sec.}$$

With a tri-alkali cathode of $150 \mu\text{A/lm}$ sensitivity, this requires an intensity of illumination of $5.1 \cdot 10^{-6}$ ft. candles of tungsten light.

If a distant perfectly diffusing white surface, illuminated with intensity I_o , is imaged on the cathode by a lens of transmission T and relative aperture F , the illumination on the cathode will be

$$I_c = \frac{I_o \times T \times F^2}{4}$$

For an $f/1$ lens with a transmission of 80%, $I_c = 0.2 I_o$, so that if I_c has a value of 5.10^{-6} ft. cd., I_o must be $2.5.10^{-5}$ ft. cd.

As an illustration of the practical meaning of this figure, the intensity of illumination at the earth's surface on a clear moonlit night is about 10^{-2} ft. cd., while on a clear starlit night with no moon the intensity is about 10^{-4} ft. cd. Thus, although the spectral response of the cathode would not be perfectly matched with the spectrum of the incident light, the sensitivity should be ample to give a satisfactory image by starlight alone.

For use with detectors other than the eye, the integration time may be varied, the limiting light level varying inversely as the integrating time. Thus, for $t = 1$ minute,

I_o becomes 4.10^{-7} ft. cd., approximately,
while for $t = 1$ hr., I_o falls to 7.10^{-9} ft. candles.

In practice, refrigeration of the cathode would be necessary for an hour-long exposure at this level.

If the resolution of the tube is increased, the sensitivity falls: it is inversely proportional to the square of the linear resolution. It seems unlikely that the channel size can be reduced below about 0.2 mm.; the limiting light level for a half-tone image would then rise to 6.10^{-4} ft.cd., so that a recognisable image should still be obtained, even by starlight.

In applications where half-tone discrimination is not required, much smaller light fluxes may be detected. Using the previously-assumed values for the parameters, the background count of the tube would be only 10 electrons/picture point/ sec. Thus if the tube were

gated by pulsing the potential of one of the electrodes, faint images of brief duration could be detected with considerable certainty, since the background could be reduced almost to zero. Single photo-electrons would then be detectable, so that observations could be made of such phenomena as particle tracks in scintillation chambers. The relatively low gain per stage would make the statistics of the tube rather unfavourable for such an application, particularly as a fairly large proportion of photo-electrons are lost in the dead area of the first dynode. Also, something between one and five per cent of those photo-electrons entering dynode cells would produce no output signal, the exact fraction depending on the yield of the surface and the efficiency of extraction of secondary electrons. The very high gain available, however, would render such tracks readily visible and enable them to be photographed.

Perl and Jones²⁶, for instance, quote a rate of photon production of 40,000 ph/cm. for a minimum ionising particle in a typical scintillator plastic. Then, in a typical chamber system they calculate that 5-10 electrons will be produced at the cathode for each cm. of the particle's path. The information about the path is thus extremely sparse - about 1 photo-electron/mm. of track - so that the high gain of the channelled tube is very useful. Further, owing to the finite depth of the chamber, and the large aperture of the optical system, the resolution is intrinsically very poor, and the limited resolution of the channelled tube is not a serious disadvantage. Perl and Jones consider two standards of definition: - 1 mm. and 0.5 mm. Tubes with channels of these dimensions have already been constructed.

Attempts to avoid the limitations due to depth of focus difficulties have led to the development of the filamentary chamber. In this the scintillator plastic is disposed in the form of fibres, which act as light pipes to transfer light from the track to an outside face of the chamber. Alternate layers of fibres are arranged at right angles.

to allow location of the track in three dimensions. Again, the resolution is not better than about $\frac{1}{2}$ mm., since smaller fibres give too low a light output at their ends for satisfactory detection. For a chamber with 1 mm. fibres, Condon⁴⁸ quotes an average of 190 photons at the end of each fibre for a minimum-ionising track. This is a factor of almost 10^4 below the level detectable by the fastest photographic emulsion, but would give quite a bright image on a tube of the type discussed. In this connection the possibility of producing tubes of large sensitive area is of great interest, since the usefulness of a scintillation chamber increases rapidly with its size.

2.3. Gain

So far, the gain of such a tube has not been discussed in detail, since within reason it may be increased to any desired value. As an example, we may consider a 15-stage tube with a gain of 3 per stage, which appears to be readily achievable, giving an overall electron gain of $1.4 \cdot 10^7$. If the amplified electron stream is then projected on to an aluminium-backed ZnS:Ag phosphor by an accelerating potential of 10 kV, each electron will release in the forward direction about 500 photons, so that each single initial photo-electron will produce about $7 \cdot 10^9$ output photons (These figures are based on the results of Brill and Klasens⁴⁹). Then for an element 1 mm. square, assuming an integrating time of 0.1 second for visual observation, the rate of emission is $7 \cdot 10^{12}$ ph/cm²/sec. This level - about a factor of 10^3 below peak white in a television image - is readily detectable by the photopic eye, and is almost three orders of magnitude above the level required to expose a fast photographic emulsion (10^9 ph/cm²), so that even allowing for optical losses, a photographic record would be readily obtained.

2.4. Resolution

When the question of resolving power in a channelled system is considered, it is seen that the situation is rather different from that obtaining in the case of most other imaging devices. In most systems, a point source is imaged as a more or less diffuse spot, and the limit of resolution is reached when two such spots are too close together to be distinguished with certainty. In a channelled tube, however, a point source is imaged as a rather sharp spot of approximately the same dimensions as a single channel, this being the size of a picture element in the output image. Thus in general two point sources will not be distinguishable unless they stimulate two separate channels, and image details smaller than one channel diameter will be lost, the brightness of each picture point in the output image depending only on the mean brightness of the corresponding area of the input image.

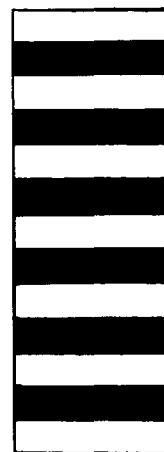
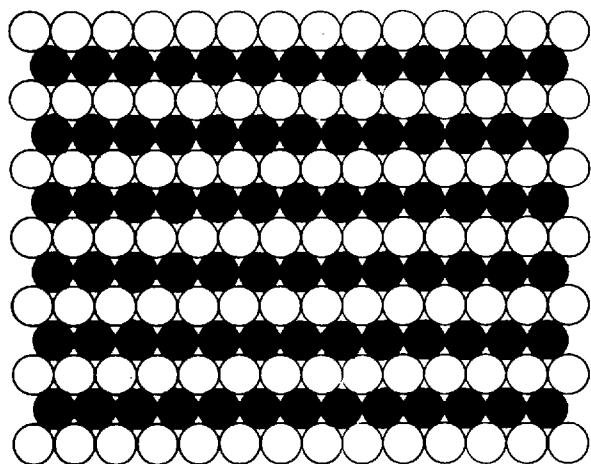
An additional feature of the channelled system is that the picture points will normally be arranged in a geometrical array, and if geometrical figures are imaged, interference between the two patterns may occur, giving a Moiré fringe effect. The importance of this effect will depend on the form of the two patterns, and on their relative size and orientation. This effect is discussed later in more detail.

Cell Form Before proceeding further, it is necessary to consider the cross-sectional form of the channels to be used. As described in Chapter III, the dynode structure finally selected was one in which each cell of a dynode consisted of a short cylinder, its end faces parallel to each other, but at an angle to the axis of the cylinder. This cell form then results in a picture point of elliptical shape, the selected angle of 55° giving a ratio of 1.22 : 1 between the major and minor axes. For reasons of simplicity, however, this discussion will be restricted to the case of circular picture elements. The results may readily be carried over to the case of elliptical picture points, the only change being a variation of 1.2:1 in the resolving

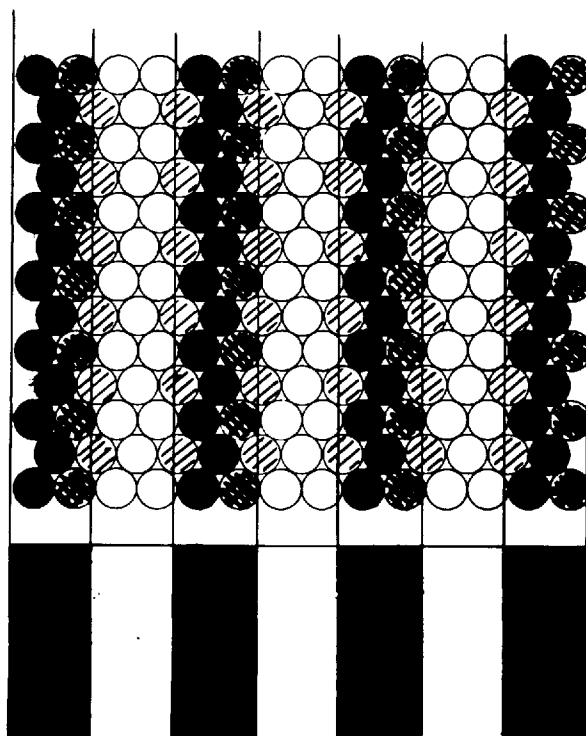
power along directions parallel to the minor and major axes respectively. The channels are best arranged in a two-dimensional version of the hexagonal close packed structure, since this enables the maximum number of channels to be accommodated in a given cross-sectional area; the dead space between the channels occupies only 9% of the total electrode area.

It is convenient to consider the image of a Foucault test pattern, i.e. one consisting of parallel black and white bars of equal width. Fig. I. shows clearly that the limiting resolution of a channelled tube for such a pattern will depend rather critically on the state of alignment between the pattern and the dynode structure. The maximum resolution is obtained when the test bars are accurately aligned with rows of cells in the dynode (Figs. 1a & 25a). For cells d mm. in diameter, the resolution is then $\frac{1}{1.74d}$ lp/mm., since the lines of centres of adjacent rows are separated by $0.87d$ mm. This is a special case, however, since such a pattern can be resolved only if the spacing is exactly correct; slightly coarser or finer patterns result in a "beating" effect of the type mentioned earlier, producing widely spaced Moiré fringes at the output screen (Fig. 25d). Further, in general the alignment will not be perfect, and varying states of misalignment will give different spurious effects. If the pattern is translated laterally by half a channel diameter, the image is completely lost, since electrons from each illuminated bar on the photocathode are then divided equally between two neighbouring rows of cells. If the image is rotated through a small angle, a zig-zag pattern results at the output (Figs. 25b and c). A pattern at the limit of resolution can thus only be resolved if it is of exactly the right spacing and arranged in one of three angular dispositions relative to the dynode, these being at intervals of 120° .

In the general case of random alignment between dynode and test pattern, good resolution is maintained down to $\frac{1}{4d}$ lp/mm. (Fig. 1b), although line patterns down to $1/3d$ lp/mm can be distinguished with difficulty.



a



b

Fig. 1.

It is of interest here to note the improvement in contrast resulting from the use of cells with finite wall thickness. It will be seen from Fig. 1a that the boundaries of cells in adjacent rows overlap slightly, so that when a pattern at the limit of resolution is imaged, those cells in the dark bars of the pattern will receive a small amount of light from the adjacent illuminated bars, if the cell walls are sufficiently thin. As the thickness of the cell walls is increased, however, more and more of this unwanted light will fall upon the wall section and be absorbed, so that the contrast of the final image will be improved.

2.5. Dynamic viewing

When viewing an image with a channelled tube, it is found that the definition and overall appearance of the image are much improved if the tube as a whole is kept in motion in the plane of the image. The improvement is not subjective; it can be photographed (Figs. 26 and 27). It is due to an integrating effect, as channels in varying states of alignment with the details of the image are swept across them. This results not only in improved definition, but also in a more acceptable output image, since the pattern of the picture elements is rendered much less obtrusive, and irregularities in the multiplication process and the phosphor screen are smoothed out. This "dynamic viewing" is possible with the channelled tube because the secondary emission process is extremely rapid; the only lag in the system is that introduced by the output phosphor.

A similar phenomenon is observed with fibre optics, where an image is transferred from point to point by an array of transparent fibres acting as light pipes. Each fibre transmits the light from a single picture element, so that the resolution properties of the array are very similar to those of a channelled tube. Kapany et al⁵⁰ have derived an expression for the improvement in resolution obtainable by

moving both ends of the fibre system in synchronism. Although their analysis is somewhat doubtful, the factor of 2.12 which they quote for the improvement in maximum resolution appears to agree fairly well with experiment, since patterns rather more than twice as fine as in the static limiting case can be resolved (see Chap. VI). A more important point is that the spatial frequency response is now continuous, and the "beating" effect previously mentioned is no longer observed. In addition, patterns are resolved in all states of alignment with the dynode structure, so that a very real increase in the information content of the image is obtained. Fig. 2 gives a qualitative idea of the spatial frequency response in the two cases, Fig. 2a representing static viewing, and 2b dynamic viewing. In Fig. 2a the isolated peak at $\frac{1}{2d}$ lp/mm. corresponds to the limiting resolution; patterns slightly coarser than this are not resolved. In 2b, however, the response is continuous down to better than $\frac{1}{d}$ lp/mm., so that the increase in the useful, continuous, portion of the curve is roughly equivalent to that which would result from an order of magnitude increase in the number of channels; a very valuable gain. In practice the effect might be utilised either by mechanical movement of the whole tube or by synchronously sweeping the input photo electrons across the first dynode and the output electrons across the phosphor. Ideally, the oscillations in the two mutually perpendicular directions should be random in amplitude and frequency, but it seems probable that a simple rotatory motion of the tube would prove quite satisfactory.

(Note: The values for the resolution given in Fig. 2. do not apply to dynodes with circular cells, but to the practical case of dynodes cut at 55° . They are measured in the direction parallel to the major axes of the cells, and are consequently poorer by a factor of 1.22 than in the case of circular dynode cells.)

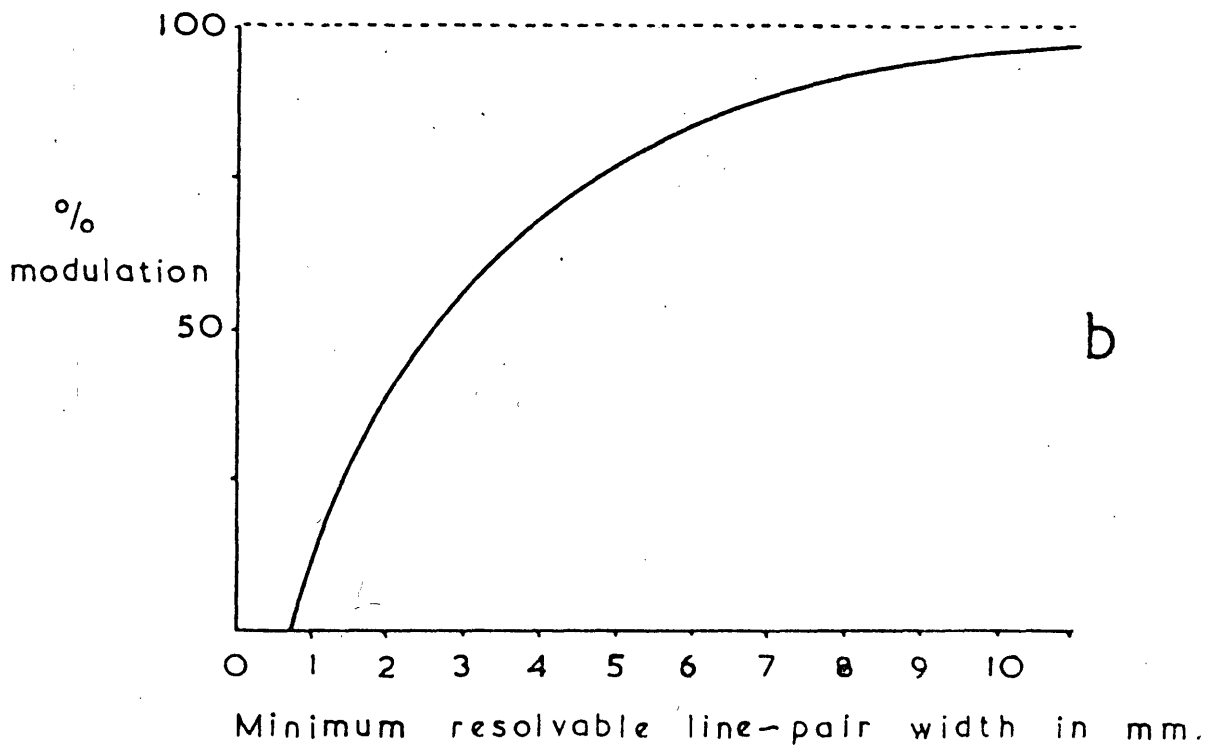
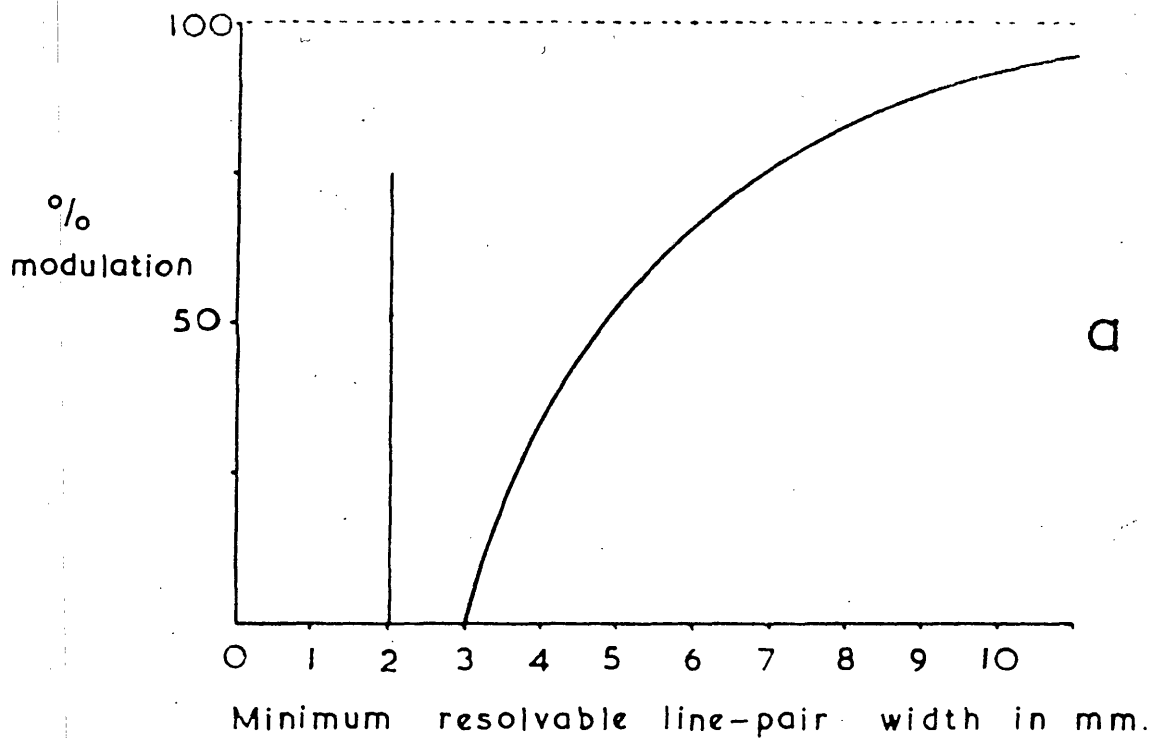


Fig. 2. Qualitative representation of resolution given by ideal tube with 1mm. diameter channels.

a) static viewing

b) dynamic viewing

2.6. Cell size, dynode area and picture quality

Dynodes with cells 1 mm. in diameter are readily constructed, and are found to be extremely strong and rigid. Those with $\frac{1}{2}$ mm. channels are notably less solid, and it seems improbable that the channel size can be reduced below about 0.2 mm. with the present techniques. Even this would present great difficulty, and it is felt that 0.4 mm. represents a more practical figure which could be attained with reasonable ease. This would then represent a limiting resolution of 2.5 lp/mm. in the dynamic case; quite reasonable definition.

An alternative to reducing the channel size lies in an increase in the area of the dynode; with 1 mm. channels, an edge-supported dynode 10 cm. square is probably feasible, giving a total of 10^4 picture points, equivalent to a 100-line square television picture. Although this is considerably below the standard of the B.B.C. transmissions, many television sets in domestic use display pictures of very little higher quality. This area could be still further increased if the dynodes were supported over their entire surface, either by an insulating material deposited on the edge of the cell walls, or by a mica grid structure with apertures a few centimetres across. In this case, the dynode size could probably be increased to something in the region of 25 cm. square, giving $6 \cdot 25 \cdot 10^4$ picture points. With dynodes of this type, a small image could be magnified, either optically or electron-optically, to cover the whole dynode area, and the output image could if necessary be demagnified, with a consequent further brightness gain.

Fig. 3, reproduced from "Television" by Zworykin and Morton, gives an idea of the picture quality given by varying numbers of picture points. Fig. 3a shows an image corresponding to that given by a dynode 7.5 cm. square, with 1 mm. picture points, while Fig. 3c corresponds to that given by a similar dynode 22.5 cm. square. From

a



75² picture elements

b



150² picture elements

c



225² picture elements

d



375² picture elements



e

original

Fig. 3. Relation between Picture Perfection and Number of Picture Elements.

this it may be seen that even 10 cm. dynodes would give a very satisfactory picture, while 25 cm. dynodes would give images acceptable for almost all purposes. The actual resolution, in lp/mm, would be closely similar to that of Fig. 3a, in which the picture points are 0.9 mm square.

Alternatively, dynodes of smaller area and with correspondingly narrower channels might be used to give pictures of equal information content and higher resolution, although it is questionable whether the resolution as such is an important parameter for visual observation.

It is of interest here to note that in a typical newspaper photogravure reproduction, the picture points are approximately 0.4 mm. square. (Those in Fig. 3b are 0.45 mm square.) This is approximately the same as the smallest readily--usable channel diameter, as discussed earlier, so that by a suitable reduction in channel diameter it should be possible to construct tubes capable of giving images of high information content, with resolution comparable to that of the average newspaper photograph (or of Fig. 3b).

Finally it is necessary to point out that apart from the difficulty of constructing and aligning dynodes with channels of very small diameter, a lower limit is set to the usable channel size by more fundamental factors. As the channel diameter is decreased, the maximum permissible spacing between dynodes is reduced in proportion. A certain minimum inter-stage voltage is required for a reasonable secondary emission yield, however, so that the field strength between dynodes is inversely proportional to the channel size. Consequently, field emission will become increasingly important, and will ultimately impose a lower limit on the diameter of the channels.

Chapter III The Choice of an Electrode Structure for a channelled Tube

3.1. Basic Requirements

Once embarked on the construction of a channelled tube, it was necessary to decide on a suitable structure for the multiplying electrodes. Many possible forms may be devised^{51, 52, 53}, e.g. the cells of each dynode may be round, square or polygonal in cross-section, they may be prismatic or conical, and their axes may be at various angles to the plane of the dynode. In selecting one from these many possibilities, four criteria may be stated, which any practical cell form must meet.

1. The structure must be robust, simple to fabricate, and easy to align on assembly in the tube.
2. It must be possible to extract a large proportion of the secondaries produced in each dynode.
3. These electrons, and photo-electrons leaving the cathode, must strike the multiplying surface of the succeeding dynode.
4. As few electrons as possible should be allowed to stray into neighbouring channels, so that contrast is maintained.

Most of the possible geometries are immediately eliminated because they do not fulfil condition 1. . For example, dynodes with conical cells whose axes were not normal to the face of the dynode would be very difficult to construct, and consequently need not be considered. Three structures were selected for preliminary investigation, all being fairly simple to manufacture (Fig. 4). They were a) an "egg-box" type of structure based on the well-known Venetian blind photomultiplier, b) an arrangement in which each dynode consists of an array of short right cylinders, placed side by side, and c) a structure similar to b), but in which the ends of the cylinders are cut at an angle to their axes.

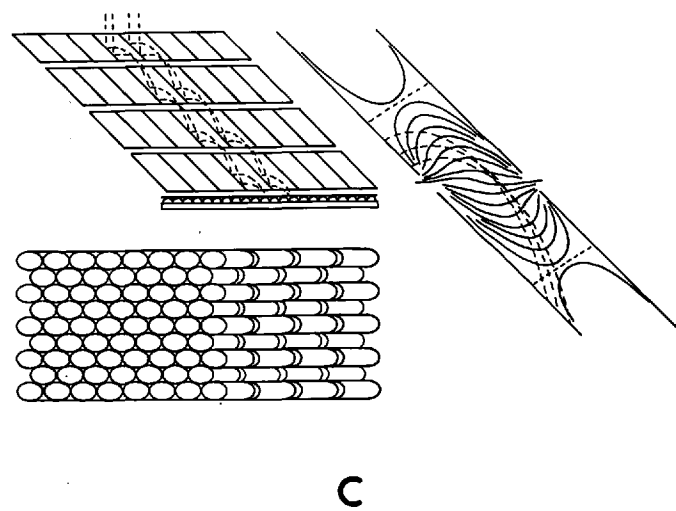
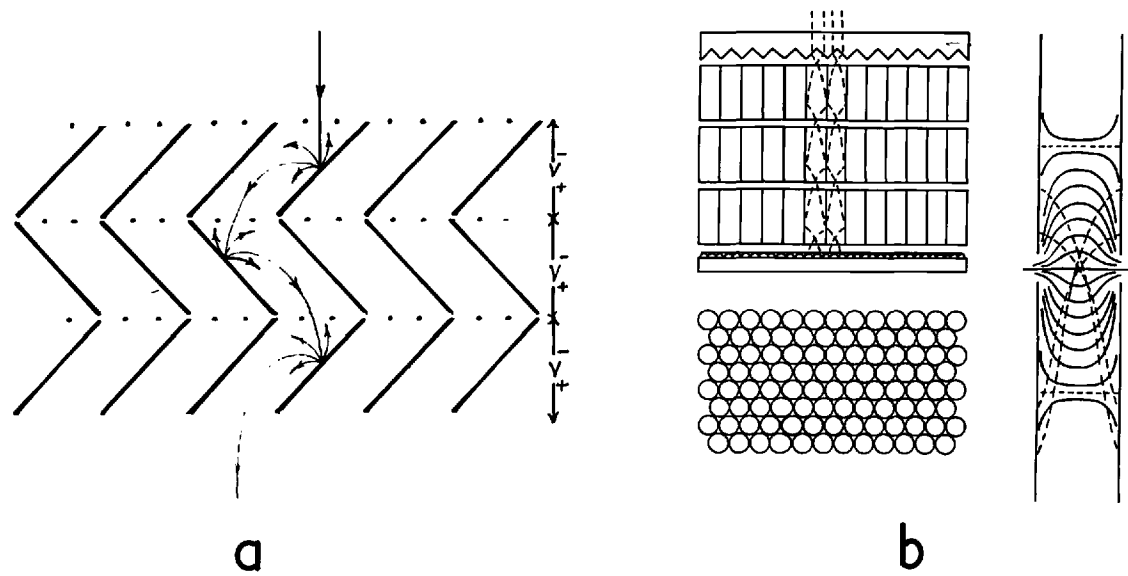


Fig. 4 .

Several possible methods of investigating the field distribution and electron paths were considered, but most proved unsuitable for this application. For instance, the rubber sheet model and the electrolytic tank allow the field to be plotted only in the plane of symmetry of the system. Consequently the trajectories of electrons not originating in this plane, or having a significant velocity component normal to it, cannot be investigated. The resistance network analogue may be extended to three dimensions, but the quantity of data to be reduced then becomes extremely large. Analytical methods may be employed for systems with cylindrical symmetry, but the calculation of the trajectory of an electron originating at the wall of such a system is rather difficult, since the usual approximations do not apply. Finally, relaxation methods may be used; in these an iterative process is used to determine the potential at a network of points in the electrode system, and the electron paths are plotted by a similar process. Again, however, this becomes prohibitively complex for a system without rotational symmetry, unless access to a digital computer is available. Consequently it was felt that the best means of investigating the various systems would be the construction of scaled-up models. The results of experiments with such models are given below.

3.2. The "Egg-Box", or modified Venetian blind structure

Each electrode in a normal Venetian blind photomultiplier (Fig. 4a) consists of an array of parallel slats, set at an angle to the plane of the dynode and coated with some secondary emitting material. Each dynode has a fine wire mesh over the face at which the electrons enter, to prevent penetration of the field from the preceding dynode, which would tend to prevent the removal of secondary electrons. The angle of the slats is comparatively unimportant, and multipliers are currently in production with slats set at angles ranging between 30° and 60° to the plane of the dynode⁵⁴. This structure is readily modified to form

an imaging system by adding to each dynode a second set of slats at right angles to the first, and perpendicular to the plane of the dynode, so that the dynode is divided into an array of rectangular cells. Each cell then corresponds to one stage of a single channel.

A large-scale model was built to represent a single cell of each of two stages in such a structure. The electrodes were made from glass, with a transparent conductive coating of stannous oxide - "Nesa". This coating is applied by spraying the glass with an acid solution of stannic chloride, while maintaining it at the annealing point. The decomposition of the stannic chloride on contact with the hot glass leaves an extremely adherent transparent coating, the electrical **resistivity** of which may be varied at will within wide limits by varying the composition of the spraying solution and the thickness of the layer. In the model under discussion, a thin layer of willemite phosphor was deposited on top of the Nesa coating. This served a dual purpose; it increased the secondary emission coefficient of the surface and also allowed visual observation of the points of impact of electrons. The wire grid was represented by a single wire across the opening of each cell, parallel to the multiplying slats (the most efficient arrangement⁵⁴). Primary electrons were supplied by an electron gun, with magnetic focusing and deflection, firing into the open end of the first cell. A plane fluorescent screen was placed across the exit from the second cell, to show the distribution of electrons leaving the system.

The results obtained were only moderately encouraging. A marked channelling effect was apparent; the electrons stayed well bunched, producing an approximately round patch of fluorescence on both the second dynode and the output screen. The position of these bright areas did not depend noticeably on the electrode potentials, and was affected to a remarkably small extent by varying the point of incidence of the primaries. Unfortunately however, the percentage of the

secondaries extracted was rather low - about 40% with the primary beam incident in the centre of the active surface of the first dynode. This improved slightly as the beam was moved nearer the lower edge of the first dynode, but decreased rapidly as the spot approached the top of the dynode.

It was anticipated that an additional problem with this form of dynode would occur during the assembly of the multiplying stack. It was proposed to manufacture the dynodes by brazing together a number of rectangular tubes, and cutting off slices from the resultant block at a suitable angle. This would produce dynodes having cells of the correct form. During assembly, however, alternate dynodes would have to be turned end for end, to achieve the Venetian blind structure. Unless the cross-section of the dynodes could be made extremely uniform, accurate alignment would then be very difficult.

In consequence of these disadvantages, it was decided that dynodes of this type were not the most suitable, and as other geometrical configurations appeared more promising, work on the "egg-box" structure was abandoned.

3.3. The Symmetrical Cylindrical Structure

A dynode in a system of this type consists of an array of short right cylinders, the cells of adjacent dynodes being accurately aligned with each other. Such dynodes are readily fabricated by assembling a number of cylindrical tubes in the desired arrangement, and brazing them together. The block of tubes is then cut into slices to yield dynodes which naturally line up with perfect accuracy.

As is seen in Fig. 4b, two cells in consecutive dynodes may be considered to form a two-tube electron lens, but with the difference that here the electrons originate at the wall of the system, instead of entering almost parallel with its axis, as is usually the case. We might thus expect a rather poor electron image of the source to be

formed on the opposite wall of the second cell. Secondaries released here would then be imaged in the next cell and so on. For this process to continue satisfactorily, the secondaries must be liberated in a region of extracting field, so that they contribute to the multiplication of the signal. The length of the cylinders is consequently of primary importance, since if they are too short, electrons will tend to be accelerated right through the cell without striking the wall, after the manner of a Cockroft-Walton accelerator. If on the other hand they are too long, the extracting field will be weak, and secondaries will be lost.

Several large scale models were built to study the electron paths in an electrode system of this type. These were basically very simple (Fig. 5a), consisting of a length of 25 mm. Pyrex glass tube, with a pumping stem and side arms for the activation of a photocathode. The multiplying electrodes consisted of short conducting cylinders of Nesa on the inner wall of the tube. These were formed by drawing 1 mm. wide bands of colloidal graphite - "Aquadag" - around the inside wall of the tube at appropriate intervals. After the Nesa-spraying process, the Aquadag was removed with hot sodium hydroxide solution, to leave a series of conducting cylinders with insulating gaps between them. Contact to the Nesa was made from outside the tube by platinum tape seals through the glass wall. A thin layer of willemite phosphor was then applied to the inside of the tube, to act as a secondary emitter and to indicate where electrons were landing. Primary electrons were supplied by a photocathode formed on the wall of the tube at one end. During the activation of this cathode, antimony, which would have produced leakage across the insulating gaps, and caesium, which rapidly attacks Nesa, were excluded from the rest of the tube by a cylindrical nickel shield, coated with Aquadag, which readily absorbs caesium. After activation of the cathode, this shield was withdrawn to the far end of the tube, where it remained out of the way. During

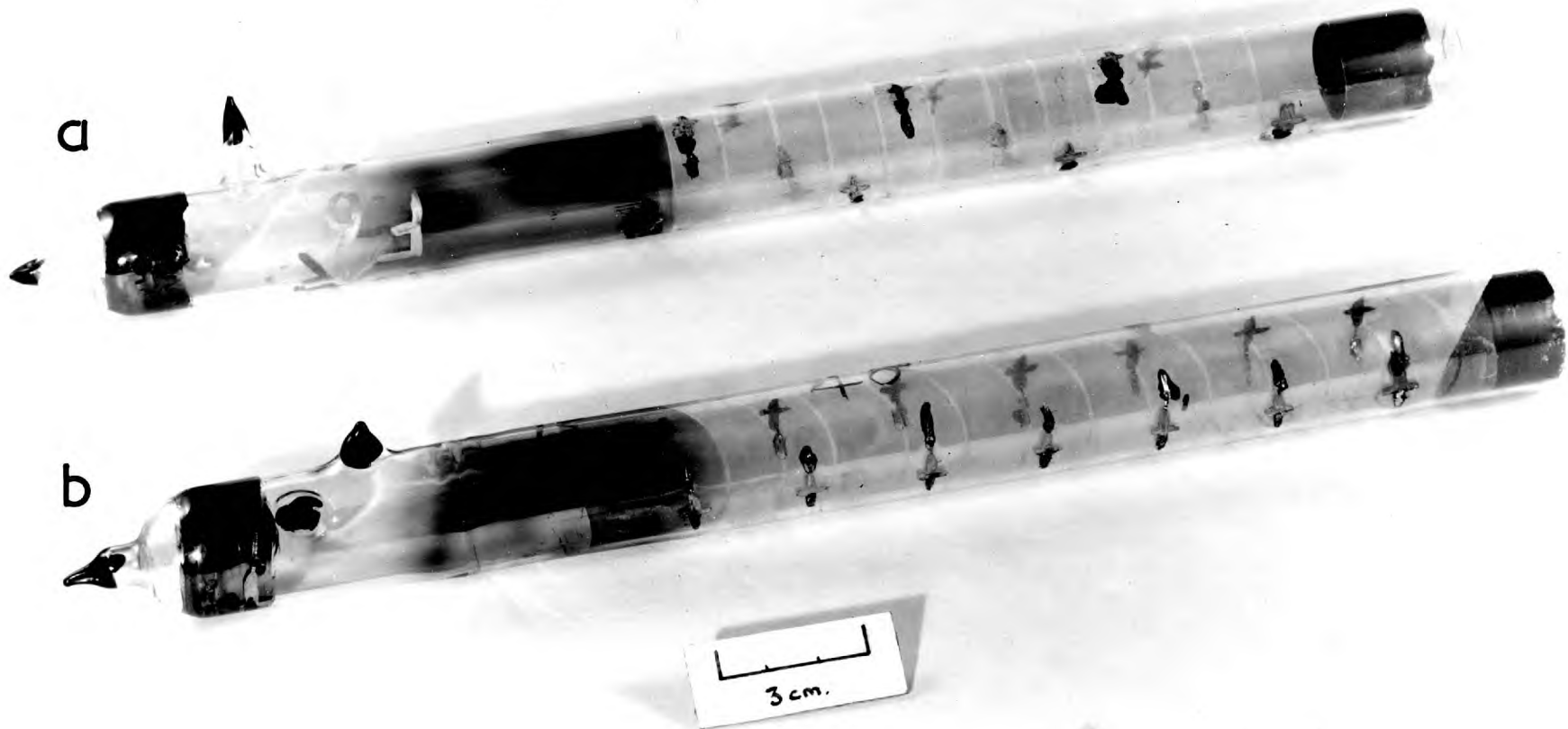


Fig. 5.

processing, the photo-current was collected by an auxiliary anode of platinum paint fired into the tube wall.

Electrons could then be generated at any desired point on the photocathode, by projecting on to it a small light spot. The photo electrons then entered the multiplying system, producing secondaries. The points where electrons struck the wall were indicated by fluorescence in the willemite layer. The effect of different electrode lengths could be studied by connecting together two, three or more of the Nesa cylinders to form a single electrode.

Once again, the results were disappointing. Previous workers⁵² had suggested that electrons in such a system did in fact follow the desired paths, but no signs were found of this, either in the tubes described here, in others of a different type described later, or even on re-examination of the original tubes in which such trajectories were reported to have been observed. In tubes with the Nesa wall electrodes, the best results were obtained when the electrodes were so connected as to give a ratio of length to diameter of two and a quarter to one. Even then, however, the desired electron trajectories were found only in the first stage. The secondaries from each stage landed farther and farther along the wall of the following cell. With the ratio of length to diameter quoted above and with photo-electrons originating at a point approximately one quarter of a dynode length from the lower edge of the cathode, some were seen to land a little over halfway along the first dynode, while the remainder went directly to the **second** stage. The secondaries from the first dynode were then incident almost two-thirds of the way down the second, and the secondaries originating here spread out along the whole of the length of the third dynode, with some going direct to the collector electrode beyond this. As the light spot on the photocathode was moved nearer the edge of the first dynode, the photo-electrons landed nearer the top of the first stage. The secondaries, however, then by-passed the second stage completely, and went directly to the lower half of the third stage. If the point of origin of the

photo-electrons were moved further from the first dynode, these then went direct to the second and third stages, spreading along the whole length of the latter.

With longer electrodes, generally similar results were obtained, except that the fluorescence was less bright, indicating that a smaller fraction of the secondary electrons was being utilised. The electrons still did not take up a stable progression, as would be indicated by their landing at corresponding points on each dynode in turn. If shorter electrodes were used, the photo-electrons tended completely to miss the first and even the second stage, unless the light spot was very near the edge of the cathode. In this case, the secondaries from the first dynode went on to skip several stages, as one would expect with short cylinders.

Later, several tubes of a different type were built, to confirm these results. These tubes, similar in structure to that shown in Fig. 6., had tubular glass electrodes, each representing a single cell of one dynode. These electrodes were coated with Nesa and willemite as before, and mounted on a large multi-pin pinch, which was drop-sealed into the vacuum envelope. The end electrode was slit along one side, and primary electrons entered the system through this slit, from an electron gun in a side arm. The electron beam could thus be deflected along the wall of the cell, and the trajectories of the secondary electrons could be investigated for various points of incidence of the primaries. Several such tubes were made, with electrodes of different lengths, and the results obtained agreed closely with those already described. The spacing of the electrodes did not exert any significant effect on the electron paths, up to a separation of about 0.15 times the length of the electrodes, the maximum investigated.

It thus appeared that a system of this type was unsuitable for a channelled multiplier. Some consideration was given to the possibility

of using a system in which each channel would consist of a single long tube of high resistance: possibly glass tubing coated inside with high-resistance Nesa. Electrons would then travel from side to side of the channel, acquiring enough energy from the longitudinal field at each transit to liberate secondaries on impact with the tube wall. Multiplication would thus occur, as in the electrostatic electron multiplier devised by Farnsworth⁵⁵. This similarly consisted of a glass cylinder coated inside with material of low conductivity and reasonable secondary emission yield, but contained in addition an axial wire electrode maintained at collector potential to assist in obtaining the desired electron trajectories. It does not appear to have been successful, possibly owing to distortion of the electrostatic field when current was drawn from the tube. In the present case, the scheme was not pursued very far, as it was considered that the difficulty of producing a uniform high-resistance layer inside a large number of channels of sufficiently small diameter was too great to be overcome with the facilities available. This situation would be altered should hollow fibres of some suitable semi-conducting material become readily available.

Before leaving this section, it is of interest to note that as early as 1937, Kubetski⁵⁶ had constructed an electrostatic electron multiplier with dynodes in the form of right cylinders. This was designed as an improvement on the Farnsworth multiplier mentioned above. In spite of the use of an axial wire electrode at high potential to improve the electron paths the tube had to be worked with increasing voltage steps between the stages, which would obviously help to prevent the effects described here.

As an alternative to the use of a non-uniform potential distribution, Kubetski suggested the use of electrodes forming a series of truncated cones, of successively decreasing diameter and angle, but no actual tube of this type appears to have been constructed.

3.4. The Asymmetrical Cylindrical Structure

This was the last possibility to be studied and the form finally adopted. In a dynode of this form (Fig. 4c), each cell consists of a short cylinder with its ends cut parallel to each other, but at an acute angle to the longitudinal axis. The effect of this asymmetry is to introduce a lateral component into the field between adjacent dynodes, so that the electron is deflected to the wall of the cell. Thus electrons will now always strike the same side of the channel, instead of crossing from side to side, as in the symmetrical form.

Again, the exact proportions of the cell are crucial. If the ratio of length to diameter is too great, the extracting field will be weakened, and gain will be lost. If this ratio is too small, the electrons will tend to miss out stages, so that the gain will again fall. In this case, too, the tendency of electrons to stray into adjoining channels will be increased. The angle of the ends of the cylinders is equally important. If this is too acute, although the electron trajectories will be very strongly controlled, the field from one dynode will penetrate too far into the cells of the succeeding dynode, and tend to prevent the escape of secondaries. If the angle is too great, the electrons will not be deflected sufficiently strongly, and will tend to miss a stage. The tendency to stray into the wrong channel will also be increased.

It was thus necessary to investigate the effect of varying both these parameters over a fairly wide range, and once more this was done by means of scaled-up models. Initially, these were of the same form as the tubes first described in connection with the right cylindrical electrode form. The Nesa cylinders were now formed with their ends at an angle (Fig. 5b), by using a template to guide the pen with which the Aquadag rings were drawn. The template consisted of a piece of metal tubing which was an easy sliding fit in the tube body, and with its end cut at the requisite angle. A slot was cut along the side of this tube,

and a guide pin engaging in the slot ensured that all the rings were parallel. In each tube, the Nesa cylinders were made short in comparison with their diameter, so that electrodes of different lengths could again be simulated by strapping together varying numbers of these cylinders. Thus, by constructing a series of tubes, each having its Nesa rings at a different angle, it was possible to investigate a wide range of the two parameters with only a few tubes.

The first tube of this type had the planes of the ends of the electrodes at 45° to their axes. The electron trajectories observed were extremely encouraging: a series of spots could be obtained equidistantly spaced along the electrode system, showing that a stable progression could be obtained over at least 4 stages of multiplication⁵². Unfortunately, however, the secondary electron extraction efficiency appeared to be rather low. It was impossible to make a direct determination of the secondary emission yield of the Nesa-willemite surface, and the percentage extraction had to be estimated indirectly. The cathode was illuminated with a fixed spot of light, and the potential between this and the first dynode was held constant, so that the input current to the first dynode remained steady. The other dynodes were strapped together as a collector, and their potential was increased in stages, the current collected being measured at each step. When this current was plotted against the collector potential, it rose asymptotically toward a limiting value. If this value is then assumed to correspond to perfect collection of the secondary electrons, the extraction efficiency of the dynodes at their normal working potential can be estimated. The estimate is rather uncertain, since it is difficult to know what fraction, if any, of the primary electrons are attracted straight through the multiplying dynode to the collector, as its voltage is raised. Later work suggested that this fraction is not large, so that the extraction efficiency determined thus is probably correct to within a few per cent. The optimum electron

paths were obtained with dynodes having a slant length of 2.2 times their internal diameter, and the extraction efficiency, estimated as described above, was approximately 45%. To raise this figure to 90%, it was necessary to raise the potential difference between the first dynode and the collector to three times that between the cathode and the dynode.

The promising results obtained with this tube encouraged further work on systems of this type. It was clear that dynodes with an angle of less than 45° between the axis and the planes of the end faces would have a prohibitively low extraction efficiency, so a series of tubes covering the range of angles from 45° to 60° was constructed. As the angle is increased, the percentage of the secondary electrons which can be extracted increases (e.g. at 50° , 50% of the secondaries are extracted), but the electrons are less and less strongly deflected. When an angle of 60° is reached, the electrons are no longer sufficiently well controlled, and spread out along the tube, so that some of them begin to miss a stage. The maximum angle at which adequate control can be maintained was found to be 55° , the corresponding optimum value for the ratio of slant length to internal diameter is 2:1.

The optimum value of this ratio was determined more exactly and the electron trajectories confirmed in a further series of tubes (Fig. 6). These were similar to those already described in connection with the study of the symmetrical cylindrical structure, having a series of Nesa-coated glass electrodes thinly covered inside with willemite. These were supported inside a glass vacuum envelope, and electrons were injected into the system through a longitudinal slit in the side of the first dynode, from an electron gun in a side arm. (The end electrode shown in Fig. 6 acts merely as a field-shaping electrode). Tubes were made with electrodes of varying lengths, and it was confirmed that the optimum ratio of length to diameter was in fact 2:1, a variation of 5% either way resulting in less satisfactory electron



Fig . 6 .

paths. Reducing the length gave a slight increase in extraction efficiency, but the electron paths were less well controlled, the electrons striking nearer and nearer the bottom of each dynode in turn.

The use of an electron gun enabled the secondary emission coefficient of the surface, and consequently the extraction efficiency, to be determined with reasonable accuracy. The efficiency found - 60% - was in good agreement with the value estimated from tubes of the earlier type when the cathode was illuminated with a large light spot at a point corresponding to the area of maximum brightness on the other dynodes.

Thus, as a result of these investigations, the asymmetrical cylindrical structure was established as the most satisfactory, the optimum cell form being one with the slant length of the cell equal to twice the internal diameter, and with the end faces at 55° to the longitudinal axis.

A large scale model with Sb-Cs secondary emitting surfaces was constructed, and a moderate gain of 20 in four stages was obtained at 450 v/stage.

Chapter IV Possible Secondary Emitting Materials

4.1.

Once the electrode structure had been selected, the remaining major decision was the choice of a suitable secondary emitting material. Since only about 60% of the secondaries produced are utilised, a secondary emission yield of at least 5 is desirable, to give a reasonable gain per stage. Moreover, the complexity of the multiplying system renders impracticable the evaporation of materials on to the active surfaces of the dynodes after assembly, so that any evaporation which may be necessary must be performed first. This raises the problem of protecting the evaporated films from attack by atmospheric moisture, and oxidation. It is consequently desirable that the material selected should be resistant to atmospheric attack, at least for brief exposures.

Consideration of these factors and the properties of the various known secondary emitters led to the selection of three surfaces for further study. These were:

- 1) Antimony - caesium. Secondary emission yields of 10 are obtainable with this material, and the surface is reputedly easy to prepare. Antimony is fairly resistant to atmospheric exposure, although the resulting yields after processing are usually not so high as with freshly-evaporated antimony layers. The caesium, however, being extremely reactive, must be admitted after the tube is evacuated, and must then diffuse throughout the dynode structure.
- 2) Potassium Chloride - KCl. Gains of 5, for transmission secondary emission, are achieved in thin film multipliers²². It was felt, and later work justified the view, that much higher yields could be obtained for multiplication at the front surface.
- 3) Magnesium Oxide MgO. Values of δ up to 18 at 1 keV⁵⁷ are quoted for thin films of this material, and the surface is reported to be fairly

easy to prepare. Various workers differ as to its resistance to contamination.

4.2. Antimony - Caesium

This is the best-known and most commonly used surface, in this country at least. Tests were made on the secondary emission yield obtainable using pre-evaporated antimony films, which were then sealed into tubes, and activated. Trials were made both with the silver chloride sealing process, and with ordinary glass-sealing techniques, but in both cases the yield was disappointingly low. It appeared that the heating suffered by the antimony films during the sealing process had deleterious effects in spite of efforts to keep the surface cool, and to maintain an inert atmosphere inside the envelope. This effect, of course, was particularly marked when the envelope was sealed with a glass blowing torch, as it proved impossible completely to exclude the combustion products of the torch, which are rather corrosive. In an effort to regenerate the antimony surface before caesiation, an R.F. discharge in hydrogen was excited in the tube, but this had little apparent effect. The results obtained were rather variable, but it was found that a secondary emission yield of 5 could be obtained at 500 eV primary energy. This is just about acceptable, so that this surface might be satisfactory. There still remain the problems of distributing caesium uniformly throughout the multiplying structure, and of preventing field emission and breakdown, since these phenomena are much more pronounced in the presence of caesium.

4.3. Potassium Chloride KCl

This material has been used in transmission secondary emission tubes, but has not found application in ordinary electron multipliers. It suffers from one serious defect, in that prolonged electron bombardment lowers its yield, liberating free chlorine atoms and generating "colour centres" in the material, which act as electron traps. The

chlorine so produced tends to attack the photocathode with a corresponding loss of sensitivity. This is not a serious defect in transmission intensifiers, with their large volume and long path between dynode and cathode, but can be important in the much more compact channelled intensifier. Figures for the loss in yield with bombardment quoted by different workers vary, but Todkill²³ of this department has measured a fall in gain to one-half the original value after bombardment with a charge density of 25 millicoulomb/cm².

KCl has one great advantage in that, after evaporation, no further activation is required: the layer is ready for immediate use. It is however extremely susceptible to attack by atmospheric moisture. After a few minutes exposure to damp air, the normally clear film becomes milky in appearance, and the secondary emission yield falls drastically.

According to Nakhodkin and Romanovsky⁵⁸, the optimum yield at moderate bombarding voltages is obtained with a layer 1,000 Å thick, so investigations were confined to layers of this thickness.

A tube was constructed to check on the yield obtainable, (Fig. 7.) Primary electrons were supplied by a magnetically focused and deflected electron gun at one end of the tube. The test surface was deposited on an aluminised glass plate, which was supported by a spring mechanism on a stainless steel annulus held in position by three tungsten pins set in the tube wall. The collector was a wall electrode of platinum paint entirely surrounding the test surface except for the aperture through which the anode cylinder of the gun projected. This slight extension of the anode cylinder prevented primaries from going directly to the collector. The tube was closed by a plane end window sealed in position with silver chloride. The potassium chloride evaporator was introduced from a side arm at this end of the tube. Initially, the tube was sealed on the pump with the test surface facing the evaporator. After evacuation the gun was activated, and a layer of KCl 1000 Å thick was deposited on the test plate. The thickness was monitored by measuring the amplitude

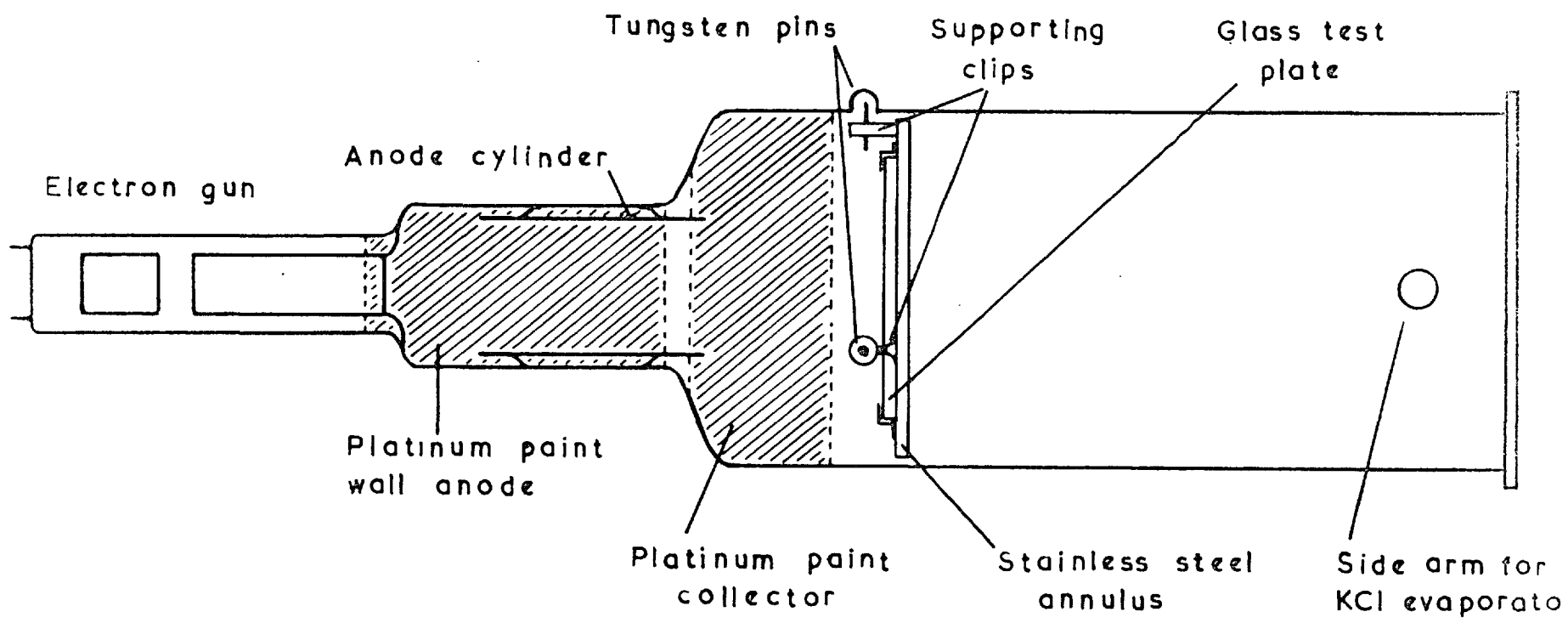


Fig. 7.

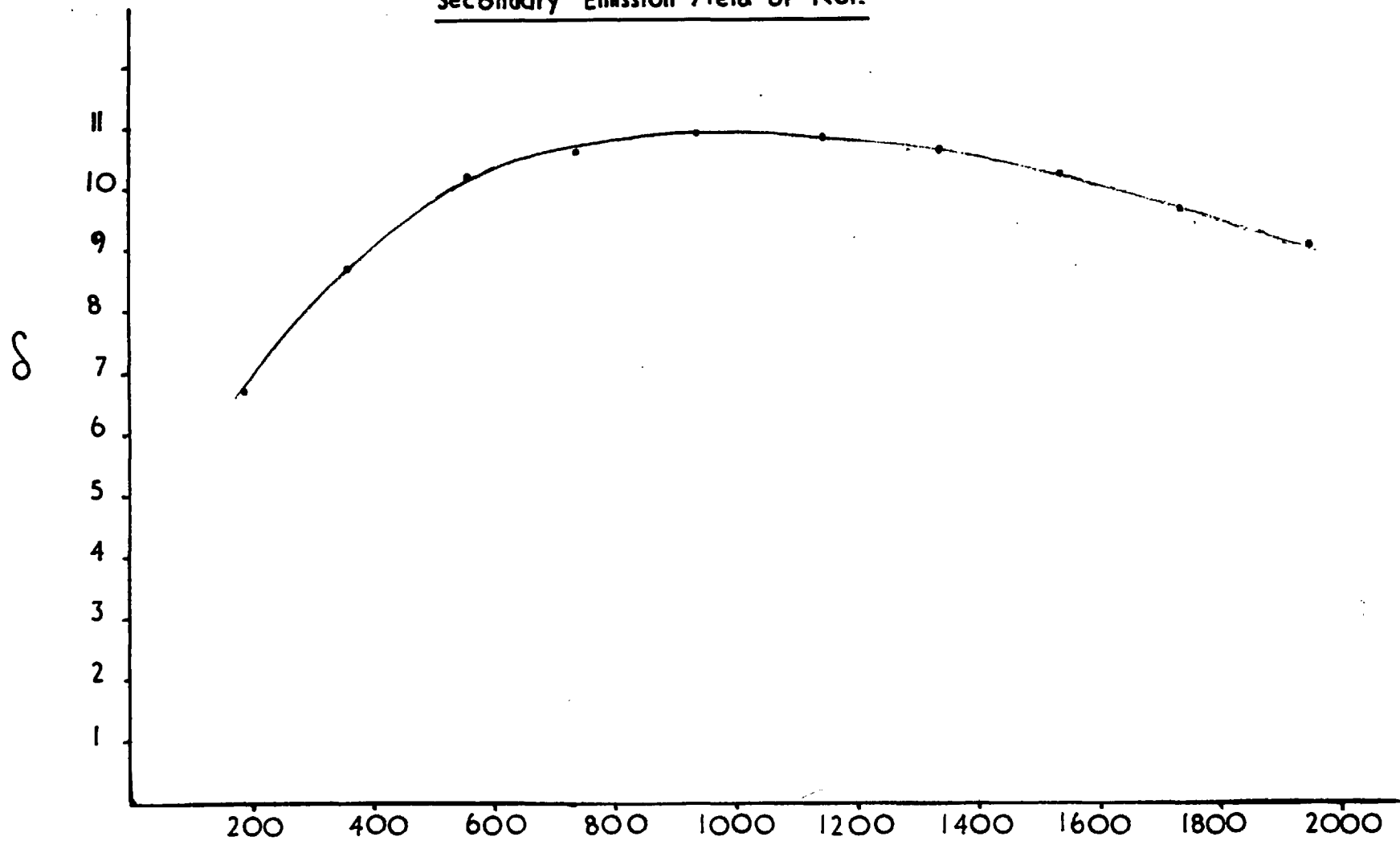
of a light beam reflected at the aluminium surface, this going through a series of maxima and minima as the thickness changed. For green light, allowing for the refractive index of the salt, the first minimum corresponds approximately to the desired thickness of $1,000 \text{ \AA}$. After this evaporation, the side arm was removed, and the tube sealed off the pump. The glass plate was then tapped free of the retaining catches and turned over to face the gun so that measurements could be made.

The results obtained are shown in Fig. 8, and were extremely encouraging. The maximum yield was approximately 11, at 1 keV primary energy, while at 300 eV, the yield was still as high as 8. It thus appeared that apart from its decay properties, KCl was an almost ideal material for use in the channelled tube.

4.4. Magnesium Oxide - MgO

This material is widely used in electron multipliers, particularly in the United States. In this application, the dynodes are generally made from an alloy of silver with about 3% of magnesium, and the active layer is generated by a baking process. During this, the magnesium diffuses to the surface, where it is oxidised by air, carbon dioxide or water vapour. Values of δ of 12 at 600 eV primary energy, and 9.5 at 300 eV, are obtained by this method^{59, 60}. Unfortunately, the mechanical properties of the silver-magnesium alloy prevent its being drawn into tubing, such as is required in the construction of dynodes for a channelled tube, and attention was turned to the use of thin evaporated films of magnesium, with subsequent oxidation. Such films have been studied by Whetten and Lapovsky⁵⁷, who report a maximum yield of 18 at 1200 eV primary energy, falling to 10 at 300 eV, for an MgO layer 800 \AA thick. They observed a marked deterioration in the yield on exposure to CO_2 or water vapour, the latter irreversibly reducing the yield by 50%. Their films were oxidised at 550°C . at a

Secondary Emission Yield of KCl.



Primary Energy (eV)

Fig.8.

pressure of 50-100 μ of oxygen. Other workers have successfully used a wide range of oxidising conditions, and have noted less sensitivity to attack by water and CO_2 .

It was felt that the best method would be to evaporate the magnesium layer in a demountable system, assemble the tube in a dry inert atmosphere, maintained inside a glove box, and seal it with a silver chloride seal, still inside the glove box. The layer would then be oxidised after the tube had been pumped and baked, so that the oxide layer would not be exposed at any time to contamination by water vapour or carbon dioxide. Several experimental tubes were then made by this method, to examine the yields given by various oxidation procedures. In each case however it was found impossible to maintain a sufficiently inert atmosphere in the dry box, and the magnesium layer rapidly oxidised during the assembly process. In fact the metal layer was observed to oxidise while still in the demountable pumping system, at an indicated pressure of 10^{-5} mm. of mercury. Surfaces were prepared by baking in pure oxygen at various temperatures, in dry air and in carbon dioxide. Oxidation temperatures above 450°C were not studied at first, since the use of an Ag Cl seal as envisaged in the construction of the final intensifier tubes would preclude baking at higher temperatures. (The melting point of Ag Cl is 455°C).

A surface oxidised in CO_2 at 420°C for 20 minutes gave a yield of slightly over 5 at 950 eV, the highest primary energy used, and of 3.9 at 560 eV. The CO_2 was generated by heating very pure Ca CO_3 in a side arm. It was later discovered⁶¹ that traces of carbon monoxide, which are very difficult to eliminate, are known to have deleterious effects on the oxide surface, and the use of CO_2 was discontinued.

Oxidation in air or oxygen at 450°C and a pressure of 50 mm. of mercury yielded very similar results, and it was clear that either the oxidation temperature was too low or the premature oxidation described above was adversely affecting the yield. Baking at higher

temperatures in tubes sealed by glass-blowing gave only a slight improvement, but in this case it proved extremely difficult to exclude the combustion products of the heating torch from the tube, and these would obviously tend to attack the magnesium surface. In spite of this, a few image tubes were made by this method with some success. In the meantime, to examine the yields obtainable from a completely uncontaminated surface a tube was constructed in which the magnesium layer was deposited after evacuation and then oxidised.

The tube was very similar in design to that used in the determination of δ for KCl, as shown in Fig. 7, the main difference being that the test plate was mounted in a pivoted frame and could be rotated magnetically to face either the magnesium evaporator or the electron gun. The glass plate was made conductive with a coating of a proprietary platinising material, a small circular area being left clear so that the magnesium thickness could be monitored. After the tube had been pumped and baked to a pressure of less than 5.10^{-7} mm. a thin (3% optical transmission) layer of magnesium was deposited on the plate. It was noticeable that this layer was much cleaner and more reflective than those deposited at the pressures attainable in the demountable pumping system (about 5.10^{-6} mm.) The accommodation coefficient of the metal appeared to be much higher, also, and geometrical shadows were observed. After oxidation of the magnesium, the plate was turned to face the electron gun, and the secondary emission yield was measured with the tube still on the pump, so that the effect of various treatments on the yield of the MgO layer could be observed.

Temperatures below 450°C were found inadequate for oxidation, but further baking for 20 minutes at 480°C in 50 mm. of dry oxygen gave good results (Fig. 9). A yield of 4.75 was observed with a primary energy of 300eV, rising to a maximum of 7.6 at 950eV. Exposure to dry air for 15 minutes had no measurable effect on the yield, but 15 minutes exposure to air saturated with water vapour at room temperature reduced

Secondary Emission Yield of Magnesium Oxide.

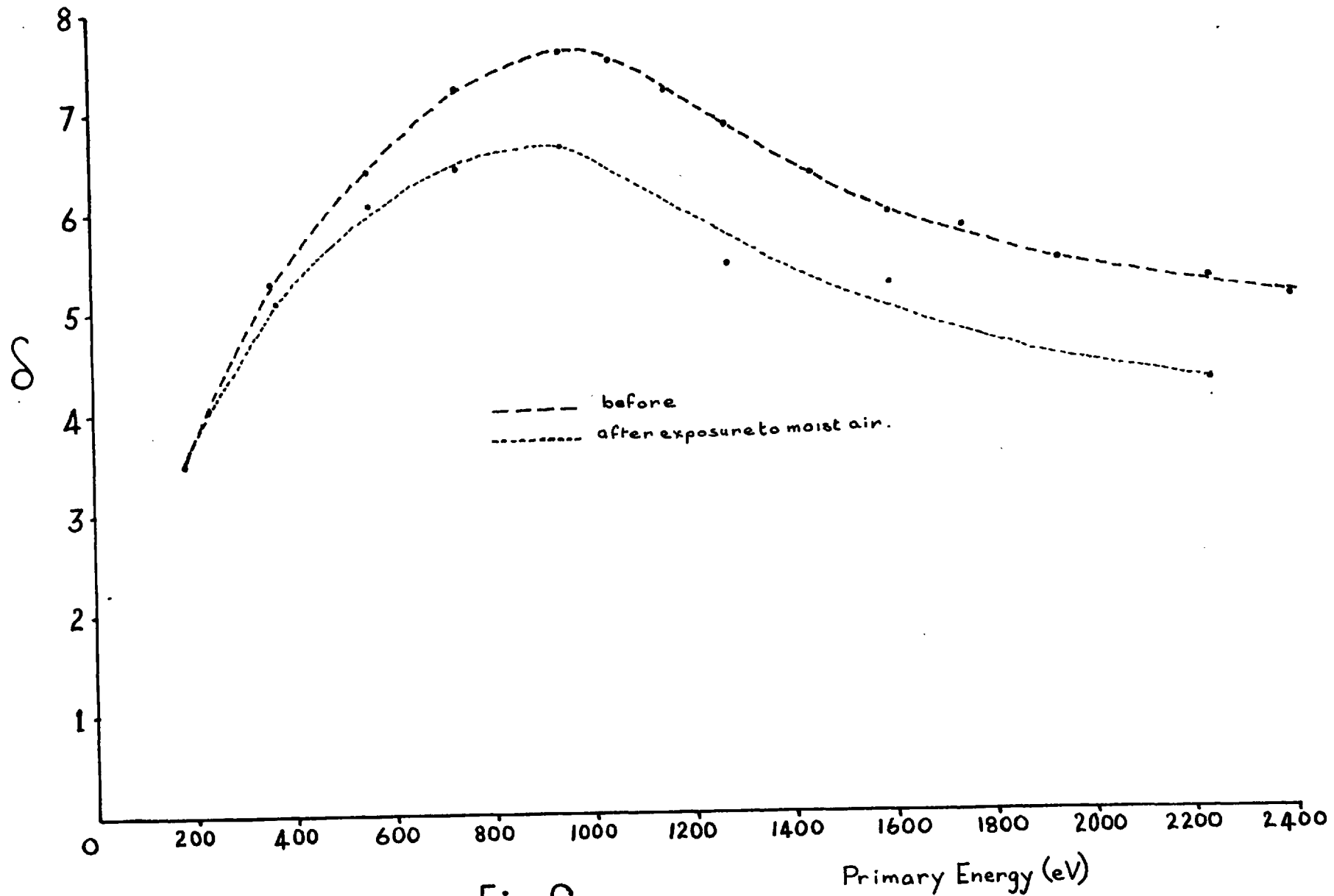


Fig.9.

Primary Energy (eV)

the maximum yield to 6.6 at 950 eV. The yield was not restored by baking, and an attempt at reoxidation caused a further fall, to 5.5 at 950 eV. Caesiation of the surface increased the yield to a new maximum of 9 at 950 eV. It was thus clear that higher oxidation temperatures were required than could be obtained in tubes closed with a silver chloride seal, and furthermore that exposure of the oxidised surface to dry air had remarkably little effect on the yield. Consequently, most of the intensifiers using MgO secondary emitting layers (Chapter V) had surfaces oxidised before the assembly of the tube.

The figures obtained for the secondary emission yield of MgO are lower than those given by some other workers, although they agree quite closely with the results of Arntz and Van Vliet⁶². These low values of δ may possibly have been due to the use of too thin a layer of magnesium, but they are in any case sufficiently high to make the MgO surface a possible secondary emitter for use in a channelled tube. The surface must be oxidised before assembly, and protected from moist air, but against these disadvantages must be set the important fact that such layers are largely free from decay effects under prolonged electron bombardment.

4.5. Summary

On the basis of these results, KCl appeared to be the best material for use in a channelled tube, owing to its simplicity of preparation and the consistently high yields obtainable. The only precaution necessary is to protect the evaporated film from attack by moist air, and this is necessary also in the case of MgO, which in addition requires a more complicated activation procedure, and was found to give somewhat unpredictable results when used in intensifiers. In spite of this, however, it was felt to be worth while proceeding with the use of MgO surfaces, owing to the absence of decay effects and the resulting attack

on the photo-surface.

Antimony-caesium surfaces were considered completely unsuitable, owing to the low yields obtained, and the difficulties attaching to the use of caesium in a closely spaced electrode system; in intensifiers in which the electrode structure was flooded with caesium, considerable field emission was found to occur at low interstage voltages, and caesium attack on the phosphor sometimes occurred. (See Chapter VI).

Recent results obtained by other workers suggest that other materials might prove satisfactory. For example BaO , BaF_2 , MgF_2 and porous layers of KCl ,⁶³ produced by evaporation in an inert atmosphere at a pressure of a few mm. of mercury, all give good secondary emission yields and appear to be resistant to contamination by dry air. It was felt, however, that with the limited effort available it was impracticable to study such a wide range of materials, and so attention was concentrated on the three already discussed. For future tubes it is felt that a study of other secondary emitters might prove very valuable, porous KCl layers in particular being claimed to give very high yields, of 50 or more, although presumably the decay effects observed in homogeneous layers are still present.

Chapter V Construction of Image Tubes

5.1. Dynode fabrication

In view of the workshop facilities available, it was felt that the dynodes could best be constructed from thin-walled nickel tubing. This is commercially available as "cathode tubing", used in the manufacture of indirectly heated thermionic cathodes for valves and cathode ray tubes. It is available in a large range of diameters, in any desired length and with wall thicknesses down to .002 in. The material - O-type nickel - is 99.5% nickel, the remainder consisting chiefly of carbon, with small controlled additions of manganese, silicon and magnesium.

Two main types of dynode were made. Initially, the dynodes consisted entirely of multiplying cells, with no specific provision for mounting. These were fixed to stainless steel supporting plates by Inconel clips engaging in recesses in the surface of the dynode. However, it was found almost impossible to align successive dynodes with this arrangement, and later tubes used dynodes having integral mounting points. As the fabrication of both types of dynode is essentially the same, it will suffice to describe the manufacture of the later, more successful, type.

The tubing was purchased in six-inch lengths, with the thinnest wall available - .002 in. The ends of each tube were plugged with "gun cement" (a mixture of alumina and potassium silicate solution), and the tubes were assembled in a mild steel brazing jig (Fig. 10) to form a rectangular block some 18 mm x 24 mm in cross section. At each corner of the array a rectangular nickel bar approximately 4 mm square was incorporated, which ultimately formed a support for the dynodes. Sheets of mica were interposed between the nickel tubes and the walls of the jig, to eliminate any possibility of brazing the jig and tubes together. The top plate of the jig was then bolted firmly down, and

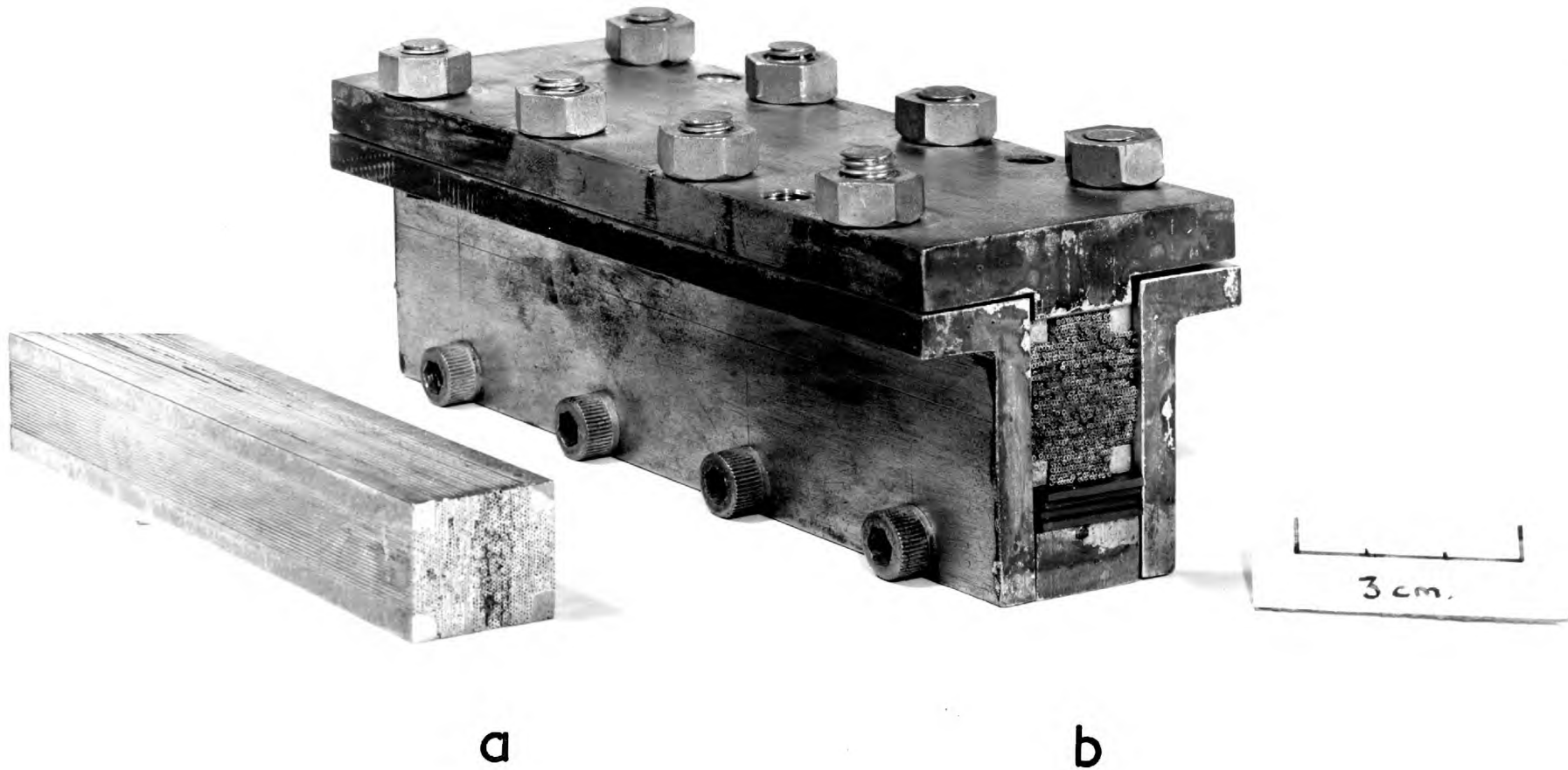


Fig . 10.

the whole assembly was placed on one end in a vacuum stove or reducing furnace. Pieces of silver-copper eutectic alloy (m.p. 772°C) were placed on top of the tubes, and the temperature was raised to 850°C . for half an hour. Under these conditions, the brazing alloy readily wetted the nickel, and so penetrated the interstices of the assembly, while the plugs of gun cement prevented the tubes from being blocked by the brazing metal. The process was repeated until a sufficient quantity - about 75 gm. - of the alloy had been administered.

After brazing, the block of tubes was removed from the jig (Fig. 10a) and cut into slices of the appropriate thickness and angle. This process was performed by a high-speed cut-off wheel, operating at a speed of 14,000 surface ft. per minute. The use of such a wheel only a few hundredths of an inch thick enabled accurate cuts to be made through heavy sections with a minimum of distortion and burr. Initially, considerable difficulty was experienced in the cutting process, as the only available means of attaining such speeds was a small pneumatic motor, primarily intended to drive low-powered hand tools. This was mounted (Fig. 11) in the head stock of a disused milling machine to give the necessary rigidity, and the workpiece was held in a small machine vice, clamped to the bed of the miller, so that motion in all directions could be obtained. The motor was powered by dried cylinder nitrogen at 100 lb/sq. in., containing a fine oil mist for lubrication. Rubber bonded aluminium oxide wheels, 4 in. in diameter and ranging in thickness from .020 in. to .030 in. were used, at a spindle speed of 14,000 r.p.m. At first wheels .020 in. thick proved satisfactory but as soon as traces of wear developed in the front bearing of the motor, wheel breakages became frequent. Replacement of the bearing provided a temporary cure or none at all, and it was found necessary to use thicker wheels to avoid breakage. Wheels .030 in. thick proved sufficiently robust, but the greater thickness severely reduced the cutting speed, and increased the amount of burr formed. Finally .025 in.

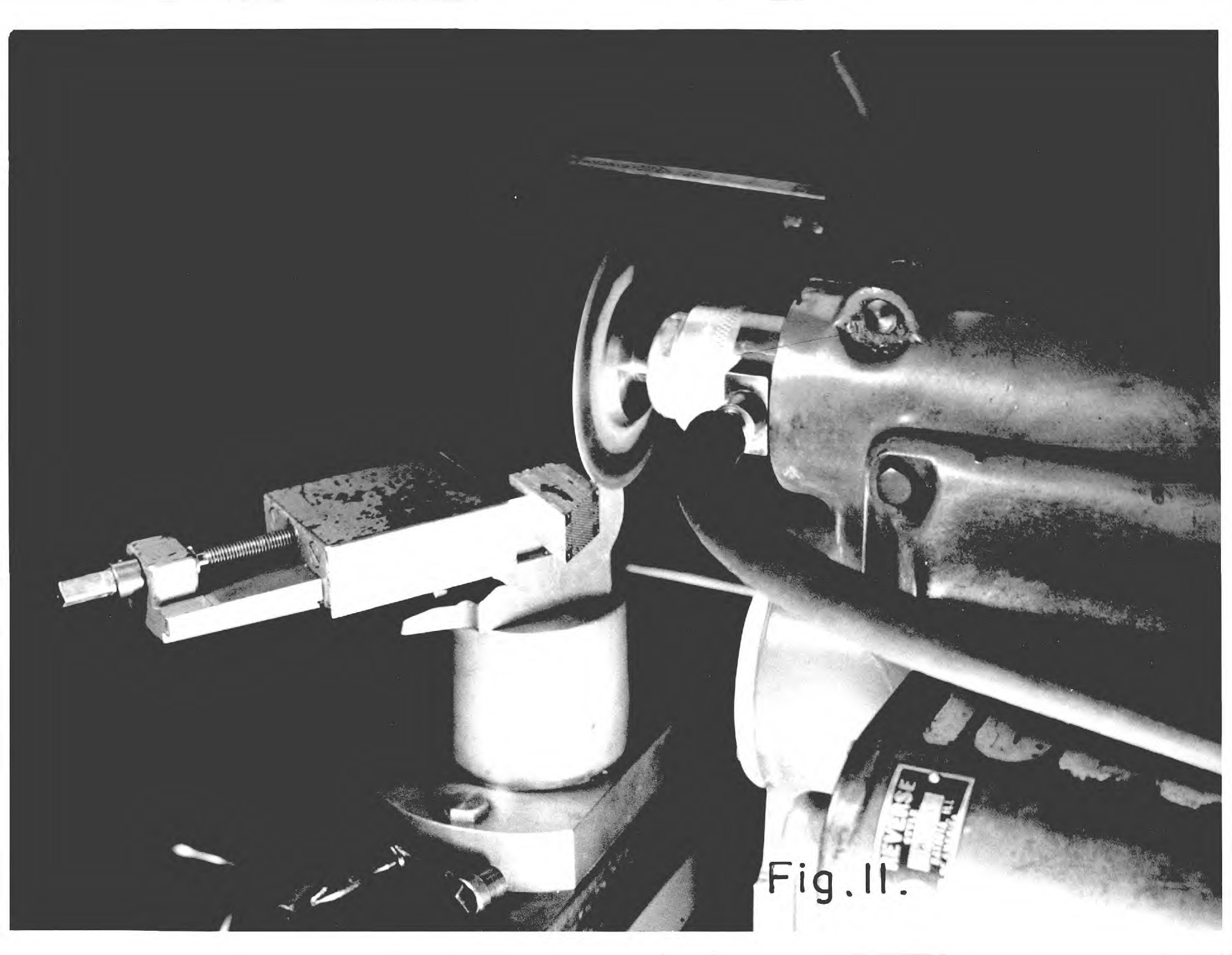


Fig. 11.

wheels were found to provide a suitable compromise, cutting much faster than the .030 in. wheels, but having sufficient rigidity to prevent breakage. Burring of the work was reduced as much as possible by the use of soft grade wheels of very fine grit size: 320 grit was found very suitable, and 280 grit almost as good. The wheel was cooled and lubricated by a continuous jet of very dilute soluble oil played on the edge of the wheel where it left the work. One part of soluble oil in 80 of water was found satisfactory, the oil being required only to prevent rusting of the machine.

Once the cutting process was perfected it was found possible to cut sections from the block of tubes previously described, with considerable accuracy. For instance, slices .060 in. thick could be cut which were uniform in thickness across their surface to within .001 in., although the section was 29 mm. across and 18 mm. deep, and had to be cut in three successive passes. Thin sections tended to bow slightly, however, and a grinding process was found desirable after cutting to produce flat slices of exactly the right thickness. At first this was done by hand on a glass plate, with carborundum powder and water, but later a surface grinder was used, as this gave much flatter dynodes. A considerable amount of burr remained after grinding, and in the case of dynodes with 1 mm. cells this was removed by hand with a small five-sided broach. The faces of the dynode were then lightly rubbed down on very fine emery cloth, to remove any irregularities.

Next the nickel rectangles at the corners of the dynodes were drilled to take the $3/32$ in. ceramic rods which supported the electrode assembly in the tube. This was done in a special jig (Fig. 12a) to ensure the necessary accuracy. After the burr produced by this operation was removed, the dynodes intended to form one complete multiplying stack were lined up together by means of fine drills passed through several channels, and the $3/32$ in. holes were reamed with a parallel reamer, to ensure accurate assembly. Finally, the completed dynodes

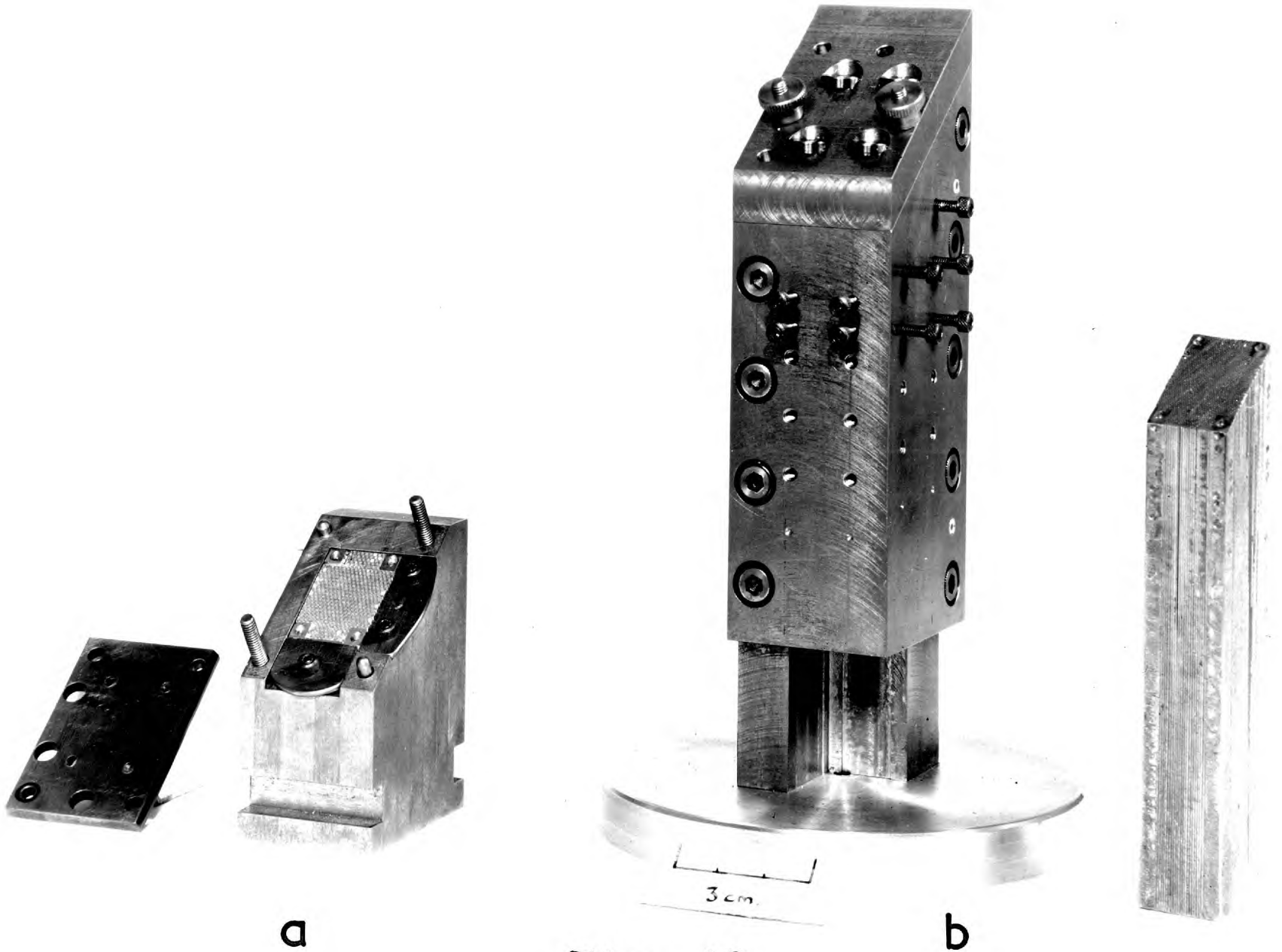


Fig . 12 .

were degreased and lightly etched in warm dilute HCl, to remove surface roughnesses which might promote field emission.

It was eventually decided that this drilling procedure was not sufficiently accurate, and the dynodes for later tubes were drilled in the block before cutting. A special jig (Fig. 12b) was used. Owing to drill wander, only a few dynodes could be drilled at a time; these were then sliced off and the block drilled a little deeper, to provide several more dynodes. As before, all the dynodes for one tube were finally reamed together to give easy accurate alignment. This process, when properly carried out, gave almost perfect alignment.

After cleaning the dynodes, nickel tapes were spot welded to them, in shallow recesses filed in the faces of the solid rectangles at their corners. These served to make contact to the dynodes after assembly, and according to the type of tube under construction, were either left free for spot welding to lead wires in the tube or were terminated in small Inconel tags, drilled to be a tight push fit over 1 mm. tungsten pins sealed through the tube wall. Fig. 16 c (page 77) shows several completed dynodes.

5.2. Preparation of Secondary Emitting Surfaces

Before deposition of the secondary emitter the dynodes were degreased and vacuum stoved at 700°C .

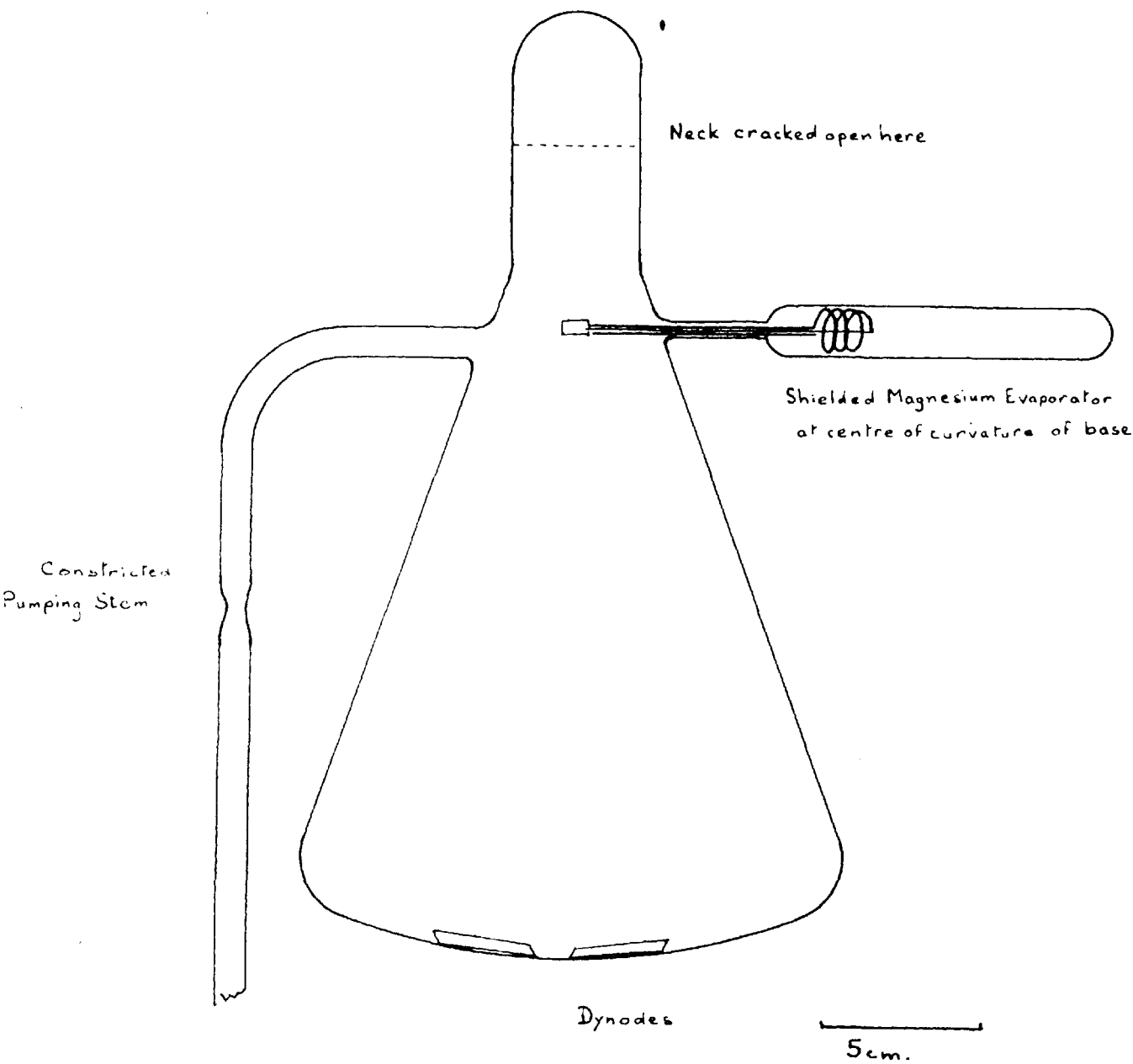
Two secondary emitting surfaces were successfully used: magnesium oxide and potassium chloride. MgO was used in the first successful tubes, but involved a lengthy activation process, and gave rather low, unpredictable yields. Furthermore, if it became necessary to reclaim the dynodes for further use, an acid rinse and prolonged vacuum stoving were necessary to clean them satisfactorily. In contrast, KCl layers were simple to prepare, gave more consistent yields, and were readily removed, if necessary, by boiling the dynodes in distilled water.

5.2.1. MgO Surfaces

As described in Chapter IV, a few early MgO tubes used pre-evaporated magnesium layers, which were oxidised inside the tube. The high temperatures found necessary for satisfactory activation then precluded the closing of the tube by a silver chloride seal, as originally intended, and conventional glass-working methods had to be used. It was then extremely difficult to prevent attack on the magnesium surface by the combustion products of the glass-working flame, in spite of all efforts to maintain a cool inert atmosphere inside the tube, and the resulting yields were generally low and variable. With pre-oxidised layers, however, the tube could be closed by a silver chloride seal, so that the problem of preventing attack on the surface was much eased. Consequently, all the later MgO tubes used pre-oxidised layers.

Activation of the secondary emitting surfaces was performed in a special chamber, shown diagrammatically in Fig. 13. This was constructed from a Buchner conical flask, a very thick-walled vessel originally intended for vacuum filtration. The neck was domed over, and a side arm was sealed on to it to contain an evaporator loaded with magnesium ribbon. The bottom of the flask was tooled to a spherical form, the centre of curvature being at the point occupied by the magnesium evaporator when in the operating position. The whole apparatus was supported and pumped by means of a wide pumping stem sealed to the side of the chamber.

To use this, the neck was cracked open, and the dynodes arranged on the bottom of the chamber as in Fig. 13. The top was then resealed, and the apparatus was sealed on to an all-glass pumping system. The chamber could then be pumped and baked to give a very low pressure of less than 5.10^{-7} mm. and the dynodes themselves could be outgassed by eddy current heating them to a dull red with a work coil held beneath the flask. When a pressure of 5.10^{-7} mm. was attained, the magnesium



Sealed-on Processing Chamber
for Magnesium Oxide Surfaces

Fig. 13.

evaporator was introduced, and a layer of magnesium, estimated at about 400\AA thick, was deposited on the dynodes. A very clean metal layer of high reflectivity was obtained by evaporating at this pressure. Monitoring the thickness proved rather difficult. This was done by measuring the optical transmission through the bottom of the flask, but even with very clean surfaces the accommodation coefficient of magnesium is lower than that of most other metals, so that the walls of the flask also received a coating of magnesium, in spite of careful shielding of the evaporator.

After the deposition of the magnesium layer, the evaporator was withdrawn and the side arm sealed off. The liquid nitrogen in the cold trap was replaced with liquid oxygen, and dry oxygen was admitted to the system to a pressure of 50 mm. of mercury. The chamber was baked to 520°C , and held there for thirty minutes, to ensure complete oxidation, then the oxygen was pumped away and the system cooled down. Finally the chamber was filled with dry nitrogen or forming gas (10% hydrogen, 90% nitrogen) and sealed off until the dynodes were required. To remove the dynodes, the neck of the chamber was cracked with a hot glass point, and the flask was placed bodily in the glove box. This was then thoroughly flushed with dry air before opening the flask and removing the dynodes for assembly of the tube.

5.2.2. Potassium Chloride Surfaces

KCl surfaces also were formed in a demountable bell-jar, but in this case a much more easily-operated one. The system is shown in Fig. 14. The evaporating chamber was a cylindrical glass bell-jar, with a wide pumping stem sealed to its dome. This stem passed through a 15 mm. glass vacuum stopcock and terminated in a standard B 24 ground joint. In this was inserted a demountable pumping line, which at the other end fitted into a similar socket on a small bell-jar sealed to the face plate of the normal pumping system by means of a Neoprene

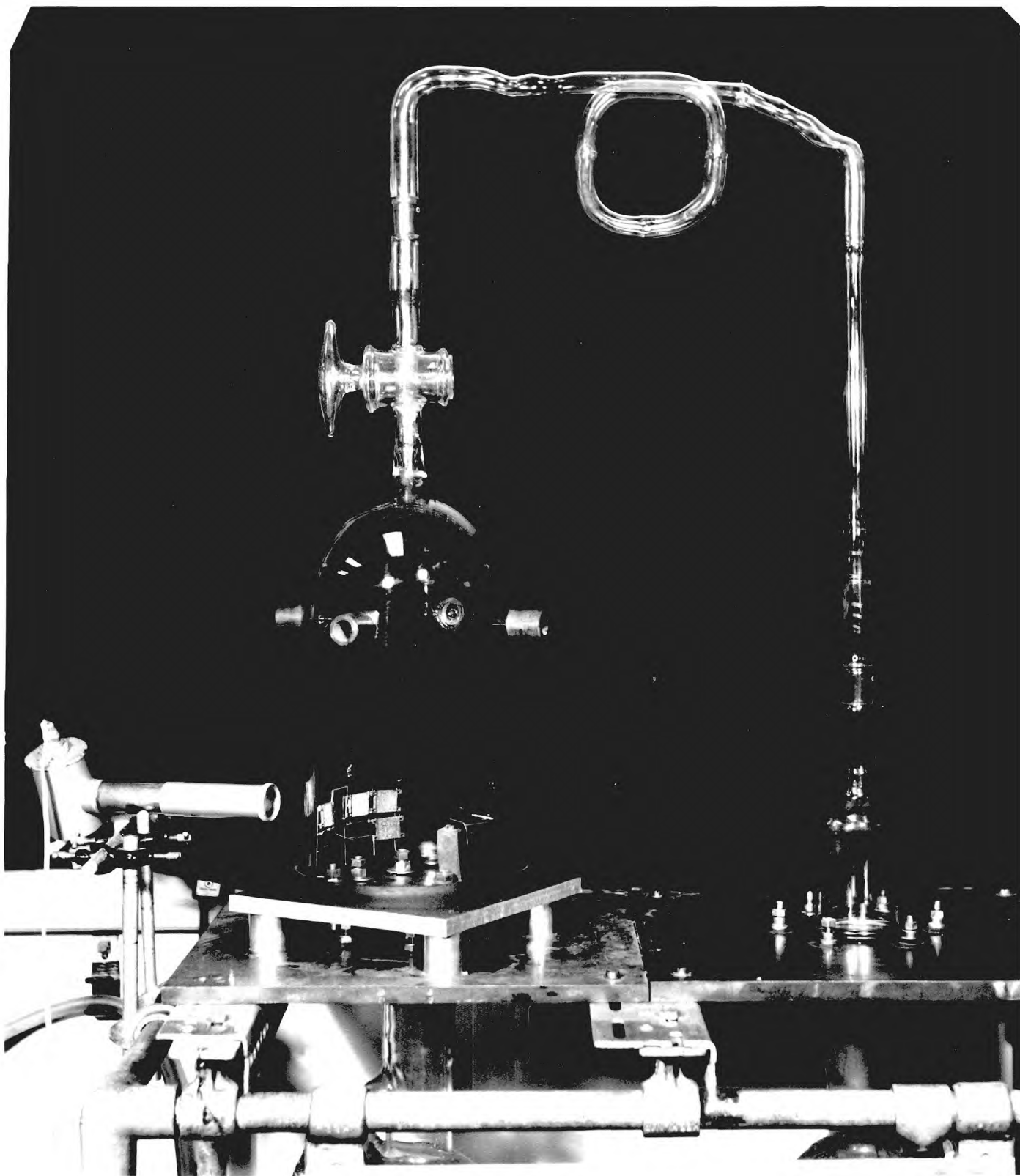


Fig. 14.

O-ring. The base-plate of the evaporating chamber consisted of a 10 in. square Duralumin plate $\frac{1}{2}$ in. thick, through which passed five brass terminals, vacuum sealed with Neoprene washers, and the seal between the bell-jar and base-plate was made by means of an L-section Neoprene gasket.

Evaporation of the KCl was carried out from a small molybdenum boat, firing horizontally across the chamber. The KCl charge was retained in this by bending the sides of the boat slightly inwards, and a nickel shield surrounding the evaporator prevented KCl from reaching the chamber wall behind the evaporator. The dynodes were supported on a nickel wire frame, forming an arc of a circle centred on the evaporator. This frame was so arranged that the dynodes were turned a few degrees away from the normal to the evaporator's line of fire, to ensure that KCl was deposited along the whole of the inside wall of each cell. The thickness of the evaporated layer was monitored by measuring the transmission of light through a thin soda glass plate supported in the same frame as the dynodes. In some cases, reflected light was used, but setting up the system was easier for transmission. As described in Chapter IV, during evaporation the transmission (or reflection) goes through a series of maxima and minima, according as the layer is an odd or even number of quarter-wavelengths thick. Light was supplied by a 240 V. pigmy bulb, run from a stabilised current supply, and was received by a selenium barrier layer cell (not shown in Fig. 14) with a response peaking at $5,700\text{\AA}$. The system was extremely stable: the output of the photo cell was constant to within 0.1%. The output of the cell was measured on a moving coil galvanometer, and since the amplitude of the modulation is only a few per cent in transmission, the larger part of the standing current was cancelled by a dry cell and rheostat connected in parallel with the photo cell, so that the most sensitive range of the galvanometer could be used. For transmission, the first extremum observed is a maximum, since the refractive index

of KCl is less than that of glass. When allowance is made for the angle of incidence of the KCl on the cell walls, and the refractive index of KCl, it is found that the optimum thickness of $1,000\text{\AA}$ ⁵⁸ on the cell walls of the dynode corresponds to a point approximately midway between this maximum and the succeeding minimum. By this method, the progress of the evaporation could be accurately controlled.

To use the system, the various vacuum seals were connected up and the bell-jar evacuated to an indicated pressure of 4.10^{-6} mm. of mercury. The KCl layer was then deposited and the stopcock closed. The pumps were stopped, and the pump system let down to air. Next the pumping stem was dismantled at the two ground joints and the entire evaporating chamber, with its base plate, was transferred to the glove box where it could be opened to the very dry atmosphere maintained inside, to permit the removal of the dynodes.

5.3. Assembly of Tubes

The image tubes constructed may be divided into two main types, although variations occurred within each group. The difference lies essentially in the fact that in the earlier, rather crude tubes, no attempt was made to exclude caesium from the multiplying system. As a result of observations made on these tubes, it became clear that the presence of caesium in the dynode structure was a serious disadvantage, and the second type of tube was devised in an attempt to prevent caesium from reaching the dynodes. The components of a tube of this second type are shown in Fig. 16, many of the components being identical with those used in tubes of the earlier design.

5.3.1. Early image tubes

In the first type of tube (Fig. 15) the electrode assembly was based on a rectangular stainless steel plate, which also served as a supporting frame for the fluorescent screen. This consisted of a

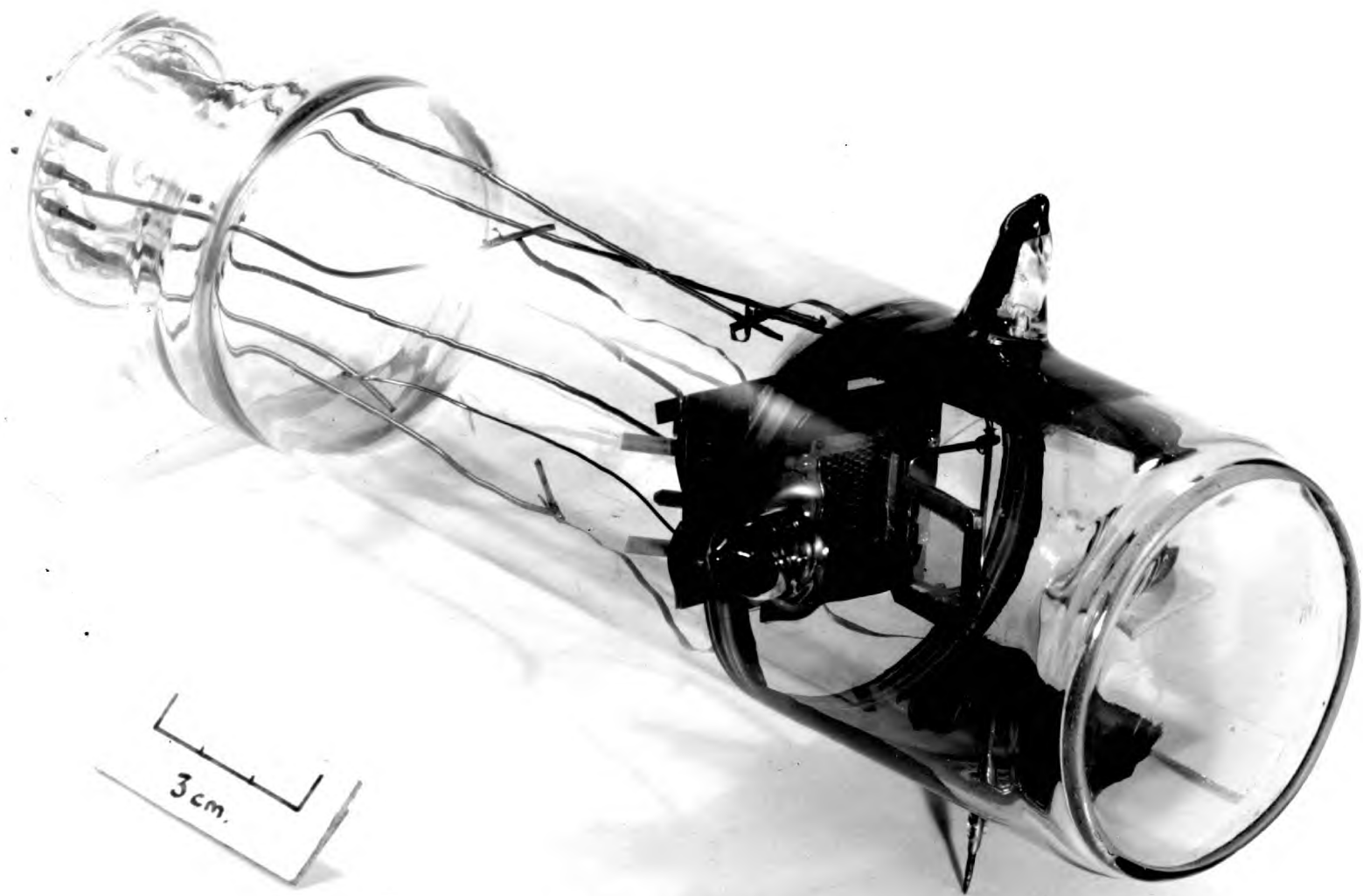


Fig . 15 .

0.7 mgr/cm² layer of willemitite with an aluminium backing, deposited on a rectangular glass plate, which was held in its frame by strips of Inconel spot-welded to the stainless steel. These strips were extended laterally outward from the plate, to support the electrode assembly in the tube. At the opposite end of the electrode system, a similar stainless steel plate supported the photocathode. This was formed on a rectangular soda glass plate, held in a nickel frame which was hinged to the stainless steel plate. For activation, the cathode plate was swung back at right angles to its normal position (Fig. 15) to face the antimony evaporator, introduced from a side arm. The cathode was caesiated in this position, and then swung back into the normal operating position after the tube was sealed off. Four steatite rods, fused at one end to form a "head", and ground at the other to a blunt point to facilitate assembly (Fig. 16f) were passed through holes in the stainless steel plates and through the holes at the corners of the dynodes, (or in their supporting plates), so holding the entire assembly in alignment. The rods were held in position by small "Spire nuts" (Fig. 16h). These are commercially-available spring clips which can be pushed along a rod in one direction, but are prevented from moving the other way by small teeth which bite into the surface of the rod. These were pushed firmly home over the pointed ends of the ceramic rods, their natural springiness ensuring the rigidity of the assembly, and then the excess length of the rods was snapped off. The dynodes were insulated from each other and from the photocathode by mica spacers approximately .005 in. thick, (Fig. 16d) and from the phosphor screen by tubular glass spacers 2.5 mm. long, cut at an angle of 55° (Fig. 16g). Contact was made to all the dynodes by means of nickel tapes spot-welded to their surfaces.

After assembly, the dynode system was inserted into the envelope. This consisted simply of a cylindrical Kodial glass body about 9 in. long and 60 mm. in diameter with a flat window sealed in at one end

and a large 15-pin pinch at the other. 1 mm. nickel wires were spot-welded to the pinch before drop sealing this in place. After the drop sealing process the envelope was leak tested, and then cut open near the pinch, for the insertion of the electrodes. The electrode structure was secured in the envelope by the four Inconel strips spot-welded to the phosphor supporting plate. These were spot welded with extension tongs inside the glove box to four of the nickel wires already mounted on the pinch. The nickel tape leads from the other electrodes were then welded in turn to the rest of the nickel wire leads, and the two halves of the body were reunited.

Resealing of the envelope was performed outside the glove box, either by means of a silver chloride seal or, more commonly, by glass-blowing. During this process, the tube was continuously flushed with forming gas, which entered via the pumping stem and left by a special side arm added for the purpose, in an effort to prevent attack on the multiplying surfaces. The gas was first dried and cooled by passing it through a phosphorus pentoxide drying tower and then through a copper worm immersed in liquid nitrogen.

Tubes of this type worked moderately well, and the first reasonable electron gain recorded was obtained in such a tube, (see Chapter VI). The design suffered from several disadvantages, however. The spot-welding process inside the glove box was a complicated procedure, since the tongs were rather large and unmanageable in the limited space available. The fluorescent screen could not be viewed normally, but only at an inconvenient angle through the side of the tube; the sealing process almost certainly resulted in some reduction in the yield of the multiplying surfaces, and the whole structure was saturated with caesium during the activation of the photocathode. The presence of caesium on the multiplying surfaces probably increased the secondary emission yields obtainable, but considerable field emission was observed at low voltages, and serious caesium attack on the phosphor occurred in some tubes. In an

attempt to remedy these defects, the second type of image tube was evolved.

5.3.2. An improved design of channelled intensifier

The components of a 4-stage tube of this type are shown in Fig. 16, and the envelope in Fig. 17. Fig. 18b shows a diagram of the assembled electrode structure. The basis of the electrode system in these tubes was the photocathode shelf (Fig. 16a). This consisted of a stainless steel disc 55 mm. in diameter, and .050 in. thick. A rectangular aperture 26 mm. x 18 mm. was cut in this, slightly off centre to allow for the angle of the electrode system, and a recess .040 in. deep and rather larger than the hole was milled around its edge, to act as a supporting ledge for the glass photocathode plate (Fig. 16b). A springy skirt of stainless steel .006 in. thick was spot-welded around the circumference of the disc, and slightly spun out so as to be a tight fit in the tooled down portion of the envelope. (Fig. 17 shows a cathode shelf in position in the envelope, for prepumping.) The shelf was held in position in the tube by three Inconel spring clips spot-welded to its upper surface, which engaged with three 1 mm. diameter tungsten pins accurately positioned in the tube wall. One of these pins was extended through the wall to form an external contact for the photocathode, while the other two were left blind to reduce the risk of leakage.

The photocathode plate itself was made from soda glass, of such a size as to be an easy fit in the recess in the photocathode shelf while completely covering the rectangular hole. Platinum paste around its edges ensured good electrical contact between the shelf and the photocathode surface and the plate was held in position by two fine Inconel springs bearing lightly on its surface. In later tubes of this type the springs were replaced by a spring loaded magnetic catch, which proved much simpler to operate when reversing the cathode.

As before, the fluorescent screen was deposited on a rectangular

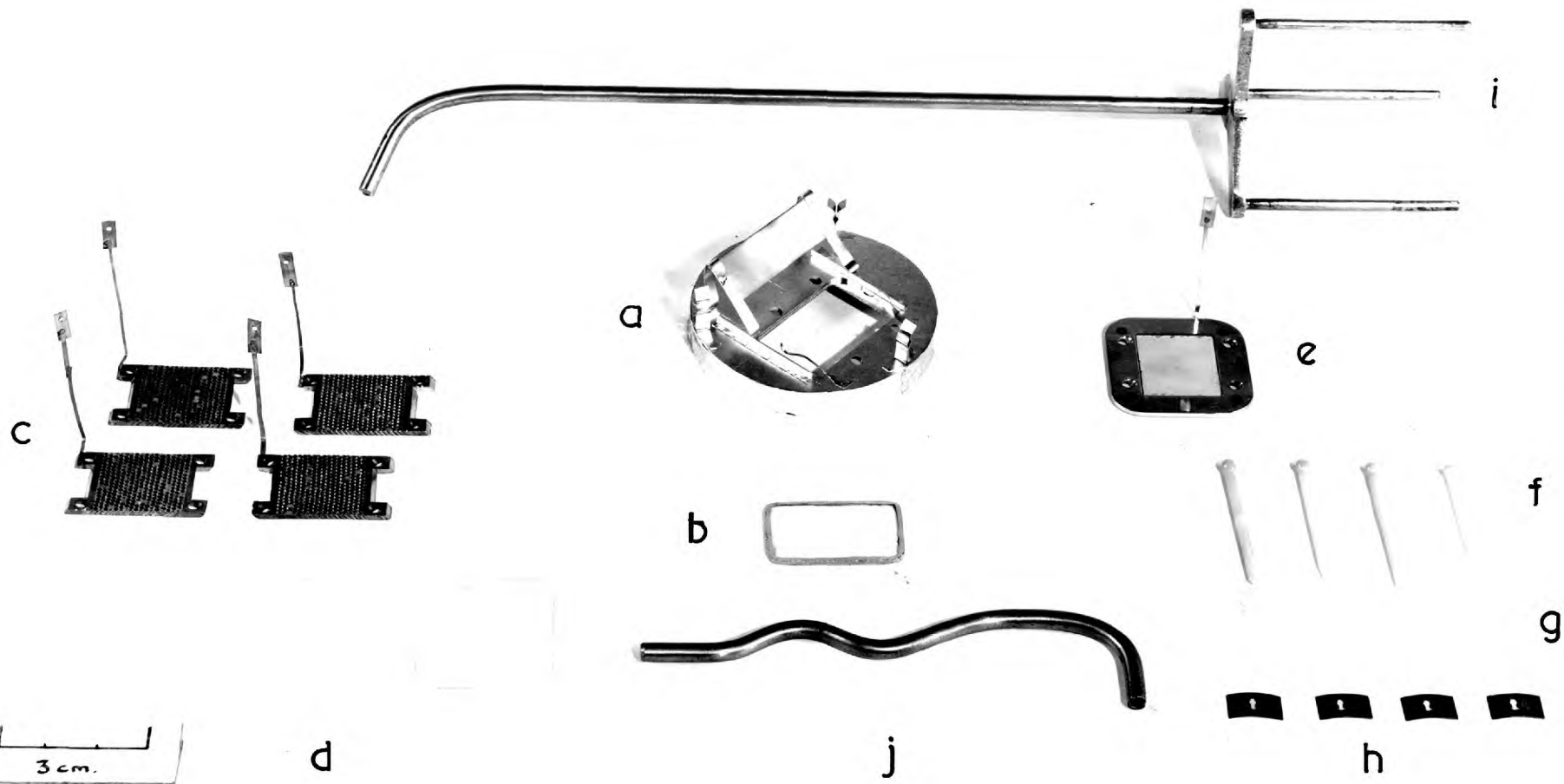


Fig 16



Fig . 17.

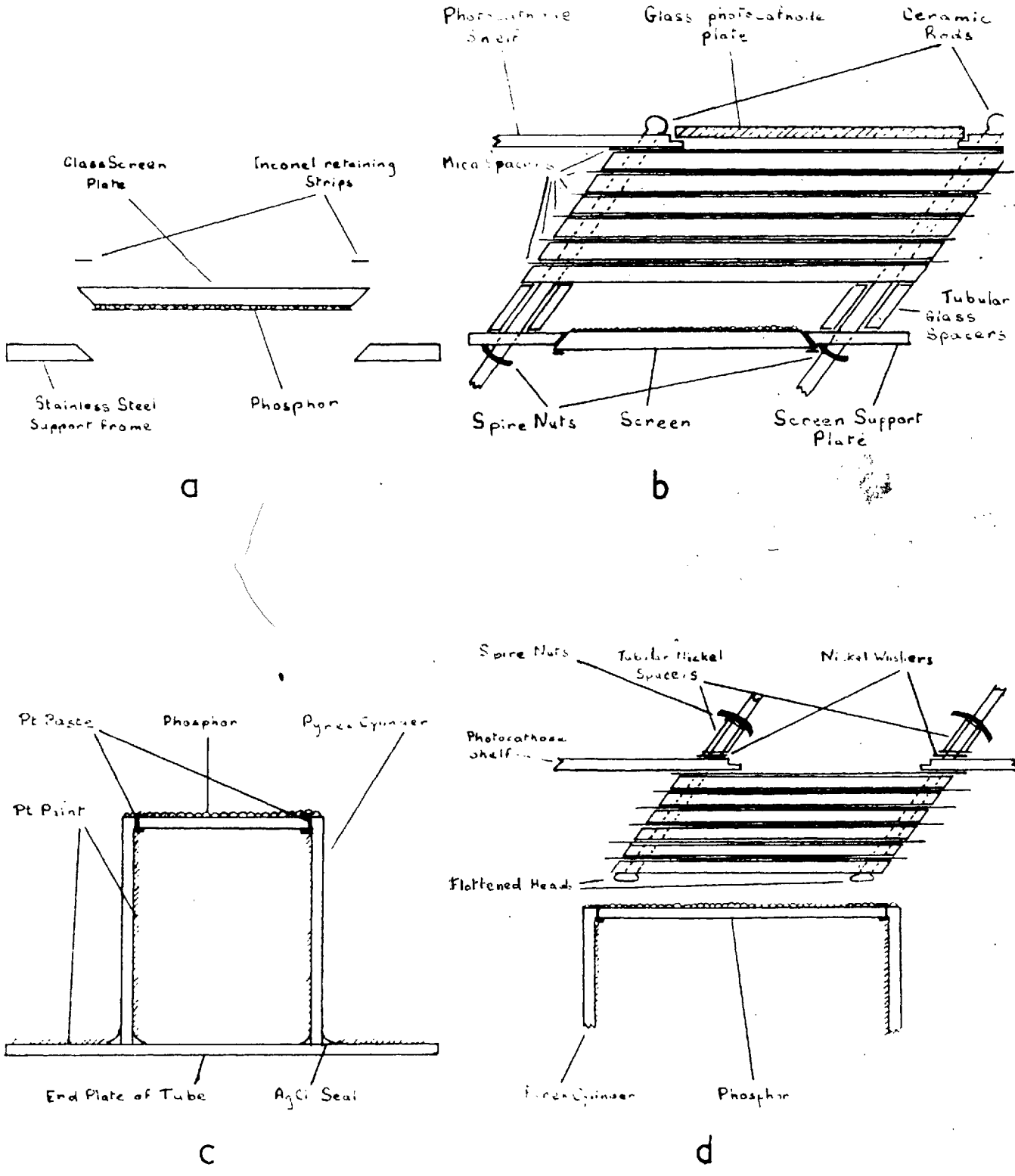


Fig. 18.

glass plate supported in a stainless steel frame (Figs. 16e and 18a). To avoid unnecessary projections on the face of the screen, this was made with two of its edges ground at an angle of 45° , and the two corresponding edges of the hole in the supporting frame were similarly shaped. The screen was then simply dropped into position in the frame, and retained in position by two strips of Inconel spot welded to the back of the frame, so that no projections disturbed the field in front of the screen. Aluminium-backed willemite or $ZnS:Ag$ was used for the screen. Contact was ensured between the aluminium layer and the stainless steel plate by a layer of platinum paste along the sloping edges of the screen.

The dynodes (Fig. 16c) were the same as for the tube described in § 5.3.1, except that the nickel tape leads were terminated in small Inconel tags. These were drilled to be a tight push fit over the 1 mm. tungsten pins set in a band around the lower end of the envelope, between the tooled down portion and the polished end. (Fig. 17).

As before, the assembled dynodes (Fig. 18b) were held in alignment by pointed steatite rods $3/32$ in. in diameter (Fig. 16f) fused at one end to form a head, and secured at the other by spire nuts (Fig. 16h). These passed through $3/32$ in. holes drilled at an angle of 55° through the photocathode shelf and the screen support plate, and through the holes at the corners of the dynodes. The dynodes were again insulated from each other by mica spacers approximately .005 in. thick (Fig. 16d) and from the screen by tubular glass spacers (Fig. 16g) 5mm. long and ground at an angle of 55° . When assembly was complete the ceramic rods were snipped off close to the spire nuts and the assembly was inserted into the envelope by means of a special tool (Fig. 16i) which engaged with three blind holes drilled in the underside of the shelf. The Inconel tags were then pressed home over the appropriate tungsten pins with the tool shown in Fig. 16j.

After assembly the tube was flushed with a steady supply of cool dry argon while the end plate was sealed in position with silver chloride,

using an electric hot plate. At this stage the glove box could be opened to facilitate the sealing process, since the flow of dry argon prevented atmospheric attack on the multiplying surfaces. A magnetically-operated ball valve (not shown in Fig. 16) was incorporated in the pumping stem of the tube to prevent ingress of moisture during the sealing of the tube on the pump, and this was closed after completion of the silver chloride seal. The argon supply was then shut off and the tube was sealed on to the pump. On completion of the glass-blowing the ball valve was opened to allow the tube to be evacuated.

5.4. Processing

During evacuation of the tube, the double pumping stem (Fig. 17) ensured efficient pumping of the space on both sides of the photocathode shelf, which formed an almost hermetic seal. The antimony layer (see App. II) was deposited by an evaporator introduced from its side arm through the upper pumping stem. This evaporator was also used as an anode during the caesiation of the photocathode, contact being made through the wall of the side arm by a platinum tape seal. This was maintained in electrical contact with the evaporator by a layer of platinum paste inside the side arm, against which was pressed a spring finger spot welded to the evaporator. During caesiation of the cathode, caesium was excluded from the main electrode structure by the skirt on the photocathode shelf, in conjunction with a thin layer of Aquadag, which readily absorbs caesium, on the tooled down portion of the tube wall.

After activation of the cathode, the antimony evaporator was withdrawn into its side arm and the image tube was sealed off the pump. The photocathode plate was then shaken free of its retaining springs, turned over to face the dynode system, and tapped back into place. The ramp and a short guide rail at each side of the cathode, clearly seen in Fig. 16a, helped to lead the plate easily into position under its springs.

This left the sensitive surface facing the first dynode and separated from it by about .01 in.

Fig. 19 shows a completed tube of this type.

5.5. Later modifications

These changes almost eliminated the disadvantages mentioned earlier; the phosphor screen was now within 4 cm. of the end window, and could be closely examined. The spot-welding and glass-blowing operations were dispensed with, and penetration of caesium to the dynode section was greatly reduced. It was however found difficult to drill the $3/32$ in. holes in the photocathode shelf with sufficient accuracy, and these sometimes had to be opened up with a fine file. In this case, caesium tended to find its way through the gaps around the ceramic rods. Also, partly as a result of this slight penetration of caesium, breakdown was found to occur between the fluorescent screen and the last dynode, along the ceramic rods. To reduce this, a new method of mounting the phosphor was introduced (Fig. 18c). The screen was settled on a pyrex glass plate drop sealed into a pyrex cylinder. The other end of this was ground and polished in the usual way, and sealed with silver chloride to the end window of the tube, using platinum paste instead of paint on the surface of the end window, to obtain good adhesion and electrical contact. Platinum paint connected the aluminised screen, via this seal, to the outer silver chloride seal, where the end plate was attached to the tube body. Since the glass in this area was also platinised, it was thus possible to make electrical contact with the aluminium layer from outside the tube. So far as possible, the platinum paint leads were kept inside the cylinder, contact being made through the drop seal by tags of platinum paste applied to the phosphor plate prior to the drop-sealing process. The ceramic rods were now made with a flattened head, and passed in the opposite direction through the dynode assembly, so that the spire nuts were now above the photocathode shelf. (Fig. 18d).



Fig. 19.

Caesium penetration was resisted by thin nickel washers, drilled to fit tightly over the ceramic rods. These were pressed down against the shelf by tubular nickel spacers, cut at one end to 55° , which also served to keep the spire nuts clear of the surface of the shelf, so that the glass cathode plate could be readily inserted into and removed from its recess. As an additional precaution, a large mica spacer covering the whole of the rear of the cathode shelf was used to reduce the chance of caesium getting around the photocathode plate.

These precautions proved quite successful, and practically no caesium reached the dynodes in a tube of this type. Much higher voltages than previously could be applied to the screen without breakdown, and higher light gains were obtained. An additional benefit was the larger area of the dynodes utilised in this case, since in the previous design the offset of the fluorescent screen (see Fig. 18b) caused an appreciable fraction of the dynode area to remain unused.

Chapter VI. Results obtained with imaging tubes

6.1. Measurement techniques.

6.1.1. Method of measuring electron gain

Potentials for the tube were supplied from a potential divider arranged as shown in Fig. 20. The E.H.T. voltage was supplied by a 10 kV or 15 kV power pack, and the various electrodes of the tube were connected by flying leads to the appropriate tapping points on the resistance chain via 4 mm. plugs and sockets. By this means, widely varying voltages could be applied to the electrodes, fine adjustment being provided by the potentiometers incorporated in the chain. Individual electrode currents were measured by means of a jack socket in series with each lead, so that a galvanometer could be rapidly connected or removed as required. All the resistors and terminal sockets were mounted on perspex sheet, and the flying leads were heavily insulated with flexible polythene tubing, as a precaution against leakage currents.

Owing to the large ratio between the input and output currents in a high-gain tube, it was found advisable to measure the electron gain in a series of steps. Initially the input light level was adjusted by means of an iris diaphragm or a variable transformer supplying the light source, until an easily measurable current was leaving the cathode. The output current was then measured with a low overall voltage applied to the tube. Next the light input was reduced until the output current had fallen by some convenient factor, and the applied voltage was increased step by step until the screen current rose approximately to the original value. The input light level was then reduced again, and the process repeated as many times as necessary. By this means the current gain of the tube could be measured without at any time drawing excessively high currents from the later dynodes. In addition, all the current measurements could be carried out on a single range of the galvanometer, so reducing instrument errors.

$R_1 = R_2 = \dots = R_{34} = 1\text{ M}\Omega$

—⊖ 4 mm. plugs and sockets

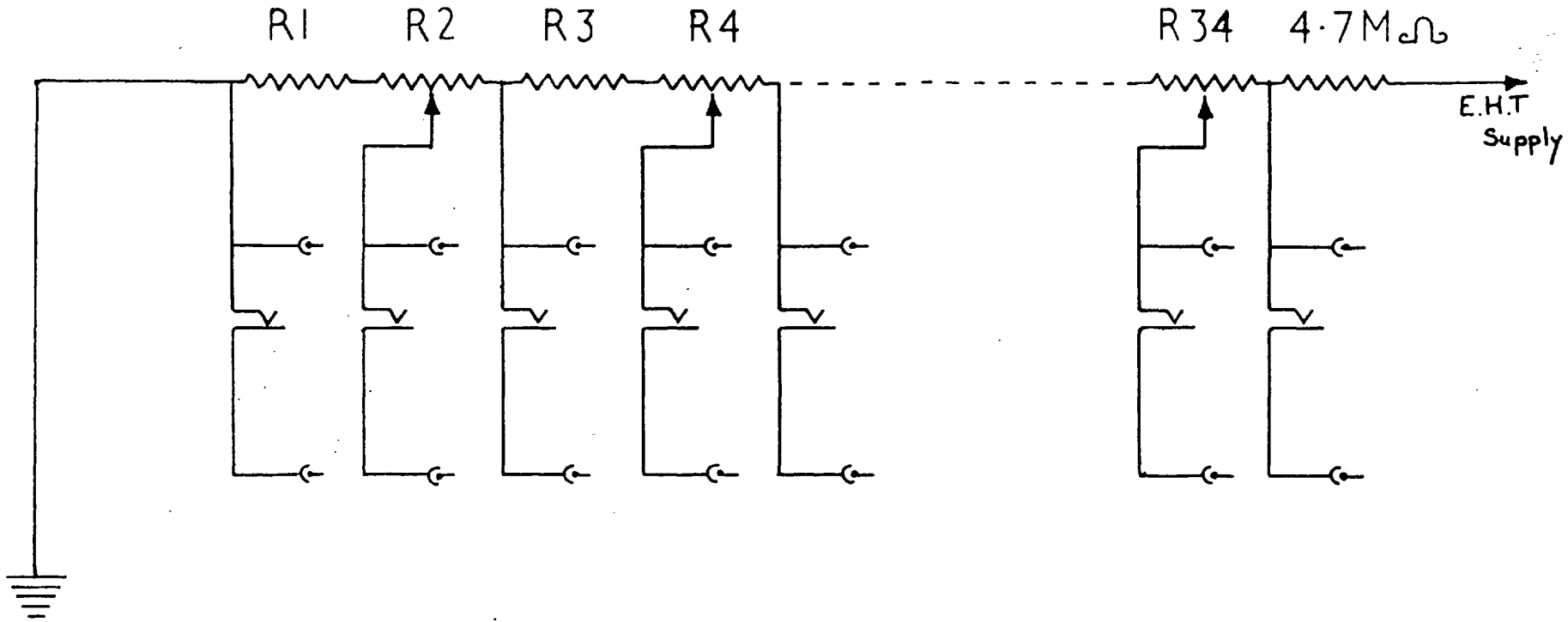


Fig. 20.

A similar procedure was used to measure the gain of individual stages. Initially, only the first few stages were connected, and the separate electrode currents were measured. Then the light input was reduced, the next few stages were connected, and their currents measured in turn. This was repeated until the gain of all the stages had been determined. When measuring the variation of electron gain with voltage, all the electrode potentials were supplied by a single power pack, to ensure that the field configuration in the tube remained constant throughout the measurements.

6.1.2. Measurement of light gain

Owing to the position of the screen in these tubes, some 4-5 cm. from the end window, it was impossible to measure the light output directly by pressing a photo cell against the screen, and some form of optical coupling had to be introduced. Two $f/1.9$ lenses of $3\frac{1}{4}$ in. focal length were used face to face, giving a measured blue light transmission of 2.6% at full aperture and unity magnification. These were used to image the output screen on a selenium barrier layer cell.

The apparatus used in the measurement of light gains is shown in Fig. 21. The light source, at the extreme right, consisted of a ZnS:Ag phosphor screen, stimulated by ultra-violet light from a heavily-filtered mercury discharge lamp. A circular diaphragm immediately in front of the phosphor was imaged on the cathode of the tube by an $f/2$ $2\frac{1}{4}$ in. lens to give a small illuminated spot. The two $f/1.9$ lenses previously mentioned were used to image the corresponding bright spot at the phosphor on the selenium cell at the extreme left. All the components of the system were supported in clamps fixed to a small optical bench.

To ensure an accurate determination of the gain, the same photo voltaic cell was used to measure both the input and output light fluxes. The potential across the dynode system and that for accelerating electrons to the fluorescent screen were supplied now by two power

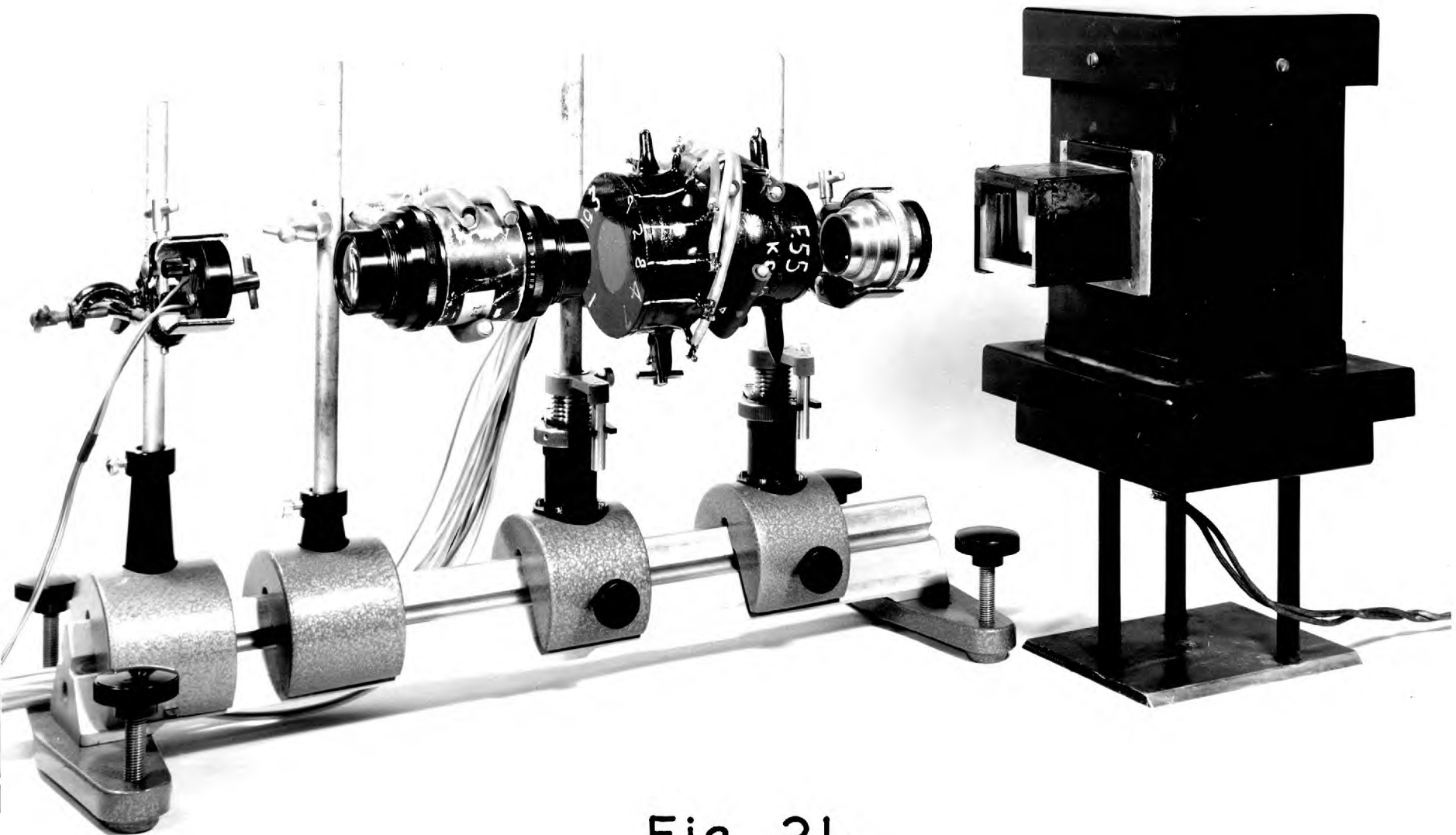


Fig . 21 .

packs which were separately adjusted for maximum gain. As with the electron gain, the light gain was measured in stages, the light input being reduced and the applied voltage increased alternately. The light input was varied by adjusting the iris diaphragm of the input lens, which had been previously calibrated to ensure accuracy.

6.1.3. Resolution

Owing to the limited resolution of these tubes, no special measurement techniques were required; the static resolution could be estimated by the unaided eye. Photographic methods were used to determine the dynamic resolution, since the relatively crude apparatus used did not allow sufficiently rapid motion of the tube to give good visual results. The use of photography overcame this limitation by allowing a longer period of integration, and also confirmed that the results obtained were not subjective.

6.2. Results of Gain Measurements

To simplify the initial investigations several tubes similar to those described in §5.3.1, were built, but in these tubes the primary electrons were supplied by an electron gun rather than a photocathode. These tubes showed that successful multiplication was possible with the chosen electrode structure, but the average stage gain obtained was disappointingly low. This was partly because the technique of producing consistent multiplying surfaces was not then sufficiently developed, but primarily because of poor alignment between the dynodes. At this time, dynodes with integral mounting points had not yet been produced, and the older type of dynode proved extremely difficult to align accurately. The resulting misalignment drastically affected the efficiency of electron transfer between stages, so that although first-stage gains of between three and four were recorded, the gain of the second and subsequent stages was typically about 1.2 with the same

primary electron energy.

The moderate success obtained with such tubes encouraged the building of actual imaging multipliers. Several were constructed to the pattern described in § 5.3.1, mostly with magnesium oxide secondary emitters. The first was unsatisfactory, owing to severe misalignment of the dynodes, but its immediate successor, the first tube in which dynodes with integral mounting points were used, was much more successful, so that dynodes of this type were used exclusively from then on. The dynodes in this tube were rather thicker than the optimum, but a moderate electron gain of about 7 in three stages was obtained at 800 V/stage, the best dynode, the second, having a gain of 2.8. The image quality was adequate, 3 mm. test bars being clearly imaged in any orientation relative to the dynode structure. There was no light gain, as the photocathode sensitivity was only $3 \mu\text{A/lm}$, and the screen voltage was limited by field emission.

Next came a four-stage tube, again with MgO secondary emitters, but this time with dynodes of the correct thickness. The tube was over-caesiated during activation of the photocathode, and severe caesium attack on the willemite screen occurred. The excess caesium also limited the inter-stage voltage which could be applied, but on the other hand it almost certainly increased the yield of the multiplying surfaces, as an electron gain of over 30 was obtained at 450 v/stage. Although the photocathode had a sensitivity of $25 \mu\text{A/lm}$, no light gain was obtained, as only about 500V could be applied to the phosphor stage before severe field emission occurred. The gains of the individual stages, in order, were 1.35, 2.65, 3.1, and 2.9, giving a mean stage gain of 2.4. It will be noted that the gains in the last three stages approached the arbitrarily-established target of a gain of three per stage. The gain of the first stage was less than half that of the others. This is partly because of the fairly large dead area of the dynode, due to the finite wall thickness of the tubes and to packing losses. In addition,

the field configuration inside the cells of this dynode is considerably different from that in the other stages, owing to the presence of the plane photocathode. The field from the following dynode does not extend so far into the cells, so that the percentage of secondaries extracted is reduced. This effect was observed in several tubes, but was reduced in later versions by making the first dynode rather thinner than the rest.

It was clear that the presence of caesium in the multiplying section of this tube was a serious disadvantage, since the onset of field emission prevented the full realisation of the potential electron gain and completely eliminated any possibility of light gain. Consequently, no more tubes of this type were constructed, all succeeding intensifiers being of the type discussed in 5.3.2.

The first tube of this type to be built had five dynodes, with KCl multiplying surfaces, and was the first image tube to use this material. Unfortunately, the surfaces were contaminated by atmospheric moisture, and the electron gain was extremely low - about 7, the best stage having a gain of 2.2. There appeared to be some light gain, but this was not measured, as it too was very low.

Several unsuccessful tubes followed this, including one with Sb-Cs multiplying surfaces. This was of particular interest in so far as the image obtained by using the first dynode as photocathode could be studied and compared with that obtained with a plane photocathode which was also incorporated in the tube. In fact, the contrast of the image so produced was considerably better than that given by the plane cathode, which would suggest that most of the loss in contrast in other tubes occurs between the photocathode and the first dynode rather than between stages. The need for extremely close spacing of these two electrodes is thus clearly seen. This tube was otherwise unsatisfactory, since field emission limited the interstage voltage to less than 300V, and the electron gain was very low.

During the construction of these tubes, the speed and ease of preparation of KCl surfaces in comparison with MgO were clearly demonstrated, and later tubes used this material exclusively.

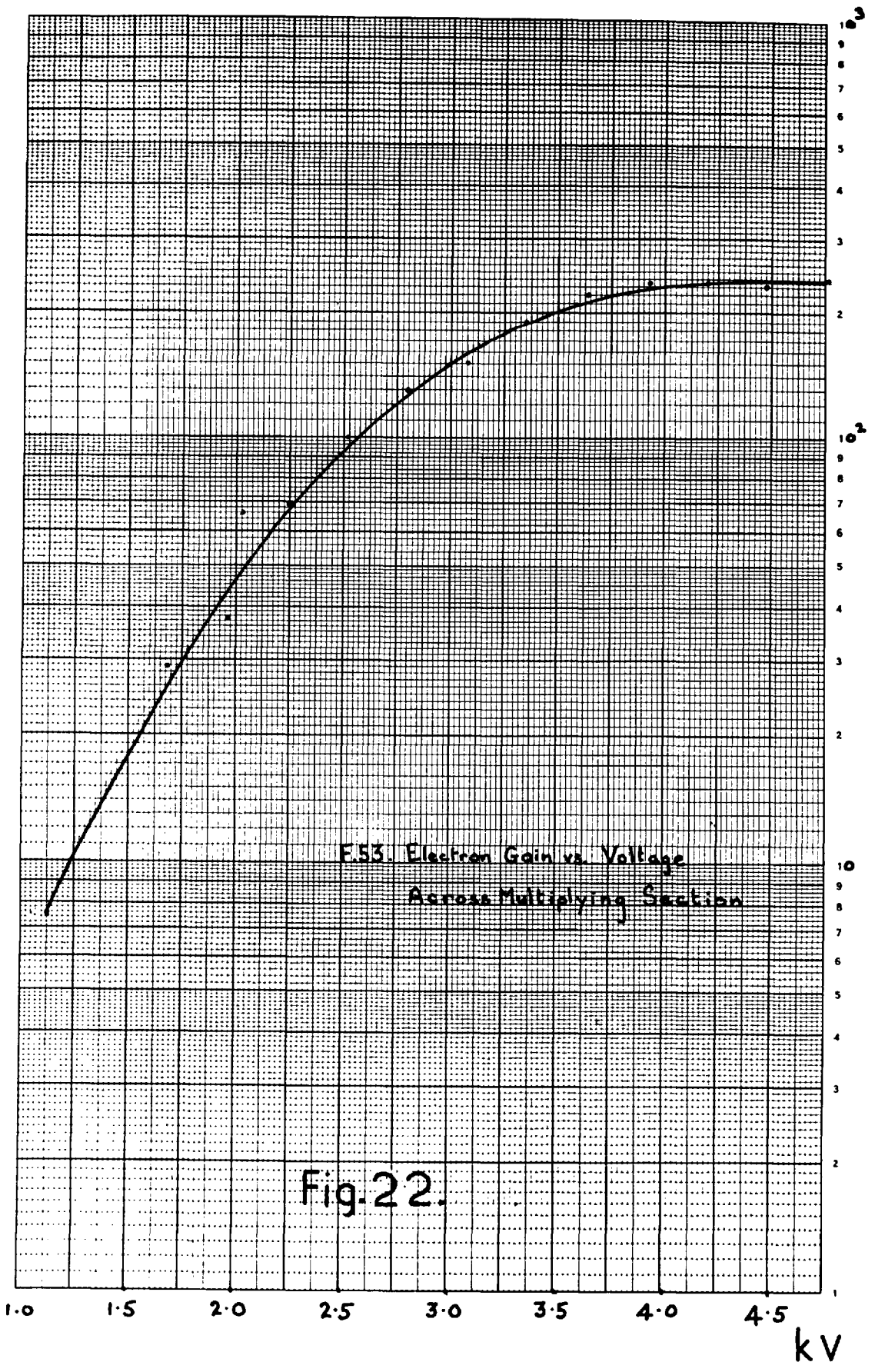
The first really successful KCl tube had an electron gain of approximately 100 in six stages at 460V/stage. Unfortunately it rapidly went soft, but it was rebuilt to give an even higher gain. In this form the tube had six dynodes, the first dynode being half the thickness of the others, and the secondary emitting material was a 1000\AA thick layer of KCl. The phosphor was aluminium-backed ZnS:Ag, settled to 1.5 ngm/cm^2 . Immediately after sealing off, the photocathode sensitivity was $6 \mu\text{A/lm}$, and an electron gain of 800 was measured at 750V/stage. This figure is of considerable interest, since it represents a mean stage gain of slightly over 3, the target figure. The improvement was chiefly due to improved techniques for preparing and handling the secondary emitting surfaces, but the reduction in thickness of the first dynode also improved its gain by over 30%. The gain in this stage was now slightly less than two-thirds that of the other stages, and since there is a theoretical loss of some 33% during electron transfer from the cathode to the first dynode, owing to packing losses and the wall thickness of the tubes, it can be seen that the thickness of this dynode was now very near the optimum value.

After these initial measurements were made, testing was discontinued for several days, while extensive alterations were carried out on the potential divider, which was beginning to break down at the high screen voltages required for this tube. During this period, the photocathode sensitivity fell noticeably.

While the tube was under test, a severe electrical leak developed between the fourth and fifth dynodes, progressively and drastically reducing the electron gain in these two stages. Initially the gain in the two together was almost 9, but this ultimately fell to less than 1. The light gain was unfortunately not measured while the tube was working at

its initial high electron gain. When the electron gain had fallen to 290 however, (at an average of 600 V/stage) and the cathode sensitivity to $3 \mu\text{A}/\text{lm}$, the tube gave a blue light gain of 920, with 8 kV on the phosphor stage. Thus, with a more sensitive cathode - say $30 \mu\text{A}/\text{lm}$ - the original electron gain of 800 would have corresponded to a light gain in the region of 25,000. In Fig. 22. the variation of electron gain with applied voltage at this time is plotted. It should be noted that the electron gain shown at 600 v/stage is not 290, but about 210. This is due to the fact that lower screen voltages were applied during the measurements of electron gain since, as previously described, all the electrodes including the screen were fed from a single power pack, to ensure that the field configuration in the tube remained constant throughout. (During measurements of light gain, the screen was fed from a separate supply, which was adjusted to give the maximum gain which could be attained without breakdown.) The curve of Fig. 22. was obtained with unequal interstage voltage increments, allowing application of the maximum voltage in each stage without breakdown. Fig. 23. shows the variation of gain with applied voltage for equal voltage increments in each stage except the last, in which field emission was particularly troublesome. At this time, with just over 500V per stage, a reasonable working figure, and with 1300V on the screen stage, the measured individual stage gain were, in order, 2.1, 3.6, 3.6, 2.2. (the fourth and fifth dynodes together), and 2.0, while the measured overall gain was 130. The leakage between the fourth and fifth dynodes was now too great to allow their gains to be measured separately, but it will be seen that these were very low. The gain in the last stage also was low, owing to the low primary energy in this stage (350 eV) and the weak extracting field applied.

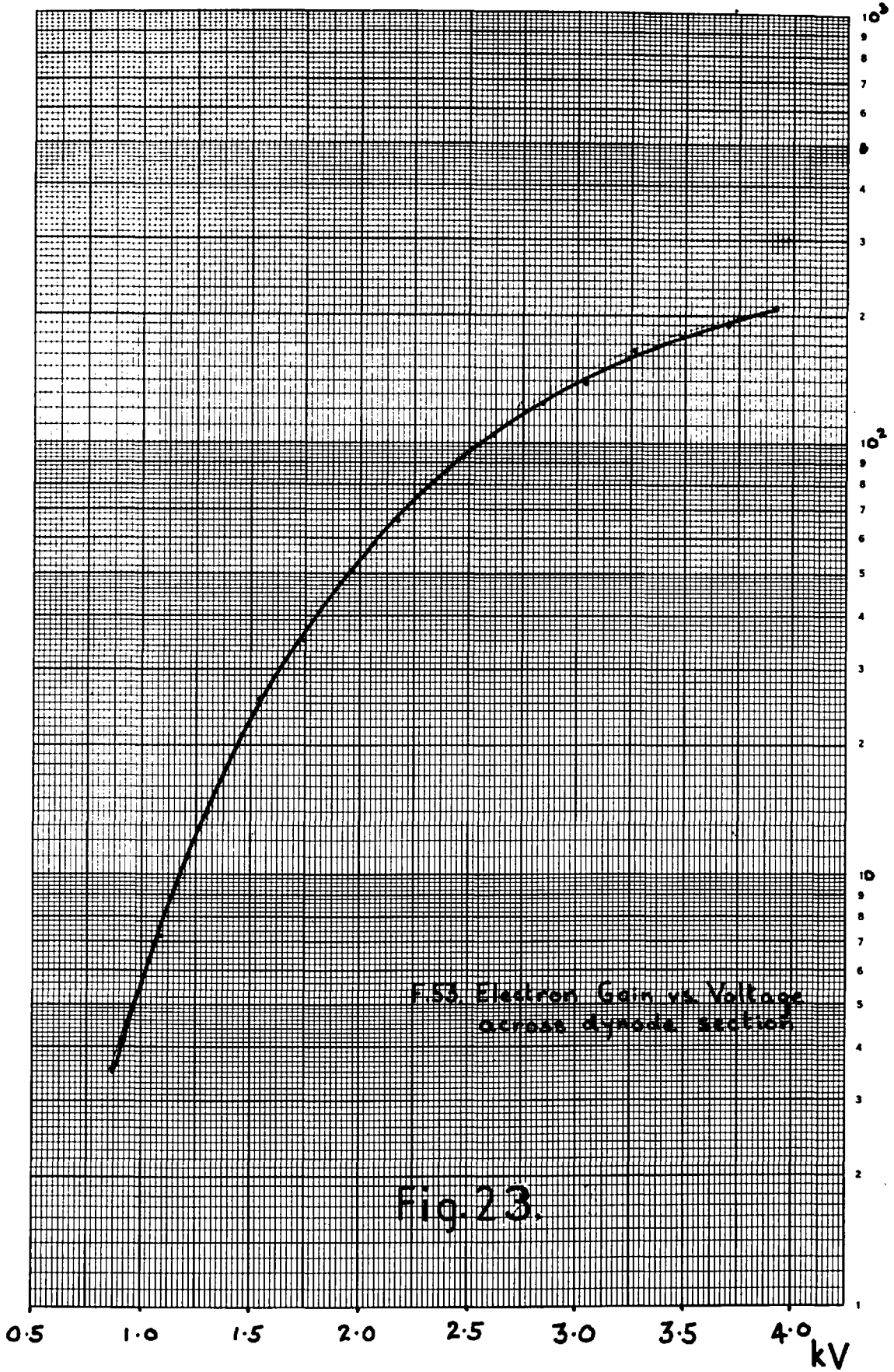
Thus the second and third stages are those most representative of conditions in a multiplying system and it will be seen that stage gains of between 3 and 4 are attainable in such a system at reasonable



F.53. Electron Gain vs. Voltage
Across Multiplying Section

Fig. 22.

kV



F.53 Electron Gain vs. Voltage
across dynode section

Fig. 23.

interstage voltages. This is borne out by the fact that initially the fourth and fifth stages gave gains of 2.5 and 3.3 respectively, at only 400 V/stage.

The very promising results obtained from this tube encouraged the building of tubes with more stages. A twelve-stage tube was planned as the next step, but the available stock of dynodes proved sufficient for only ten stages. This tube also had KCl secondary emitting surfaces, in this case a little thinner than the optimum, and a thin first dynode. The phosphor was again aluminium-backed ZnS:A₂, but this time the screen was mounted by the method described in § 5.5. This allowed accelerating voltages of up to 10 kV to be applied to the phosphor stage. The aluminium layer, however, proved too thin for the high gains achieved in this tube.

The photocathode had a sensitivity of $18 \mu\text{A}/\text{lm}$ after reversal, and immediately after sealing off an electron gain of 8,500 was measured at approximately 370V/stage. With an accelerating voltage of only 5 kV on the screen stage, the light gain was then 1.4×10^5 . At this gain, however, the image was extremely poor, owing to optical feed back through the aluminium backing of the phosphor, which would also increase the apparent light gain. The angle of the electrode stack caused the fed-back image to be considerably out of register with the original, so that the image deteriorated rapidly as the gain was increased. It was found that an adequate image was obtained with the tube working at a photon gain of $5 \cdot 10^4$. As in the previous tube, progressive shorts appeared between several dynodes over a period of a few days, and the photocathode sensitivity fell rapidly (to $6 \mu\text{A}/\text{lm}$ after 5 days). It was felt that both these effects might be due to localised breakdown, which would liberate chlorine from the KCl to attack other surfaces in the tube. This particular cathode had been slightly under-caesiated on activation, and so would be particularly sensitive to chlorine attack. The inclusion of some suitable chlorine-absorbing material in the tube might help to

reduce these effects (see Chapter 7).

The variation of electron gain with multiplying voltage for this tube is shown in Fig. 24. The gain was measured with a low screen voltage to prevent optical feedback, so that the values obtained are not so high as those which would be recorded with the tube in normal operation. In spite of this, an electron gain greater than 2.10^4 was recorded, at 530 V/stage, the maximum voltage which could be applied without breakdown. This gain corresponds to an average stage gain of 2.7, slightly below the target figure discussed above. The individual stage gains were not measured, owing to the electrical leakage.

All these tubes had channels 1 mm. in diameter. A single nine stage tube was constructed with $\frac{1}{2}$ mm. channels, but inaccuracies in the drilling process caused severe misalignment, with the result that almost all the electrons were lost inside the system. No image was obtained.

6.3. Resolution - Static and Dynamic

The resolution obtained in these tubes was in good agreement with that expected from a structure of this type. (Chapter II).

Test patterns consisting of parallel black and white bars of equal width were normally employed, the width of adjacent bars being either equal (a Foucault test pattern) or graduated across the pattern. The use of lines of graduated width enabled the minimum resolvable line width to be determined: test fans were also used in some cases for this purpose.

As discussed in Chapter II, the limiting resolution is obtained only when the test bars are of exactly the right width and in perfect alignment with the dynode structure. Variations in the size or orientation of the pattern produce various spurious effects. Examples of this are shown in Fig. 25. Fig. 25a shows a line pattern at the limit of resolution; 25b shows the same pattern rotated through a slight angle, and 25c the same pattern turned through a slightly greater angle.

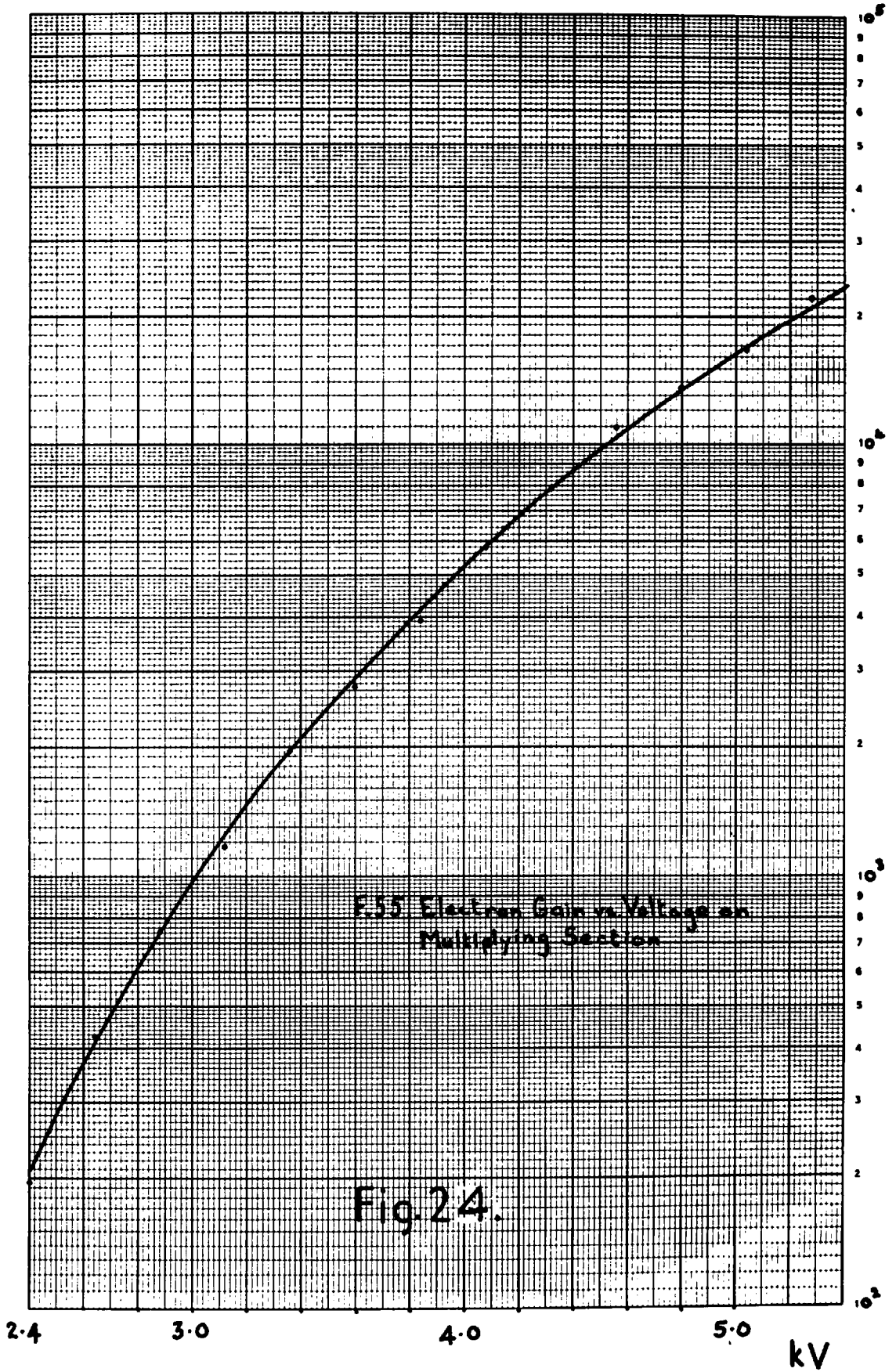
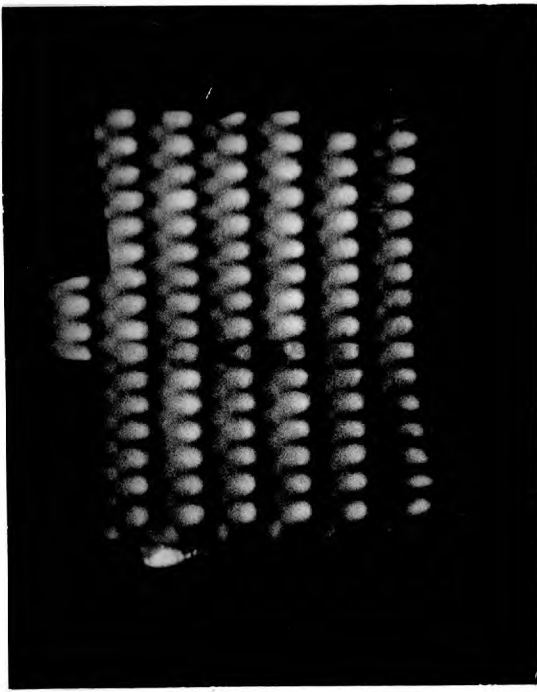


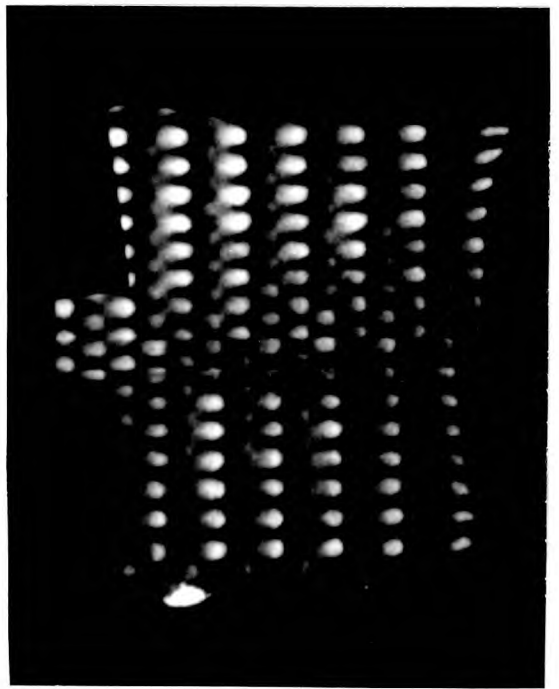
Fig. 25d shows the "beating" effect produced by a pattern just too fine to be resolved. All these photographs were taken from tubes with 1 mm. channels.

A notable improvement in resolution is obtained by movement of the image - "dynamic viewing". Figs. 26 and 27 show examples of patterns too fine to be resolved with the tube static, but which are clearly resolved when the tube is reciprocated in one dimension. Fig. 26 b and d and Fig. 27b were obtained by reciprocating the tube in the plane of the image, with a period short compared with the exposure time and an amplitude of two or three channel diameters. In fig. 26a, the image of a Foucault test pattern of approximately $\frac{2}{3}$ lp/mm. is seen; this is not resolved, the beating effect mentioned in Chapter II being clearly seen. In fig. 26b, however, obtained by reciprocating the tube in the direction perpendicular to the lines of the pattern with an amplitude of two channel diameters, the pattern is clearly seen. Similarly, Fig. 26c shows a fan test pattern graduated from $\frac{1}{3}$ lp/mm. to 1 lp/mm. This is not clearly resolved in the static case, except for the extreme coarse end of the fan, but in Fig. 26d, obtained by reciprocating the tube with an amplitude of three channel diameters, the whole of the pattern is clearly resolved. It should be noted that here the larger amplitude of motion has considerably reduced the obtrusiveness of the dynode structure and the visibility of imperfections in the phosphor layer. Finally, Fig. 27 shows a fan test pattern graduated from $\frac{2}{3}$ lp/mm. to $1\frac{1}{3}$ lp/mm. which is not resolved at all in the static case (Fig. 27a) but is clearly seen in Fig. 27b, obtained with an amplitude of motion of two channel diameters.

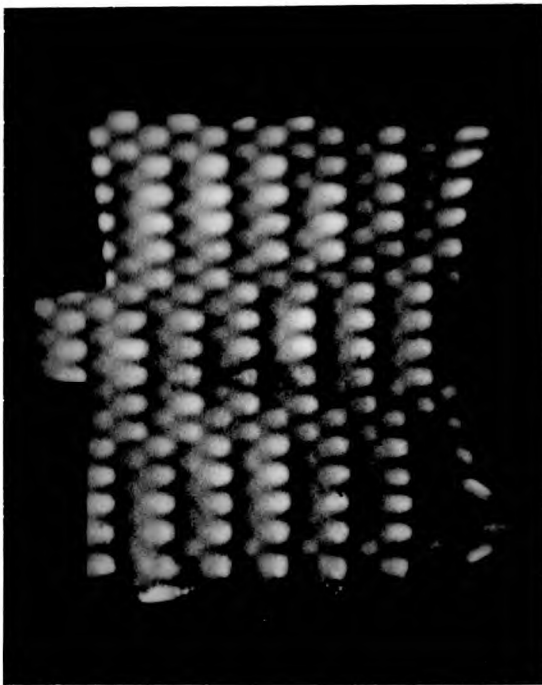
In all the photographs seen in Figs. 25, 26 and 27, the relative orientation of the dynodes and the test patterns is such that the theoretical limiting resolution for a Foucault test pattern is slightly worse than $\frac{1}{2}$ lp/mm. owing to the ellipticity of the picture points. It is thus seen that the limiting resolution in the dynamic case is rather better than twice that in the static case, while for a randomly oriented



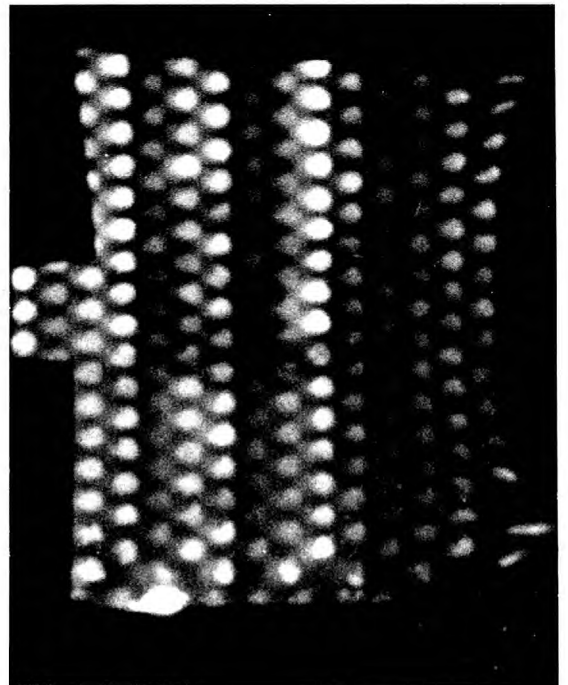
a



b

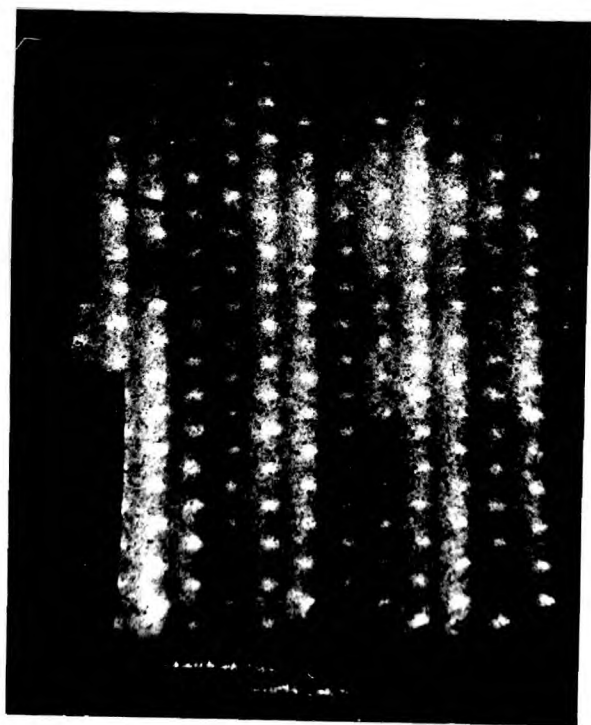


c

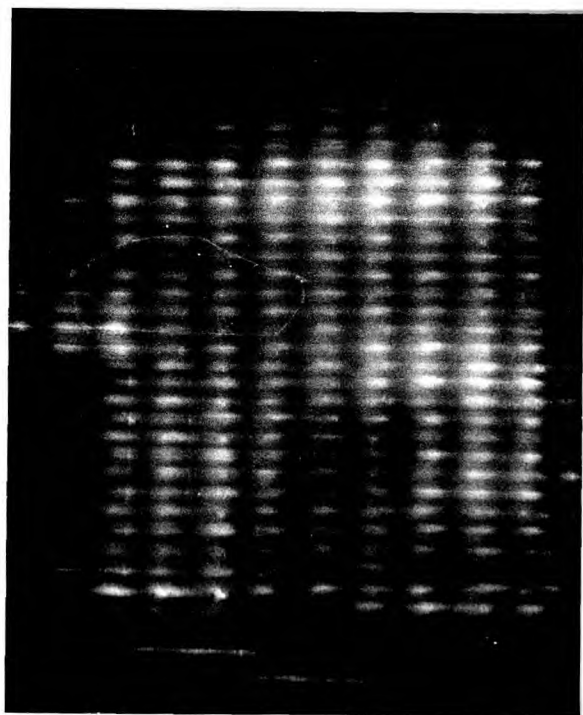


d

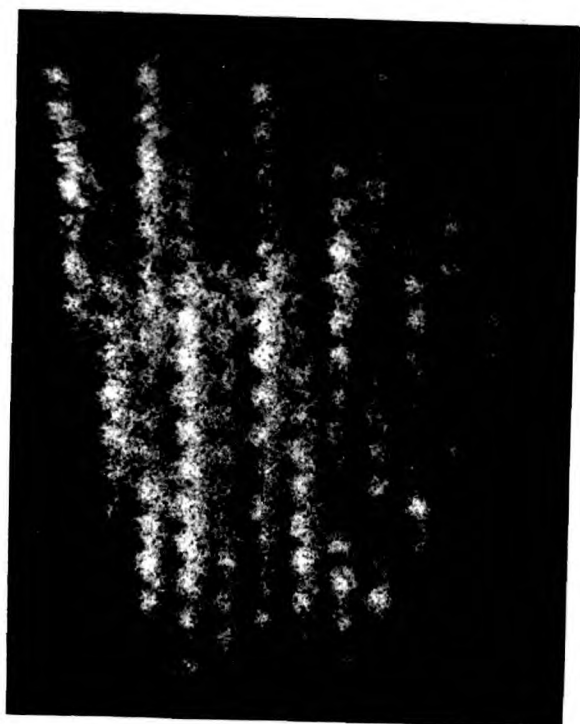
Fig. 25.



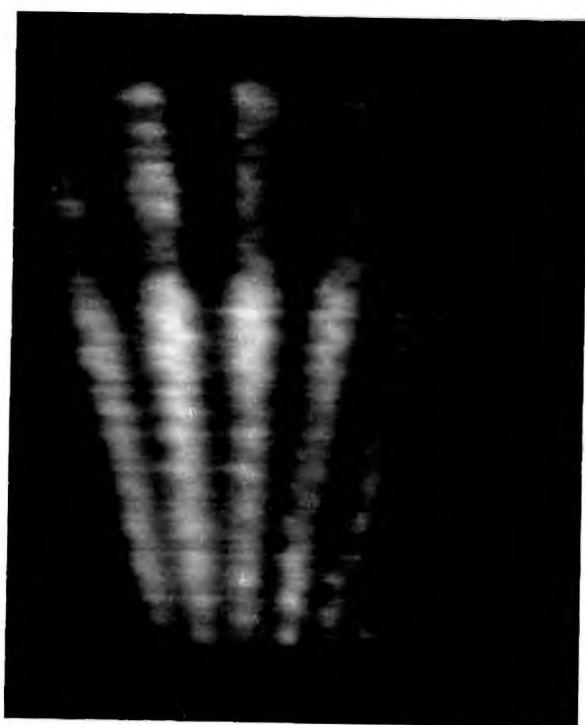
a



b

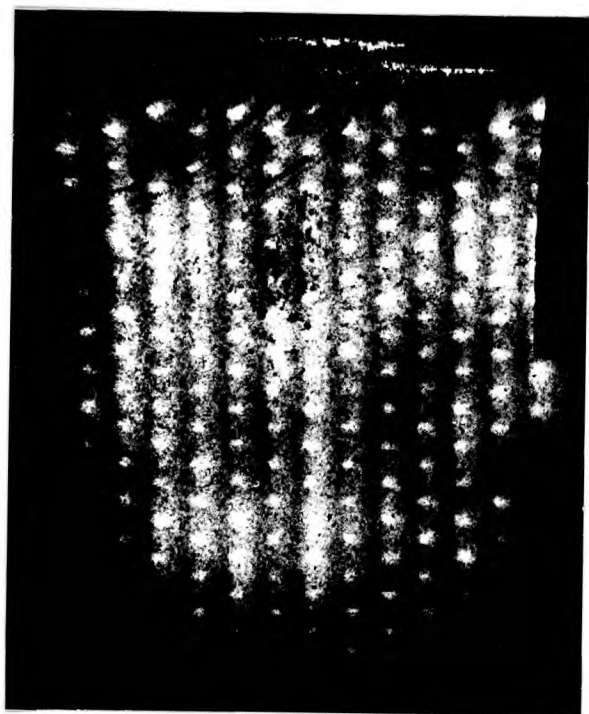


c

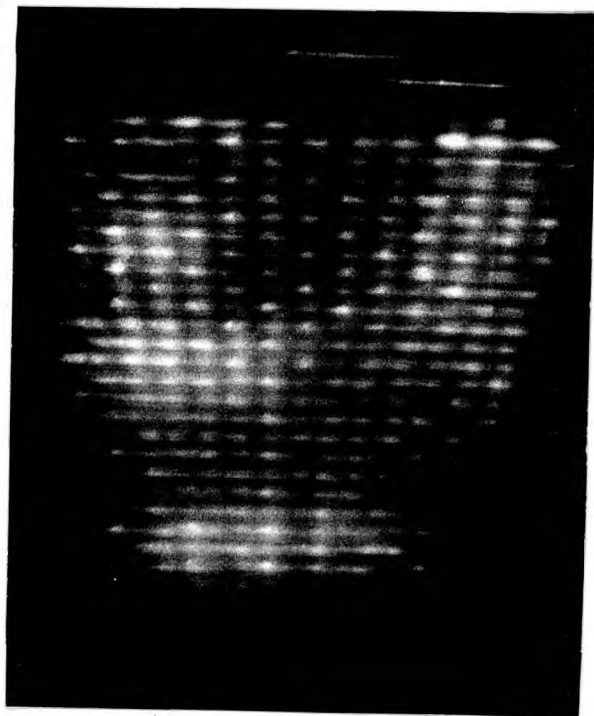


d

Fig. 26.



a



b

Fig. 27.

pattern such as a test fan, an improvement in resolution of almost four times is found. A similar gain in resolution along the other axis could be obtained by simultaneously reciprocating the tube in the direction perpendicular to the first motion, still in the plane of the image. The total effect would be a gain of between three and four times in the linear resolution in any direction, equivalent to increasing the number of channels by more than an order of magnitude.

Ideally the two mutually perpendicular motions should be random in amplitude and frequency, but in practice movements of constant and equal amplitude and frequency should prove satisfactory. This corresponds to a circular (or elliptical) motion, which could readily be achieved in a practical installation using such an intensifier.

6.4. Contrast

It will be seen from Fig. 25a that the contrast ratio in the tubes constructed was not 100%, the dark areas of the pattern showing some illumination. As discussed in § 6.2, this was probably due rather to excessive spacing between the cathode and the first dynode, imposed by the method of construction, than to straying of electrons from one channel to another during multiplication. There are two possible causes; first, the finite emission velocity of the photo-electrons, although this is small, and second, reflection of light from the front face of the first dynode to strike the cathode a second time, away from the original point of incidence. The latter appears to be more important, since increasing the potential of the first dynode had little or no effect on the contrast. In either case, a reduction in the spacing between the cathode and the first dynode would give a considerable improvement. It is unfortunately impracticable at present to form the cathode on the cell walls of the first dynode, as this would make it almost impossible to exclude caesium from the rest of the dynode system.

Should straying of electrons between channels later prove in fact

to be a serious problem, the effect could be largely eliminated by coating the edges of the cell walls with an insulating material such as MgF_2 , to act as a physical barrier to the electrons.

6.5. Background

The ten-stage tube discussed in § 6.2 showed very little background illumination at the voltages required to give a light gain of $5 \cdot 10^4$. As the voltage was increased beyond this, however, field emission from the dynodes became noticeable. It would appear that a tube with 1 mm. channels can be run at some 450 v/stage with no trouble from field emission, and there is no reason to suppose that dark emission from the cathode should be a more serious problem than in a normal photomultiplier (see Chapter II).

6.6. Conclusion

It has been satisfactorily demonstrated that an electron gain of between three and four per stage can be achieved in a channelled tube, and that very high light gains can consequently be achieved in a tube much smaller and simpler in operation than other types of intensifier. The resolution is limited, but is found to agree with that expected from a channelled structure, and various possible means of improving the resolution are apparent (see Chapter II). It is felt that the important advantages of this type of intensifier have been sufficiently clearly demonstrated to justify further development of the tube, since on the basis of the results so far obtained, a fifteen stage tube might be expected to give a light gain of 10^8 or more with an applied voltage of only 12 or 13 kV.

Now that the potentialities of the channelled intensifier have been demonstrated by the tubes described here, it is useful to consider modifications in the design and the techniques of construction which might be made, to eliminate some of the remaining defects. The method of manufacturing dynodes described here is laborious in the extreme, and requires considerable care to ensure accurate alignment. The assembly process is rather difficult, and in addition, even with the modified design described in § 5.4.3. and § 5.5. there remains some risk that caesium will penetrate to the dynodes.

It seems possible that the dynodes might be fabricated by a process similar to that currently in use for the manufacture of miniature klystron grids. In this process lengths of aluminium wire are electroplated with copper to a suitable thickness, and stacked in an array to give a cross-section similar to that required of the finished grids, but considerably larger in scale. This assembly is then drawn down to the appropriate size, the copper tubes being cold-welded together by the drawing process. Thin slices are cut from the block and etched to remove any burr. Finally the aluminium is dissolved in a caustic bath to leave a grid-structure of extremely good shadow-ratio. If this process, or a modification of it, could be used with nickel or some other suitable material, possibly by starting with small bore tubing and packing this with aluminium, it would be possible to produce dynodes with integral supporting frames, already perforated to take the aligning rods. This would eliminate the boring process, the prime cause of misalignment in the finished assembly. In addition, dynodes with very thin cell walls might be manufactured, added strength being supplied by a thick-walled tube enclosing the whole of the original assembly.

It is proposed that these dynodes should be activated, and stacked up on ceramic rods as at present, interleaved with mica spacers. The assembly would then be inserted into a tightly-fitting Kodial glass

envelope, with an end window sealed in at an angle of 55° . The electrode assembly would be separated from this end window by suitable spacers, and a rectangular-section side arm would allow the photocathode to be inserted into the resulting space, after processing in a separate compartment. Contact to the dynodes would be made by small springs attached to the dynodes, pressing against platinum tape seals through the tube wall. The dynode assembly would be held in position by a second glass spacer at the screen end of the tube. This end of the envelope would also be cut at 55° , and carry a Nilo-K flange. The phosphor would be settled on a Kodial glass window of the appropriate shape, also sealed to a Nilo-K flange. Assembly of the tube would be completed by argon-arc welding the two metal flanges together.

This would produce a tube little larger than the electrode assembly itself. The output screen would be on one end window, and the photocathode would be very close to the other, allowing good optical coupling. The dynodes would be accurately aligned, and the thin cell walls would reduce the dead area of the first dynode - an important point with cells of small diameter. As the photocathode would be processed outside the tube, caesium vapour would be completely excluded, and field emission would be reduced to a minimum.

An additional modification might reduce the effect of chlorine attack in tubes using KCl secondary emitters. A suitable chlorine-absorbing material might be deposited inside the tube, as close as possible to the active surfaces; in fact the ideal position for such a layer would be inside the channels themselves, on the wall opposite that occupied by the secondary-emitting layer. Almost all the chlorine liberated under electron bombardment would then strike the absorbing layer and react with it, before reaching the photocathode. By this means, it should be possible to make tubes combining the several advantages of KCl secondary emitting layers with the long life required of a practical device, since in the tubes investigated, chlorine attack

on the photocathode appeared to take effect much more rapidly than the corresponding fall in the secondary emission coefficient of the multiplying layers.

7.2. A colour image intensifier.

A further possible development of the channelled tube may be mentioned; a colour image intensifier. Since each picture element of the photocathode stimulates always the same section of the output phosphor, in contrast to most intensifiers, each channel could be used to intensify light of a single primary colour. Colour separation would be effected at the cathode by a tricolour mask consisting of an array of tiny colour filters, each operating on a single channel. This mask might be formed by evaporation through a suitably-modified dynode, so ensuring perfect alignment of the filter elements with the corresponding channels. The phosphor would be deposited in discrete dots, each the size of a single dynode cell, and giving output light of the colour appropriate to its particular channel. Thus a fairly simple tube could be produced which would combine the other advantages of the channelled tube with the ability to intensify full colour images. The resolution of such a tube would be rather poorer than that of a normal channelled tube, owing to the effective reduction in the number of channels, but this would to some extent be compensated by the fact that the eye will accept a coloured image of much poorer definition than that required of a monochrome image.

The channelled tube is unique in its suitability for this application, since with other types of intensifier, the accurate registration required for a colour image is almost impossible to maintain in practice; slight image distortion, or a very small drift in the power supplies, would completely destroy the colour rendering.

Acknowledgments

Thanks are due to Professor J. D. McGee, who first conceived the channelled intensifier, for his continued interest and encouragement during this work.

The author is indebted also to Mr. D. Theodorou and Mr. M. Whillock for their valuable assistance in much of the work described here.

The project was supported throughout by the National Research Development Corporation and the Department of Scientific and Industrial Research.

a) Exponential distribution

A single input electron is found empirically to give an output pulse of N electrons with probability

$$P_1(N) = \frac{1}{N_0} e^{-N/N_0}$$

Then the probability that n input electrons produce N output electrons follows:-

If the r th electron produces μ_r electrons at the output, the n th electron must produce $N - \mu_{n-1} - \dots - \mu_r - \dots - \mu_1$

The product of the probabilities is then

$$P_n(N) = \frac{1}{N_0^n} e^{-N/N_0} \int_0^N d\mu_{n-1} \int_0^{\mu_{n-1}} d\mu_{n-2} \dots \int_0^{\mu_{n-1} - \dots - \mu_2} d\mu_1$$

$$\int_0^{N - \mu_{n-1} - \dots - \mu_2} d\mu_1 = \left[\mu_1 \right]_0^{(N - \mu_{n-1} - \dots - \mu_2)} = N - \mu_{n-1} - \dots - \mu_2$$

$$\text{Put } N - \mu_{n-1} - \dots - \mu_r = U_r$$

$$\text{Then } U_r = U_{r-1} + \mu_{r-1}$$

$$\begin{aligned} \text{Then we have } \int_0^{U_3} (U_3 - \mu_2) d\mu_2 \\ = \frac{U_3^2}{2} \end{aligned}$$

$$\text{Similarly } \int_0^{U_4} d\mu_3 \text{ gives } \frac{1}{3!} U_4^3$$

After completing all $n - 1$ integrations, we get

$$P_n(N) = \frac{1}{(n-1)!} \frac{N^{n-1}}{N_0^n} e^{-N/N_0}$$

The centroid is determined by taking $\int_0^\infty N P(N) dN$

and is given by $\bar{N} = N_0 n$

The variance σ^2 is then determined by considering

$$\int_0^{\infty} (N - N_0 n)^2 P(N) dN$$

Integrating by parts, we get

$$\sigma^2 = N_0^2 n$$

Then $\frac{\bar{N}}{\sigma} = \sqrt{n}$ - signal to noise ratio for the multiplication process.

The noise generated during multiplication is additive with the natural statistical noise \sqrt{n} present in the original signal.

$$\text{Then } \left(\frac{\text{signal}}{\text{noise}} \right)_{\text{output}} = \sqrt{\frac{n}{2}}$$

Thus the signal : noise ratio is reduced by 30% during the multiplication process.

b) Probability distribution of photo-electrons

In the visible region, only first-order interactions need be considered, since for most surfaces the work function is of the same order as the photon energy.

If the quantum efficiency of the cathode is σ , and the number of photo-electrons produced is n , the probability distribution of n for a single photon is:

$$P(n) = 1 - \sigma, n = 0$$

$$P(n) = \sigma, n = 1$$

$$P(n) = 0, n > 1$$

$$\text{Then } \bar{n} = \sum_n n P(n) = \sigma$$

$$\text{and } \overline{\Delta^2 n} = \sum_r (n_r - \bar{n})^2 P(n) = (1 - \sigma) \sigma$$

For p input photons,

$$\overline{\Delta^2 p} = \bar{p}$$

These liberate M photo-electrons,

$$\text{where } \bar{M} = \bar{p} \bar{n} = \sigma \bar{p}$$

$$\begin{aligned} \text{and } \overline{\Delta^2 M} &= \bar{n}^2 \overline{\Delta^2 p} + \bar{p} \overline{\Delta^2 n} \\ &= \sigma^2 \bar{p} + \bar{p} (\sigma - \sigma^2) = \sigma \bar{p} \end{aligned}$$

$\therefore \overline{\Delta^2 M} = \bar{M}$, so that the photo-electrons also follow a Poisson distribution.

a) Activation of an SbCs₂ photocathode

The antimony was deposited from a retractable tungsten wire evaporator, loaded with a small bead of antimony, and heated by an eddy current heater in conjunction with a nickel wire pick-up coil. This evaporator was also used as an anode during caesiation, to monitor the cathode sensitivity. For this purpose, it was fitted with a small Inconel spring at the rear end, which pressed against a layer of platinum paste inside the side arm. Contact was made through the wall of the side arm by a platinum tape seal.

Caesium was generated in a second side arm, by means of a nickel capsule containing a mixture of caesium chromate with powdered tungsten and aluminium.

The first step was to outgas the caesium capsule by eddy current heating it to a dull red. When the pressure fell to a satisfactory level, the temperature was raised further to initiate the reaction which liberated free caesium. The metallic caesium was then flamed into the upper part of the side arm, and the now useless nickel capsule was sealed off. Next the antimony layer was deposited to an optical transmission for white light of 80%, as this was found to give the most sensitive semi-transparent cathodes⁶⁴. The whole tube was then baked to 150°C, and the photo sensitivity was monitored while caesium was driven in from the side arm by means of a heating coil. After the photo sensitivity reached a maximum, caesiation was continued until the sensitivity declined to 80% of the maximum value. The tube was then cooled, when the sensitivity could be seen to rise rapidly. The caesium side arm was sealed off, and when the tube was completely cold, the cathode was superficially oxidised by admitting oxygen produced by heating potassium chlorate in a side arm, after isolating the tube from the pumping system. When the sensitivity reached its new maximum, the oxygen was pumped away and the tube sealed off. The

better cathodes produced by this procedure typically had a sensitivity after reversal of 25-30 $\mu\text{A}/\text{lm}$.

b) Settling and aluminising of Fluorescent Screens

As discussed in Chapter V, two types of phosphor were used; willemite, and silver-activated zinc sulphide. The willemite was stored in an aqueous suspension containing 31.5 gm/litre of ammonium carbonate in solution to prevent aggregation. This suspension was diluted 20 : 1 with distilled water before settling, and the phosphor was settled to a density of $0.7 \text{ mgm}/\text{cm}^2$, the optimum for 10kV electrons according to Zworykin and Morton⁶⁵.

The ZnS was treated rather differently. This material was stored dry, in the form of a powder with a particle size of less than 5μ . Immediately prior to use, the necessary quantity of phosphor was weighed out and suspended in 100 ml. of 0.22 gm/litre barium nitrate solution, any aggregates being broken up by gentle ball milling. 12 ml. of potassium silicate solution (S.G. 1.020) was added to the suspension, and the mixture was immediately poured into the settling vessel, a 10 cm. diameter crystallising dish. After fifteen minutes, the remaining suspension was syphoned off and the phosphor was dried under an infra-red lamp. The ZnS phosphor was settled to a density of $1.5 \text{ mgm}/\text{cm}^2$.

After drying, the aluminising procedure was the same for both phosphors. The screen was placed in a beaker fitted with a drain tube and tap and covered with distilled water. A small quantity of filming agent (primarily collodion dissolved in a mixture of iso-propyl alcohol and amyl and butyl acetates, with dibutyl phthalate as a plasticizer) was placed on the surface of the water. This spread out to leave an extremely thin (a few hundred \AA) film of collodion as the solvents evaporated or dissolved. The water was drained off, allowing the film to settle on the surface of the phosphor, and after drying, the screen was baked to 120°C . to eliminate all traces of water.

It was then placed in a bell jar which was evacuated to a pressure below 10^{-5} mm., and the aluminium layer was deposited from a tungsten wire evaporator, to give an optical transmission of about 0.2%. Finally the screen was baked at 350°C . for thirty minutes to decompose the organic film, and it was then ready for use.

References

1. Burton, J. A. Phys. Rev. II, 72, 531 (1947)
2. Spicer, W. E. Phys. Rev. 112, 114 (1958)
3. Sommer, W. Trans. I.R.E. Nucl. Sci. NS-5, 3, 120 (1958)
4. Engstrom, R. W., Stoudenheimer, R. G., Palmer, H. L., and Bly, D. A. Trans. I.R.E. Nucl. Sci. NS-5, 3, 120 (1958)
5. Lawrence, E. O., & Beams, J. W. Phys. Rev. 29, 903 (1927)
6. Hiltner, W. A. Trans. I.A.U. IX, 687.
7. Baum, W. A. Trans. I.A.U. IX, 681.
8. Fellgett, P. B. "The Present and Future of the Telescope of Moderate Size", p. 51, University of Pennsylvania Press (1956)
9. Rose, A. J.O.S.A. 38, 2, 196 (1948)
10. Brumberg, E. M., Vavilov, S. I., and Sverdlov, Z. M. J. Phys. USSR 7, 1 (1943)
11. Hecht, S., Schlaer, S., and Pirenne, M. H. J. Gen. Physiol. 25, 819 (1942)
12. Rose, A. "Advances in Electronics", I, 131, Academic Press, New York (1955)
13. Mandel, L. J. Sci. Inst. 32, 405 (1955)
14. Krassovsky, V. I. Trans. I.A.U. IX, 693 (1955)
15. Zacharov, B. Ph. D. Thesis, University of London (1960)
16. McGee, J. D., Airey, R. W., and Wheeler, B. E. "Advances in Electronics and Electron Physics", XVI, Ed. McGee, J. D., Wilcock, W. L., and Mandel, L., p. 61. Academic Press, New York (1962)
17. Philips Gloeilampenfabrieken. Brit. Pat. No. 326,200. (5.11.28)
18. Zavoiskii, E. K., Butslov, M. M., Plakhov, A. G., and Smolkin, G. E., Dokl. Akad. Nauk. SSSR 100, 2, 241 (1955)
19. Stoudenheimer, R. G., Moor, J. C., and Palmer, H. L., Proc. I.R.E. Scintillation Counter Symposium, Washington (1959) p. 136.
20. Davis, G. P. Reference 16, p. 119.

21. Anderson, A. E. Reference 19, p. 133.
22. Wilcock, W. L., Emberson, D. L., and Weekley, B.
Reference 19, p. 126.
23. Emberson, D. L., Todkill, A., and Wilcock, W. L.,
Reference 16, p. 127.
24. McGee, J. D. Brit. Pat. No. 790,416 (5.6.53)
25. Roberts, W. L., and Kruper, A. P. U.S. Pat. No. 2,821,637 (30.11.53)
26. Perl, M. L., and Jones, L. W. "Advances in Electronics and
Electron Physics", XII, Ed. McGee, J. D., and Wilcock, W. L.,
p. 153, Academic Press, New York (1960)
27. Morton, G. A., and Ruedy, J. E. Reference 26, p. 183.
28. Lallemand, A. C.R. Acad. Sci. Paris, 203, 243, ~~296~~, (1936)
29. Lallemand, A., Duchesne, M., and Wlerick, G. Reference 26, p. 5.
30. Lallemand, A. Reference 16, p. 1.
31. Duchesne, M. Reference 16, pp. 19, 27.
32. McGee, J. D., and Wheeler, B. E. Journ. Phot. Sci. 9, 106 (1961)
33. McGee, J. D. and Wheeler, B. E. Reference 16, p. 47.
34. Hiltner, W. A., "The Present and Future of the Telescope of
Moderate Size", p. 11, University of Pennsylvania Press (1956)
36. Hiltner, W. A., and Pesch, P. Reference 26, p. 17.
36. Hall, J. S., Ford, W. K., and Baum, W. A. Reference 26, p. 21.
37. Hiltner, W. A., and Niklas, W. F. Reference 16, p. 37.
38. Zworykin, V. K., and Morton, G. A. "Television", p. 56,
2nd Edn., Chapman and Hall, London (1954)
39. Morton, G. A. R.C.A. Rev. X, 4, 525 (1949)
40. Mandel, L. Brit. Journ. Appl. Phys. 10, 233 (1959)
41. Ziegler, M. Physica 3, 307 (1936)
42. Lombard, F. J., and Martin, F. Rev. Sci. Inst. 32, 200 (1961)
43. Baicker, J. A. Reference 19, p. 74.
44. Mandel, L. Proc. Phys. Soc. 7, 1037 (1958)
45. Hiltner, W. A. Reference 8, p. 22.

46. Sharpe, J. Trans. I.R.E. Nucl. Sci. NS-5, 3, 202 (1958)
47. Zworykin, V. K., and Morton, G. A. Reference 38, p. 184.
48. Condon, P. E. Reference 26, p. 123.
49. Brill, A., and Klasens, H. A. Philips Res. Rep. 7, 401 (1952)
50. Kapany, N. S., Eyer, J. A., and Keim, R. E. J.O.S.A. 47, 423 (1957)
51. Burns, J., and Neumann, M. J. Reference 26, p. 97.
52. McGee, J. D., Flinn, E. A., and Evans, H. D. Reference 26, p. 87.
53. Chilowsky, C. U.S. Pat. No. 2,495,697.
54. Gorlich, P., Krohs, A., and Pohl, H-J. Brit. J. Appl. Phys. 12,
525 (1961)
55. Farnsworth, P. T. U.S. Pat. No. 1,773,890.
56. Kubetski, L. A. Proc. I.R.E. 25, 421 (1937)
57. Whetten, N. R., and Laponsky, A. J. Appl. Phys. 30, 432 (1958)
58. Nakhodkin, N. G., and Romanovsky, V. A. Izv. Akad. Nauk. SSSR
Ser. fiz. 22, 454, (1958)
59. Wargo, P., Haxby, B. V., and Shepherd, W. G. J. Appl. Phys. 27,
1311 (1956)
60. Rappaport, P. J. Appl. Phys. 25, 3, 288 (1954)
61. Daghish, H. N. Private communication.
62. Arntz, F. O., and Van Vliet, K. M. J. Appl. Phys. 33, 4, 1563 (1962)
63. Goeze, G. W. Reference 16, p. 145.
64. Rome, M. J. Appl. Phys. 26, 2, 166 (1955)
65. Zworykin, V. K., and Morton, G. A. Reference 38, p. 399.

Reprinted from a Symposium on E. A. FLINN

PHOTO-ELECTRONIC IMAGE DEVICES

held at London, September, 1958

Published by Academic Press Inc., New York,

An Electron Image Multiplier

Ph.D.

1963

J. D. MCGEE, E. A. FLINN, AND H. D. EVANS

*Instrument Technology Section, Physics Department, Imperial College,
University of London, England*

INTRODUCTION

The multiplication by secondary emission of a stream of electrons has been developed to a very high degree, and electron gains of 10^8 or 10^9 are now readily achievable. Thus the detection, either optically or electronically, of single photons incident on a photocathode is rendered possible.

This fact suggests the possibility of constructing a tube in which the photoelectrons from an array of image points on the photocathode are separately multiplied, but retained as a coherent electron image after multiplication, to give an image of much higher electron density.^{1,2} The electrons may then be accelerated on to a phosphor screen, or other detecting element, which might, for example, be the charge storage target of a television pick-up tube.

Secondary emission image intensifiers have been previously suggested, by Lubszynski,³ McGee,⁴ Sternglass,⁵ Wachtel† and others, but while these offer the possibility of very high gains, they all require the use of electron optical focusing techniques, with a consequent increase in complication and weight, due to the need for focus coils and stabilized power supplies.

A channelled multiplier tube will have much more modest voltage requirements than a magnetically or electrostatically focused tube, as the potential required between consecutive stages will be determined only by the secondary emission characteristics of the multiplying surfaces, and not by focusing conditions. The definition will, moreover, be independent of variations in the supply potential, only the brightness being affected. It would seem possible to operate a tube of this type with about 5kV across the entire multiplier section, while other types of intensifier tube require voltages of this order or greater for each stage.

It is clear that the main difficulty is to make such a device with a sufficient number of parallel channels to give adequate definition. From

† M. M. Wachtel. The Transmission Secondary Emission Image Intensifier. *See* p. 59.

television experience it seems that about 10^4 channels should be somewhere near the practical minimum, except for a few special purposes where relatively poor definition would be acceptable. Thus for channels 1 mm. square a structure 4 in. square should give sufficiently good definition. To improve the definition, the channels could be made smaller, or the dynodes larger. In the first case, the voltage difference between consecutive dynodes must remain constant, at or near the optimum value for secondary emission, and consequently, as the dynode structure is scaled down, the field strength between dynodes increases, increasing the risk of insulation breakdown or cold emission. Thus there appears to be a practical lower limit to channel cross-section, below which it would be difficult to go. However, there is no apparent reason why the dynodes should not be considerably larger than 4 in. square, as the optical image, or the electron image produced from it, may be magnified to 10 in. square, or even larger. Hence, by reducing the area of each channel as far as is practicable, and increasing the area of the dynodes, it seems possible that a picture of 2×10^5 elements might be achieved.

The essential features of such a channelled electron image multiplying system are three:

- (1) Electrons from the photocathode, or secondary electrons from any stage, must strike the secondary emitting surface of the following dynode.
- (2) A high percentage of the secondaries must be extracted from each stage to the next.
- (3) Straying of electrons between adjacent channels of the tube must be held to an absolute minimum.

Thus the crux of the problem is the choice of dynode geometry, and the fabrication of the resultant electrode structure. Work on this problem is at the moment being independently carried out by Burns† and his collaborators at Chicago Midway Laboratories, and by ourselves at Imperial College. Most of the work at Imperial College has been done on the construction of large-scale single-channel models, to investigate the electron trajectories in various possible dynode systems, although a certain amount of work has been carried out in the past on the problems of fabricating and processing multi-stage structures of small dimensions in actual tubes.

Probably a variety of electrode structures will be found suitable for this purpose. We have experimentally investigated the following three types:

† J. Burns and M. J. Neumann. The Channelled Image Intensifier. *See* p. 97.

- (1) A modification of the well-known "Venetian blind" type photo-multiplier.
- (2) A symmetrical cylindrical structure.
- (3) An asymmetrical cylindrical structure.

INVESTIGATION INTO ELECTRODE FORMS

1. Modified "Venetian blind" electrodes

This construction, illustrated in Fig. 1, utilises electrodes of "Venetian blind" type,⁶ with the addition of partitions to divide the dynode surface into a series of square picture channels. This results in an "egg-box" type of structure.

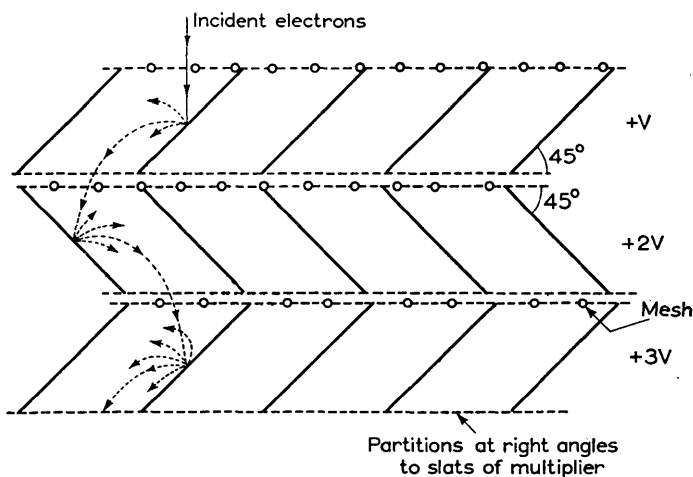


FIG. 1. Section of "Venetian blind" image multiplier.

A large model was built to simulate one cell of each of two adjacent dynodes, and a fluorescent screen was added to enable the exit points of the outgoing electrons to be observed. The electrodes were constructed of glass, carrying a transparent coat of conducting stannous oxide and a thin layer of willemite phosphor. The phosphor served as a source of secondary electrons, and also to indicate the points where electrons were incident. A beam of primary electrons was provided by a high velocity electron gun, with magnetic focusing and deflection, and was fired into the open end of the egg-box structure. It was possible by means of the phosphor to observe the points of impact of the secondary and tertiary electrons for various positions of the incident beam.

The results obtained were encouraging, as the electrons were found to be strongly canalised in passing from one dynode to the next. This

focusing effect was substantially independent of the relative voltages applied to each stage, and largely independent of the point of impact of the primary electron beam. It thus appears that the problem of electron straying between adjacent channels would be of minor importance in a structure of this type. It was concluded that dynodes of this form are perfectly practical from an electron-optical point of view. They are, however, difficult to make in small dimensions with sufficient accuracy, and to assemble in exact alignment. Hence a search was made for an electrode form more satisfactory from these points of view. The first to be investigated was a simple system of coaxial cylinders.

2. Symmetrical cylindrical electrodes

A single channel of two stages of such dynodes is drawn in Fig. 2a, while a three-stage multiplying system is illustrated in Figs. 2b and 2c. As illustrated in Figs. 2b and 2c, each of the dynodes, D_1 , D_2 , D_3 ,

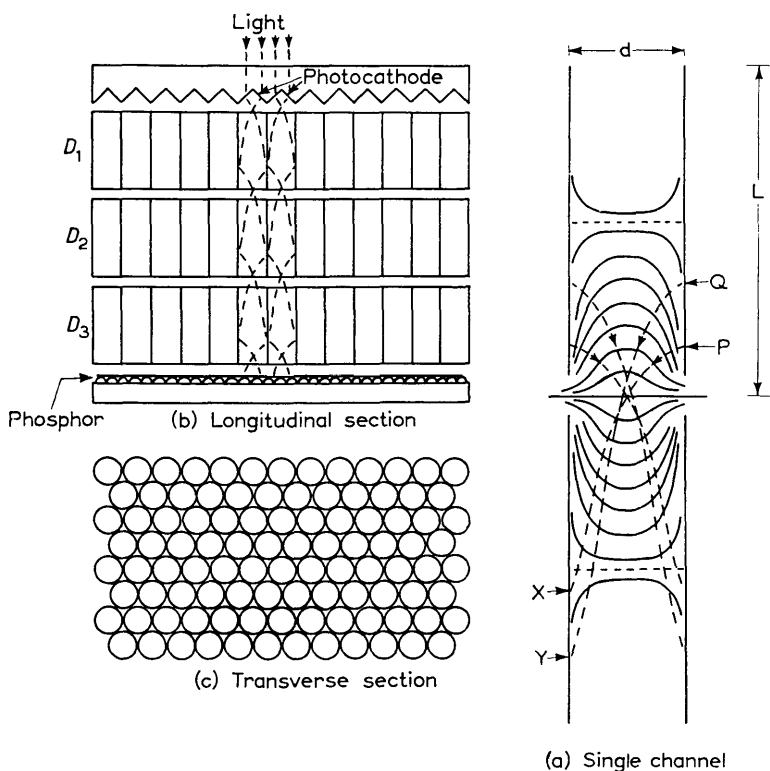


FIG. 2. Symmetrical cylindrical dynode structure.

consists of an array of short cylinders. The cylinders of consecutive dynodes are mounted accurately coaxial. Each consecutive pair of cylinders may in fact be regarded as a two-tube electrostatic lens, as shown more clearly in Fig. 2a, with the electron object, or source, lying on the wall of the first tube. Thus we might expect a crude electron image to be formed on the opposite wall of the second tube. If secondaries are released by the incident electrons at this point, it is then essential that they should be accelerated on to the third tube, and so on in successive stages.

It seemed probable that the ratio of length to diameter (L/d in Fig. 2) of each cylinder would be an important factor in controlling the operation of such a tube. If the cylinders are too short, electrons will not strike the opposite wall of the next tube, but will merely be accelerated through it, without multiplication. If, on the other hand, the segments are too long, extraction of the secondary electrons will be poor, and multiplication will again fall off.

If the dynode cylinders are all the same length, and the voltage steps applied between them are equal, then it is clear that only those electrons liberated below the mid-plane of each cylinder find themselves in a field which will accelerate them on to the next dynode. Hence it seemed desirable to make an investigation of the passage of electrons through such a dynode system on large scale models, before proceeding to the construction of small-scale multi-channel systems.

This was carried out in an experimental tube, illustrated in Fig. 3, in which the electrodes consisted of a cylindrical transparent photocathode C followed by a series of short transparent "Nesa" cylinders N , all formed on the inside wall of the Pyrex tube T . Contact was made to the electrodes and to the photocathode by means of platinum tape seals⁷ P through the walls. The separate cylinders N were about $\frac{1}{2}$ in. long and 1 in. in diameter, and could be connected externally in groups, to vary the effective dynode length. The inner surface of each cylinder was coated with a thin layer of willemite W to indicate the point of impact of primary electrons, and to serve as a source of secondaries.

The point of origin of the slow primary photoelectrons could be altered by moving about a spot of light on the photocathode, and the corresponding point of arrival of these electrons on the first dynode observed. Similarly the point of arrival of these secondaries on the second dynode could be seen, and so on.

The experimental results obtained with the tube shown in Fig. 3 are illustrated in Fig. 2a. As the exciting spot of light is moved from the position P to Q , the photoelectrons released by it are found to arrive in quite well defined spots at X and Y respectively. The photoelectrons from P arrive at a point X rather more than one tube-diameter below

the top of the next cylinder and as the spot of light is moved above Q the point at which the photoelectrons reach the opposite wall moves far below the point Y . Hence it appears from these preliminary tests

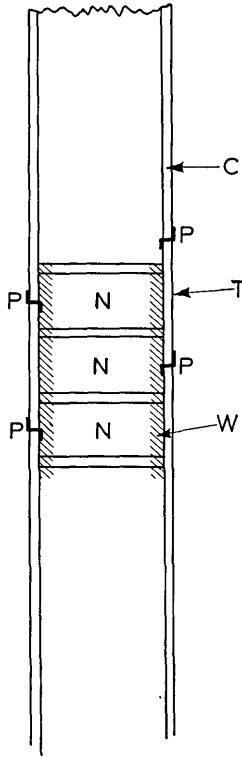


FIG. 3. Large scale model of symmetrical cylindrical structure. N - "Nesa" rings. P - Pt tape seals. C - Antimony caesium photocathode. T - Pyrex tube. W - Willemite coating inside tube.

that a ratio of L/d of about 2 would satisfy the conditions 1 and 2 listed above for such a system.

Further investigations are being carried out on this structure.

3. *Asymmetrical cylindrical electrodes*

Here, the dynodes again consist of many short segments of tube, arrayed side by side, but in this case the tube ends are cut at an angle, instead of normally, to the axis. A single channel is illustrated in Fig. 4a and a three-stage multiplier of this type in Fig. 4b. This structure is roughly equivalent to a two-tube lens with a pair of transverse deflecting plates positioned across the junction of the two cylinders. Instead of

travelling from side to side of the tubes as they pass through the dynode assembly, the electrons now impinge always on the same side of successive tubes, as shown in Fig. 4b.

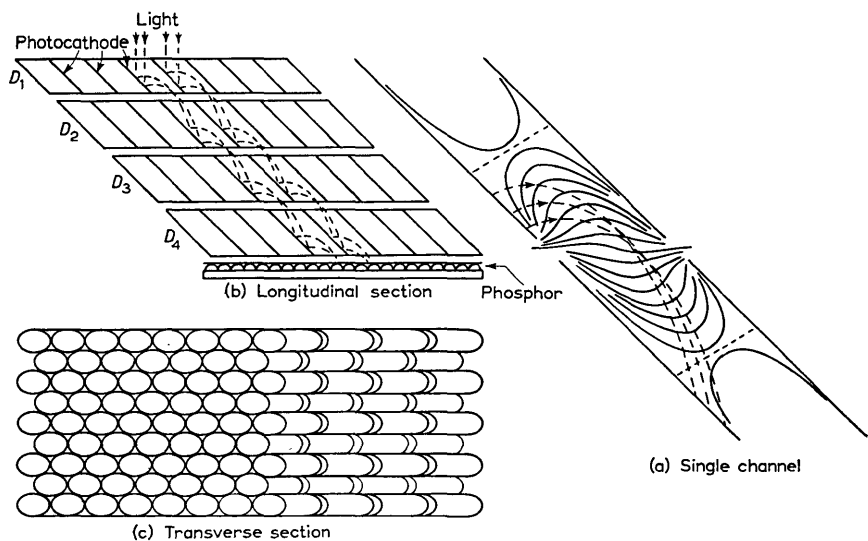


FIG. 4. Asymmetrical cylindrical dynode structure.

An experimental tube was made to simulate this structure on a large scale. Basically, the design was the same as for the tube of Fig. 3 for the investigation of the symmetrical cylindrical structure, except that the planes of the ends of the photocathode and of the "Nesa" rings were now arranged at an angle of 45° to the tube axis. The results obtained from this tube are illustrated in Figs. 5a and 5b and show a very desirable system of electron trajectories.

In Fig. 5a the whole tube is visible and the spot of light (1) projected on to the photocathode by the projector (5) is just visible. The four resulting spots of fluorescence indicated by (2) represent the successive points at which the primary, secondary, tertiary, etc., electrons impinge on the tube walls.

The behaviour of the tube is shown more clearly in Fig. 5b which is a photograph taken with low general illumination: this shows very clearly the successive areas (2) of impact of the electron stream on the wall of the tube, starting from the light spot (1) on the photocathode. It is worth noting that the first fluorescent spot (2) is smaller than the other three; this is attributed to the fact that the first spot is produced by photoelectrons having small initial velocity while the other three are

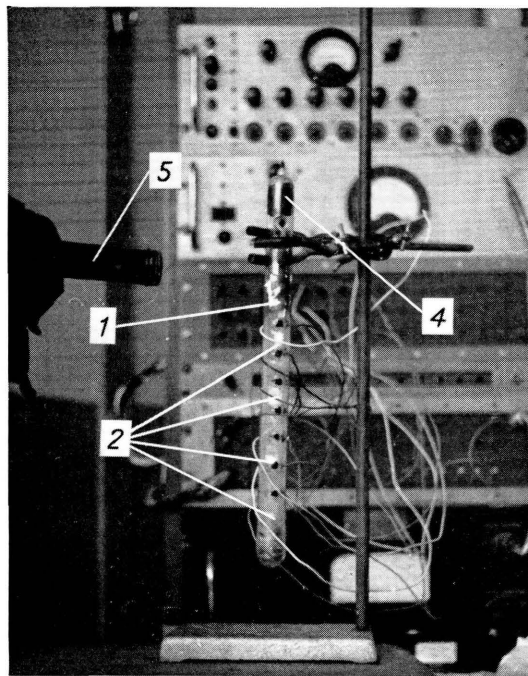


FIG. 5(a). Double exposure showing large scale model of asymmetrical cylindrical electrode system. 1. Incident light spot. 2. Luminous patches caused by secondaries. 4. Auxiliary processing anode. 5. Light source.

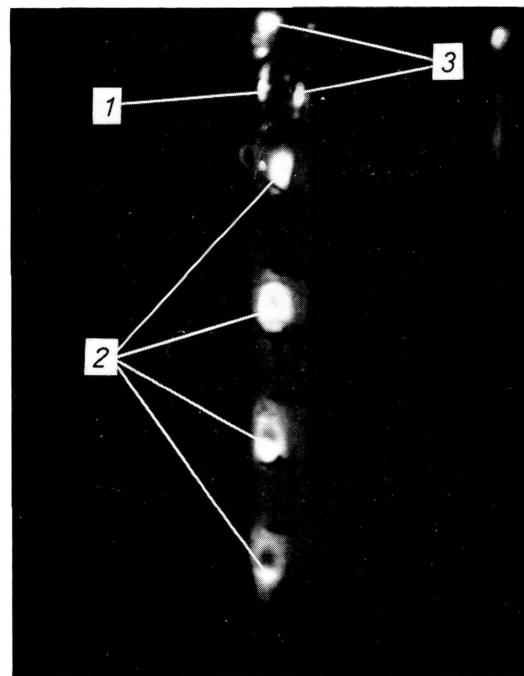


FIG. 5(b). Close-up of same tube in operation, showing: 1. Incident light spot. 2. Luminous patches caused by secondaries. 3. Scattered light (inside tube).

produced by secondary electrons which have a much greater spread of initial velocity and hence are not so easily focused. However, the enlargement of the fluorescent spot is not progressive, indicating that a fairly stable progression from stage to stage has been reached.

The position of the first fluorescent spot was to a large extent independent of the position of the spot of light on the photocathode, which indicates a useful concentrating effect of the electrons in this type of dynode structure. Moreover, it is anticipated that the optical image will be projected on to a photocathode formed on the inner surfaces of a preliminary electrode D_1 of Fig. 4b. Hence it is to be expected that the photoelectrons so produced would be directed efficiently on to D_2 .

Work is now proceeding on large-scale model tubes utilising less acute angles than 45° , and also on a large-scale model tube utilising antimony-caesium secondary emitting surfaces, to investigate the actual emission ratio obtained.

CONCLUSION

On the basis of the work so far done, there appears to be no doubt that the construction of a system of channelled secondary emission dynodes, of a form that will satisfy the conditions postulated in the introduction to this paper, is feasible. The essential problem appears to be to determine the most suitable form to give efficient operation and convenience in construction.

Even if high definition intensified images may never be achieved by such a device, the very large multiplication factors that are to be expected would enable single primary photoelectrons to be detected visually or photographically with relatively uncomplicated apparatus. This would almost certainly render it a most powerful tool in many fields of scientific observation.

ACKNOWLEDGMENTS

The authors would like to acknowledge, with thanks, the support given to this work in its initial stages by the Paul Instrument Fund Committee of the Royal Society and the present support by the National Research and Development Corporation. They also thank Mr. H. E. Holman, of the E.M.I. Research Laboratories, for much practical advice and assistance.

REFERENCES

1. McGee, J. D., Brit. Pat. No. 790, 416 (5 June, 1953).
2. Roberts, W. L., and Kruper, A. P., U.S. Pat. No. 2,821,637 (30 November, 1953).
3. Lubszynski, H. G., Brit. Pats. Nos. 457,493 (30 May, 1935) and 515,564 (27 May, 1938).

4. McGee, J. D., Brit. Pat. No. 504,927 (28 October, 1937).
5. Sternglass, E. J., *Rev. sci. Instrum.* **26**, 1202 (1955).
6. McGee, J. D., and Lubszynski, H. G., Brit. Pat. No. 508,106 (24 November, 1937).
7. Davis, E. J., *J. sci. Instrum.* **35**, 308 (1958).

Published by Academic Press, London and New York
Progress Report on a Channelled Image Intensifier

E. A. FLINN

*Instrument Technology Section, Physics Department, Imperial College,
University of London, England*

INTRODUCTION

The channelled image intensifier is fundamentally similar to a normal non-imaging photomultiplier.^{1, 2, 3, 4} The difference lies in the structure of the dynodes, which, as the name implies, consist of an array of channels so arranged that electrons from each element of the photocathode are confined to one particular channel during the multiplication process. After multiplication, they are projected on to a phosphor screen to give an intensified reproduction of the incident image. The relatively coarse structure of the dynodes is imposed on this image, since brightness variations at the photocathode occupying less than one channel diameter are destroyed during the process of intensification.

It thus appears feasible to produce a tube which, although having fairly limited resolution, has a very high potential brightness gain. This can be achieved with a very modest voltage across the dynode section; a typical photomultiplier, for instance, may give a gain of 10^6 or more with a total applied voltage of about 1.5 kV. A few kilovolts must also be supplied to accelerate the electrons to the fluorescent screen, but the overall voltage is still less than that required for a single stage of other intensifiers. No magnetic field is required since the focusing is an inherent property of the electrode structure, and there is consequently no need for a solenoid, with its stabilized current supply. Also the e.h.t. supplies need not be so accurately stabilized as when magnetic focusing is used. Finally, since the resolution is determined only by the dynode structure, the addition of extra multiplying stages causes no loss in resolving power, so that within reason any desired gain may be achieved by increasing the number of stages.

The resulting simplicity of operation, combined with the small size of such a tube and its potentially high gain, make it a very attractive proposition, in spite of its limited resolution and the practical difficulties involved in its construction.

DYNODE FORM

Various possible electrode forms have been investigated,³ chiefly by means of large-scale models. The structure finally selected is one in which each cell of the dynode consists of a short cylinder with its ends sliced at 55° (Fig. 1). The inside walls of the cells are coated with a suitable secondary electron emitter.

With this arrangement, electrons striking a cell wall in the first dynode produce secondaries which are drawn into the corresponding cell of the second dynode. At the same time they are deflected to the wall by the asymmetrical field resulting from the oblique cell structure. Multiplication then occurs, and the process is repeated.

It will be clear that the geometrical proportions of the elementary cells are of prime importance. If the cylinders are made too short, electrons may completely miss one stage, and so electron gain is lost. Such electrons also have a much higher than normal chance of straying into an adjacent channel. If, on the other hand, the cylinders are too long,

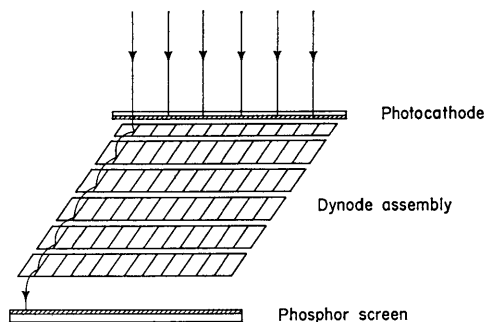


FIG. 1. Diagram of channelled image intensifier.

the extracting field of the following dynode is weakened, so that some of the secondaries fall back into the surface, and are lost to the multiplication process. Similarly, the angle between the axis of a cell and the plane of its ends is an important parameter. If this angle is too acute, the field due to one dynode penetrates too far into the succeeding dynode, and tends to inhibit the escape of secondary electrons. If, however, the angle is too obtuse, the electrons are not sufficiently strongly deflected to the wall of the following cell, and again tend to miss a stage.

The structure finally adopted after the investigations previously mentioned seems to be a reasonable compromise between these various factors. The cells used have a slant length equal to twice their diameter, and the plane of the ends of the cylinders is at 55° to the longitudinal axis.

Tests on large-scale dynodes of this form suggest that about 65% of the secondaries produced reach the following stage and later results obtained from small-scale tubes are in agreement with this. In these tubes, dynodes activated by a method giving a true secondary emission yield of about five were found to give a stage-gain of a little over three.

Dynode Fabrication

The dynodes are manufactured from nickel tubing as used for the manufacture of thermionic cathodes. In the tubes so far constructed, 1 mm diameter tubing with walls 0.002 in. thick has been used, although dynodes using 0.5 mm diameter tubing are now being constructed.

Six-inch lengths of this tubing are assembled in a steel brazing jig, so that the array, viewed from one end, exhibits a hexagonal close-packed structure. This enables the maximum number of channels to be used, and in the present dynodes there are 291 tubes, forming an array 18 mm × 15 mm. At each corner of the array, a rectangular nickel bar is incorporated. The whole assembly is brazed together in a vacuum stove, using silver-copper eutectic alloy at 850°C. This material readily wets the nickel of the tubes, but is prevented from entering them by plugs of gun cement (a mixture of alumina and potassium silicate) in their ends.

Slices are cut at the requisite angle from the resultant block of tubes with a high-speed cut-off wheel. These are then ground to the exact thickness required. This process also removes the larger part of any burr formed in the cutting operation. The slices are placed in a drilling jig and a $\frac{3}{32}$ in. diameter hole is drilled in each of the four nickel rectangles at the corners. After a light etching in warm dilute hydrochloric acid the dynodes are then ready for use.

Tube Assembly

The electrodes are fitted with nickel leads, and vacuum stoved to 700°C. The chosen secondary emitter is evaporated on to them in a special demountable bell jar, which is then transferred bodily to a glove box in which a dry and, if necessary, inert atmosphere is maintained. There the bell jar is opened and the dynodes are removed.

The electrode assembly is built up on a stainless steel base plate, fitted with a springy stainless steel skirt which presses tightly against the tube wall and excludes caesium from the dynode system during activation of the photocathode. The cathode is formed on a rectangular glass plate which fits into a shouldered recess on the other side of the base plate, and is held in position by light springs. After the photocathode is processed, the glass plate is turned over so that its sensitive surface faces the dynode assembly. The dynodes are attached to this plate and held with individual channels aligned by ceramic rods passing through the four holes at their corners. They are separated from each other and from the photocathode plate by mica spacers of suitable thickness. Tubular glass spacers separate the fluorescent screen from the last dynode. The whole assembly is fixed together by spring clips

which fit tightly on the ceramic rods, and is held in place in the tube by clips attached to the stainless steel shelf, which engage with tungsten pins set in the tube wall. Contact to the dynodes from the outside of the tube is made via a further set of tungsten pins, to which the dynode leads are attached. Finally the glass end-plate of the tube is sealed in place with silver chloride.

RESULTS

So far MgO has proved the most satisfactory secondary emitter. Attempts have also been made to use SbCs_3 and KCl, but these have been less successful.

In one four-stage tube, using MgO as secondary emitter, a total electron gain of over 30 was recorded, at 480 V per stage. The four stages had respectively gains of 1.35, 2.65, 3.1 and 2.9. With KCl emitters, the best stage gain achieved has been a little over 2. In all cases the gain of the first stage has been significantly less than that of the others, which indicates the need for further study of the problems of electron transfer from the photocathode to the first dynode, and the extraction of secondaries from this dynode.

The resolution obtained agrees well with that to be expected from a structure of this type. Three hundred elements are too few to reproduce anything other than the simplest of images, but test patterns of parallel bars are adequately imaged. For a dynode having circular elements 1 mm in diameter, arranged in a hexagonal close-packed array, the theoretical resolution for a randomly oriented pattern of equal width parallel black and white bars is about $\frac{1}{4}$ lp/mm. The maximum possible resolution is obtained when the lines of the test pattern are aligned with those of the dynode array, when about 0.6 lp/mm can be resolved. With obliquely cut dynodes, however, the elements are not

Note added in proof.

Since the original presentation of this paper, rather better results have been obtained using KCl layers. Six-stage and ten-stage tubes have been built with KCl secondary emitting surfaces. One of the six-stage tubes gave an electron gain per stage of slightly over 3 at 750 V/stage, while a ten-stage tube had an overall electron gain greater than 2×10^4 at 530 V/stage. This tube had a photocathode sensitivity of 25 $\mu\text{A}/\text{lm}$ but the aluminium backing layer on the phosphor was too thin, and the consequent optical feedback limited the useful light gain to about 5×10^4 , obtained with an overall voltage of 11 kV. Above this value, the image deteriorated progressively, since the arrangement of the channels causes the fed-back image to be considerably out of register with the original (see Fig. 1). In all these tubes, the first dynode was made only half the thickness of the others, as this was found to improve the gain of the stage by some 35%.

circular, but elliptical, and the resolution is reduced in the direction parallel to the major axes of these ellipses, the maximum resolution falling to slightly less than 0.5 lp/mm.

Results obtained with actual tubes tally well with these figures; and the theoretical resolution of 0.5 lp/mm can in fact be obtained when the test pattern is accurately aligned with the dynode structure (Fig. 2). The systematic arrangement of the picture elements gives rise to some effects not found in other types of image tube. If, for instance, a

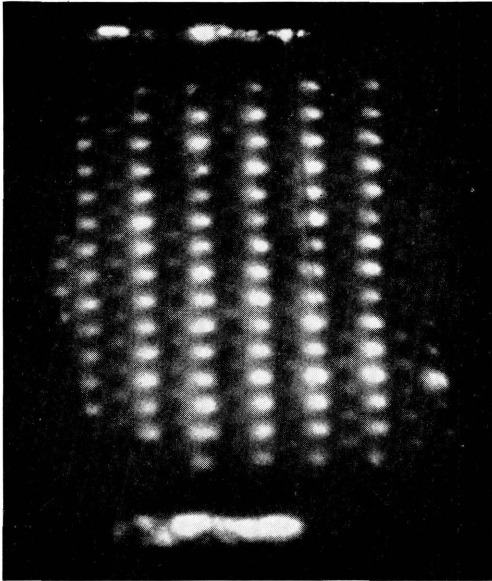


FIG. 2. Limiting resolution: 0.5 lp/mm. Test pattern aligned with dynode structure.

pattern at the limit of resolution is moved laterally by 0.5 mm, the lines totally disappear, since the electrons from a bright bar are then equally divided between two adjacent rows of apertures. Similarly, a zig-zag effect is produced by rotating such a pattern through a small angle. Patterns slightly coarser than this are not perfectly resolved; they "beat" with the dynode structure, and a widely spaced periodic intensity variation across the screen results. A similar effect is seen with patterns just too fine to be resolved. These phenomena are very similar to those observed with fibre optics, which possess the same type of ordered structure.

It has been found⁵ when using fibre optical systems that the resolution is much improved if both ends of the fibre system are moved in

synchronism, preferably with random direction and amplitude, an amplitude of a few fibre diameters being sufficient. Theoretically, the limiting resolution is more than doubled, and this has been observed in practice with our tubes. For example, Fig. 3 shows two images of a test fan having 1 lp/mm at the fine end, and approximately 0.33 lp/mm at the coarse end. In Fig. 3(a), with the tube static, only the extreme coarse end of the fan is resolved, and that very poorly, while in Fig. 3(b), obtained while reciprocating the tube with an amplitude of two channel diameters, the whole of the fan is clearly resolved. The factor of three

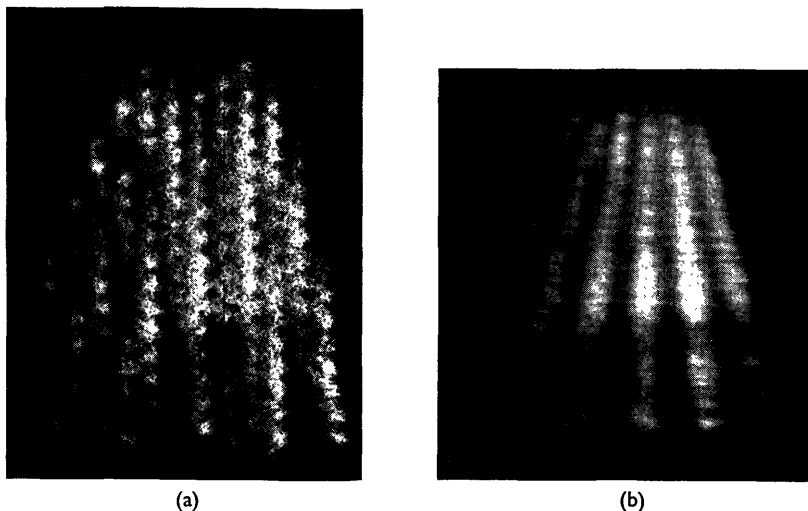


FIG. 3. (a) Image of fan pattern, tube stationary, 1 lp/mm at top. (b) Image of the same fan pattern; tube reciprocated with amplitude of two channel diameters.

thus gained in the linear resolution is equivalent to an order of magnitude increase in the total number of channels. Furthermore, with line patterns near the limit of resolution, the "beating" effects mentioned above are eliminated, and such patterns can be resolved in any orientation. The pattern of dots which form the static image is rendered much less noticeable in the dynamic case, so that a more pleasing image results. In practice, these advantages might be realized either by mechanical movement of the whole tube, or by synchronously sweeping the input electrons across the first dynode and the output electrons across the phosphor. Some additional complication in the tube and its associated equipment would be involved, but the very valuable increase in information capacity might well justify this.

In the tubes discussed, cross-talk between adjacent channels has not appeared to be a serious problem, at least at the gains so far achieved. Illumination of the photocathode with a bright pin-point image produces a single bright spot at the phosphor, with no visible halo. Should cross-talk prove troublesome at higher gains, it should be relatively easy to coat the edges of the dynode apertures with some suitable insulator, to act as a physical barrier to straying electrons.

FUTURE DEVELOPMENTS

Plans for the future include the construction of tubes with smaller channels, with a consequent improvement in resolution. This is the most obvious method of improvement, although the scanning method mentioned earlier, or an increase in dynode area, coupled with magnification of the input image, are alternative possibilities. Dynodes with 0.5 mm channels are now almost ready for use; they are otherwise exactly the same as those now in operation, and no serious difficulty is anticipated in their assembly. The resulting 1200 channels should be able to convey sufficient information to give a recognizable picture of a quite complex object, such as a human face.

To scale down the channel size still further, however, will require improvements in the technique of fabrication. Alignment becomes considerably more difficult as the scale is decreased, and in addition to this the finite wall thickness of the tubes becomes even more important. About 0.0015 in. is the thinnest wall which can readily be produced, although this can be considerably reduced by etching the completed dynode. The 0.5 mm tubes mentioned above initially have walls 0.002 in. thick, so that about 36% of the cross-sectional area is occupied by the wall. This is primarily of importance in the first stage, where it reduces the efficiency of utilization of photoelectrons.

Efforts are also being made to produce secondary emitting surfaces with a higher consistent yield. The next stage will be the construction of tubes with more stages, and consequently, it is hoped, higher gain.

CONCLUSIONS

It is felt that the results obtained to date are sufficiently encouraging to justify the continuation of our attempts to construct a channelled intensifier; the compactness of such a tube, its simplicity of operation, and potentially high gain may compensate for the considerable practical difficulties involved in its manufacture. The possibility of making tubes of very large sensitive area is also attractive, particularly in the fields of scintillation chamber work and X-ray fluoroscopy, where the small area of other intensifiers is a serious disadvantage.

ACKNOWLEDGMENTS

The author would like to thank Professor J. D. McGee who first conceived the channelled tube, and has been of continual assistance in its development. Thanks are due also to Mr. D. Theodorou and Mr. M. J. Whillock, who have assisted in much of the work described here. The project has been financially supported by the National Research Development Corporation and the Department of Scientific and Industrial Research.

REFERENCES

1. McGee, J. D., Brit. Pat. No. 790,416 (5:6:1953).
2. Roberts, W. L. and Kruper, A. P., U.S. Pat. No. 2,821,637 (1953).
3. McGee, J. D., Flinn, E. A., and Evans, H. D., "Advances in Electronics and Electron Physics", Vol. XII, ed. by J. D. McGee and W. L. Wilcock, p. 87. Academic Press, New York (1960).
4. Burns, J. and Neumann, M. J., "Advances in Electronics and Electron Physics", Vol. XII, ed. by J. D. McGee and W. L. Wilcock, p. 97. Academic Press, New York (1960).
5. Kapany, N. S., Eyer, J. A., and Keim, R. E., *J. opt. Soc. Amer.* **47**, No. 5, 423 (1957).

DISCUSSION

A. E. HUSTON: Have you found differences in the multiplication obtained in the different channels?

E. A. FLINN: Not at the gains we get at present. Non-uniformity of the photocathode sensitivity has proved to be a more serious cause of variation in gain across the sensitive area of the tube.

W. F. NIKLAS: As you have (a) packing losses, (b) losses due to dynode channel thickness, and (c) difficulties in collecting the photoelectrons in the first stage, the "effective" quantum yield of the photocathode should be quite low. Is this effect an inherent limitation?

E. A. FLINN: The possibilities of reducing the effects of these three factors can be summarized as follows.

- (a) When cylindrical channels are used in a hexagonal close-packed arrangement, there is a packing loss of about 9% of the total dynode area. It is doubtful if anything would be gained here by the use of square or hexagonal channels, as the extracting field in the corners of these would be rather weak. A periodically shaped photocathode surface would help to reduce this loss.
- (b) Losses due to the wall thickness of the channels can readily be cut down by reducing the wall thickness; to do this for very small-scale dynodes will necessitate an alternative method of construction. The shaped photocathode suggested above would help to reduce this loss also.
- (c) The difficulty here lies not in collecting the photoelectrons—this is caused by (a) and (b)—but in extracting the secondaries produced, since the field in the cells of the first dynode is not the same as in other dynodes. The optimum thickness for the first dynode has not yet been determined, but it is probable that a significant improvement can still be obtained.

An attractive possibility is the deposition of the photosensitive surface on the inner walls of the cells in the first dynode. Losses would still be present, but the possibility of photoelectrons entering the wrong channel would be eliminated, and the extraction of secondaries from the first multiplying stage would be improved.